INFORMATION TO USERS

This reproduction was made from a copy of a document sent to us for microfilming. While the most advanced technology has been used to photograph and reproduce this document, the quality of the reproduction is heavily dependent upon the quality of the material submitted.

The following explanation of techniques is provided to help clarify markings or notations which may appear on this reproduction.

1. The sign or "target" for pages apparently lacking from the document photographed is "Missing Page(s)". If it was possible to obtain the missing page(s) or section, they are spliced into the film along with adjacent pages. This may have necessitated cutting through an image and duplicating adjacent pages to assure complete continuity.
2. When an image on the film is obliterated with a round black mark, it is an indication of either blurred copy because of movement during exposure, duplicate copy, or copyrighted materials that should not have been filmed. For blurred pages, a good image of the page can be found in the adjacent frame. If copyrighted materials were deleted, a target note will appear listing the pages in the adjacent frame.
3. When a map, drawing or chart, etc., is part of the material being photographed, a definite method of "sectioning" the material has been followed. It is customary to begin filming at the upper left hand corner of a large sheet and to continue from left to right in equal sections with small overlaps. If necessary, sectioning is continued again—beginning below the first row and continuing on until complete.
4. For illustrations that cannot be satisfactorily reproduced by xerographic means, photographic prints can be purchased at additional cost and inserted into your xerographic copy. These prints are available upon request from the Dissertations Customer Services Department.
5. Some pages in any document may have indistinct print. In all cases the best available copy has been filmed.

University
Microfilms
International

300 N. Zeeb Road
Ann Arbor, MI 48106

Karimi, Majid

PMO POTENTIAL AND DIPOLE MOMENT FUNCTIONS OF HF WITH CORRECT ASYMPTOTIC BEHAVIOR

The University of Oklahoma PH.D. 1984

University
Microfilms
International 300 N. Zeeb Road, Ann Arbor, MI 48106

UNIVERSITY OF OKLAHOMA
GRADUATE COLLEGE

PMO POTENTIAL AND DIPOLE MOMENT FUNCTIONS OF HF WITH CORRECT ASYMPTOTIC BEHAVIOR

A DISSERTATION
SUBMITTED TO THE GRADUATE FACULTY
in partial fulfillment of the requirements for the
degree of
DOCTOR OF PHILOSPHY

By
MAJID KARIMI
Norman, Oklahoma
1984

PMO POTENTIAL AND DIPOLE MOMENT FUNCTIONS OF HF WITH CORRECT ASYMPTOTIC BEHAVIOR

A DISSERTATION

APPROVED FOR THE DEPARTMENT OF PHYSICS AND ASTRONOMY

By

J N Huffaker

Ronald Kantowski

Gregory A. Parker

DISSERTATION COMMITTEE

Dedication

This dissertation is dedicated to my parents,Mr. Mahmood Karimi and Mrs. Sedigheh Karimi.

Acknowledgement

I wish to express my deepest appreciation to Dr. J. N. Huffaker for suggesting this problem, for his constant help and guidance throughout the completion of this research work, and especially for encouraging me to gain an extensive ability of computer programming.

I also wish to thanks Dr. R. Kantowski,Dr. H. Fischbeck,Dr. G. Parker, and Dr. G. Atkinson for reading the manuscript,giving many useful suggestions, and for being on my committee.

Special thanks are due to Dr. Loc B. Tran for his many helpful discussions with me on the problem and for his moral support during my long years of research.

TABLE OF CONTENTS

LIST OF TABLES

LIST OF ILLUSTRATIONS

FIGURES Page

ABSTRACT

A perturbed Morse oscillator potential function for the $X^1\Sigma^+$ state of HF is improved for large internuclear separation (r) by adding a function of several parameters from which "synthetic" higher-order PMO parameters can be evaluated. These parameters can then be varied until the asymptotic condition ($V(r) \rightarrow D_e$ as $r \rightarrow \infty$ where D_e is the dissociation energy) is achieved.

Values of the PMO parameters (including the non-adiabatic correction parameter Δ and higher-order PMO parameters) have then been obtained by fitting experimental values of G_v, B_v, and D_v directly in terms of model parameters. The quality of the PMO potential function found is determined by the agreement between the eigenenergies it predicts (in this work, through solving the radial Schrödinger equation) and the spectroscopically observed ones.

The PMO potential thus obtained has been improved even more by a special method in which some of its parameters are varied in very small step size until the differences $G_v^{cal} - G_v^{ex}$ and $B_v^{cal} - B_v^{ex}$ become as small as possible.

The vibrational wave functions for this PMO potential were com-

puted by numerical methods. These wave functions were then used in the determination of the dipole moment of $X^1\Sigma^+$ state of HF as a function of r by fitting it to the experimentally deduced vibrational matrix elements.

The dipole moment of the $X^1\Sigma^+$ state of HF were calculated as cubic polynomials in $u = r - r_e$, $y = 1 - e^{-a(r-r_e)}$, and $z = e^{a(r-r_e)} - 1$. In addition, we found a suitable functional form by which we have been able to obtain the dipole moment of HF with correct asymptotic behavior at both large and small r.

PMO POTENTIAL AND DIPOLE MOMENT FUNCTIONS OF HF WITH CORRECT ASYMPTOTIC BEHAVIOR

CHAPTER I

Introduction

Since a relatively large amount of effort has been made by theoreticians on the hydrogen fluoride molecule in the past several years [1-4], it was felt that it would be worthwhile to have an accurate internuclear potential energy curve for this system. The potential function is of great importance since its knowledge is necessary for calculations of many quantities (such as dipole moment, Frank-Condon coefficients, *etc.*).

In the framework of the Born-Oppenheimer approximation, the molecular wavefunction is expressed as the product of electronic and nuclear wavefunctions [6-8]. In the particular case of a diatomic molecule, one can further separate the variablesfor the nuclear wave function, so that the total molecular wave functions may be written as

$$\psi_N = \psi_n^{(el)} \psi_\gamma^{(nucl)} = \psi_n^{(el)}(\underline{r}_e, \underline{R}_\alpha) \psi_{v,J}^{(vib)}(r) \psi_{Jm_J}^{(rot)}(\theta, \phi), \qquad (1.1)$$

where n, v, J, m_J are electronic, vibrational, rotational and magnetic quantum numbers.

The ro-vibrational part $\psi_{v,J}^{(vib)}(r)$ is the solution of the following equation

$$\left[-\frac{\hbar^2}{2\mu}\frac{d^2}{dr^2} + V(r) + \frac{\hbar^2 J(J+1)}{2\mu r^2}\right]\psi_{v,J}(r) = E_{v,J}\psi_{v,J}(r), \tag{1.2}$$

where r is the internuclear distance, μ reduced mass, and $V(r)$ is the nuclear potential energy. Dunham using the WKB method expanded the eigenvalue $E_{v,J}$ of Eq. (1.2) as a double power series in vibrational and rotational quantum numbers $(v+1/2)$ and J [10] as follows:

$$E_{v,J} = hc\sum_{j=0}\sum_{k=0} Y_{jk}(v+\frac{1}{2})^j[J(J+1)]^k. \tag{1.3}$$

1.1. Internuclear Potential Functions for Diatomic Molecules

Several different potential functions have been used with varying degrees of success. One of the standard potentials for describing diatomic molecules is the Morse potential [13] given by

$$V(r) = D_e[1 - e^{-a(r-r_e)}]^2 = D_e y^2, \tag{1.4a}$$

involving the three parameters D_e (well depth), r_e (equilibrium value of r), and a. For convenience, we define the Morse potential by three parameters ρ, σ, and τ, which related to D_e, r_e, and a by the following relations

$$\rho = ar_e, \qquad 1.4b$$

$$\sigma = [2\tau D_e]^{\frac{1}{2}}/_{ah}, \qquad 1.4c$$

$$\tau = \frac{D_e}{hc}, \qquad 1.4d$$

where $\sigma = \frac{w_e}{2w_e x_e}$ is approximately the number of bound states of the Morse potential. For the Morse potential, Eq. (1.2) is exactly soluble when $J = 0$. In this case, the vibrational term values are found to be [13,14]

$$G(v) = 2\tau(\frac{v+\frac{1}{2}}{\sigma}) - \tau(\frac{v+\frac{1}{2}}{\sigma})^2. \tag{1.5}$$

The drawback of this potential is that there are not enough parameters to accurately reproduce experimental results.

Another potential is the Dunham potential [11,12], which can be written as

$$V_D(\xi) = hca_0\xi^2(1 + a_1\xi + a_2\xi^2 + \cdots), \tag{1.6a}$$

where $\xi = \frac{(r-r_e)}{r_e}$. The eigenvalues and parameters a_0, a_1, ... of this potential have been found by the WKB method [12]. The drawback of this potential is its poor convergence[7] and not producing analytic wave functions.

Another potential similar to Dunham but with a different variable than Dunham is the Simons-Parr-Finlan (SPF) potential [15]

$$V_{SPF}(r) = hcT\eta^2(1 + \sum_{n=1} A_n\eta^n), \tag{1.6b}$$

where $\eta = (r - r_e)/r$.

The generalization of the Dunham and SPF potentials were introduced by Thakker[47]:

$$V(r) = e_0(p)\lambda^2(p)(1 + \sum_{n=1} e_n\lambda^n(p)), \tag{1.7}$$

where $\lambda(p) = s(p)(1-(r_e/r)^p)$, and

$$s(p) = \begin{cases} +1, & p > 0 \\ -1' & p < 0 \end{cases}$$

Thakker potential contains both the Dunham and the SPF potentials as special cases corresponding to p=+1 and p=-1.

One of the most practical procedures for obtaining a potential function directly from spectroscopic constants is a numerical procedure known as the Rydberg-Klein-Rees (RKR). This method is based on the semi-classical JWKB method [16,17]. In this method the turning points in the potential curve are given by

$$r_{\substack{max \\ min}} = C\left[\left(f_v^2 + \frac{f_v}{g_v}\right)^{\frac{1}{2}} \pm f_v\right], \tag{1.8a}$$

$$\text{where} \quad C = \left(\frac{h}{8\pi^2 c\mu}\right)^{\frac{1}{2}},\ f_v = \int_{v_0}^{v} [G_v - G_{v'}]^{-\frac{1}{2}} dv', \tag{1.8b}$$

$$\text{and} \quad g_v = \int_{v_0}^{v} B_{v'} [G_v - G_{v'}]^{-\frac{1}{2}} dv'. \tag{1.8c}$$

The lower limit of the integrals, v_0, introduced by Kaiser [18] may be defined by

$$E_{v,J} = 0 = Y_{00} + G_{v_0} = 0. \tag{1.9}$$

Huffaker and Dwivedi [19] showed that the perturbed Morse oscillator (hereinafter abbreviated as PMO) with potential function of the form

$$V(r) = \tau(y^2 + \sum_{n=4}^{\infty} b_n y^n), \tag{1.10}$$

where $y = 1 - \exp(-a(r - r_e))$, provides an accurate model for the vibrational-rotational motion of diatomic molecules. Model parameters ρ, σ, τ, b_4, ..., b_n can be determined from spectroscopic constants [10,11]. The PMO potential parameters are related to the dissociation energy D_e by

$$D_e = \tau(1 + \sum_{n=4}^{\infty} b_n). \tag{1.11}$$

The PMO potential converges for all values of r except for a singularity at $r = 0$. A method was proposed by Huffaker [20] to relate an RKR potential to a PMO one, through an explicit relationship between their parameters. The PMO potential has a longer range of convergence than the Dunham potential,and its leading term represents a potential with finite number of bound states; therefore it is a suitable model to describe vibrational-rotational states of a diatomic molecule. The SPF potential also has a long range of convergence, but because its leading term gives a potential with an infinite number of bound states it is not as useful as the PMO potential.

The vibrational term values G_v, the rotational constants B_v, and the centrifugal distortion constants D_v, H_v, *etc.*, are related to the Dunham coefficients Y_{jk} as follows:

$$G_v = \sum_{j=1} Y_{j0}(v + \frac{1}{2})^j, \tag{1.12a}$$

$$B_v = \sum_{j=0} Y_{j1}(v + \frac{1}{2})^j, \tag{1.12b}$$

$$D_v = \sum_{j=0} Y_{j2}(v+\frac{1}{2})^j, \tag{1.12c}$$

$$H_v = \sum_{j=0} Y_{j3}(v+\frac{1}{2})^j, \tag{1.12d}$$

The energy eigenvalues $E_{v,J}$ are related to G_v, B_v, D_v, and H_v by

$$E_{v,J} = Y_{00} + G_v + B_v[J(J+1)] + D_v[J(J+1)]^2 + H_v[J(J+1)]^3 + \cdots. \tag{1.13}$$

1.2 The Born-Oppenheimer Approximation

One of the most fundamental approximations of molecular physics is the Born-Oppenheimer separation of nuclear and electronic motion. For a system of electrons and nuclei interacting through Coulombic interactions, the Hamiltonian [5-8] is

$$H = T_e + T_N + V(r,R). \tag{1.14}$$

where $T_e = -\frac{\hbar^2}{2m}\sum_i \nabla_i^2$, $T_N = -\frac{\hbar^2}{2}\sum_\alpha \frac{1}{M_\alpha}\nabla_\alpha^2$,

and $V(r,R) = V_{ee} + V_{NN} + V_{eN} =$

$$\sum_{i<j}\frac{e^2}{|r_i - r_j|} + \sum_{\alpha<\beta}\frac{z_\alpha z_\beta e^2}{|R_\alpha - R_\beta|} - \sum_{\alpha,i}\frac{z_\alpha e^2}{|R_\alpha - r_i|}.$$

T_e and T_N are electronic and nuclear kinetic energy respectively, and $V(r,R)$ includes electron-electron, nuclear-nuclear, and electron-nuclear interactions. Because T_N is a very small term in this Hamiltonian, we may calculate the eigenvalues and eigenfunctions of Eq. (1.14) by treating T_N as a small perturbation [7].

The Schrödinger equation for the molecule is then

$$[T_e + V(r,R)]\varphi_n(r,R) = E_n(R)\varphi_n(r,R). \tag{1.15}$$

where $E_n(R)$ and $\varphi_n(r,R)$ are energy and wave functions of the electronic state. Since the eigenfunctions of equation (1.15) form a complete set of states [7], we may expand the total molecular wave function in terms of them

$$\psi(r,R) = \sum_n \psi_n(R)\varphi_n(r,R). \tag{1.16}$$

The molecular wave function $\psi(r,R)$ satisfies the Schrödinger equation

$$[T_e + T_N + V(r,R)]\psi(r,R) = E\psi(r,R). \tag{1.17}$$

Substituting $\psi(r,R)$ from Eq. (1.16) into Eq. (1.17) and using Eq. (1.15), we find

$$\sum_m (E_m(R) + T_N)\psi_m(R)\varphi_m(r,R) = E\sum_m \psi_m(R)\varphi_m(r,R). \tag{1.18}$$

Multiplying Eq. (1.18) on the left by $\varphi_n^*(r,R)$, integrating over all electronic positions, and using the orthogonality of φ_m, we have

$$\sum_m \langle\varphi_n(r,R)|T_N|\psi_m(R)\varphi_m(r,R)\rangle + E_n(R)\psi_n(R) = E\psi_n(R), \tag{1.19}$$

which can be written as

$$[T_N + E_n(R) + A_{nn}(R)]\psi_n(R) = E\psi_n(R) - \sum_{m\neq n} A_{nm}\psi_m(R), \tag{1.20}$$

where

$$A_{nm}\psi_m(R) = -\hbar^2 \sum_\alpha \frac{1}{2M_\alpha}\langle\varphi_n(r,R)|2\nabla\psi_m \cdot \nabla\varphi_m + \psi_m\nabla^2\varphi_m\rangle.$$

By neglecting the off-diagonal elements of A (i.e., considering $\sum_{m\neq n} A_{nm}$ $\psi_m(R) = 0$) we get the adiabatic approximation. We then have

$$[T_N + E_n(R) + A_{nn}(R)]\psi_n(R) = E\psi_n(R), \qquad (1.21)$$

where the adiabatic potential energy $V_n^{ad}(R)$ is given by

$$V_n^{ad}(R) = E_n(R) + A_{nn}(R).$$

It can be shown that both the adiabatic and nonadiabatic terms are of the order of magnitude $(\frac{m}{M})$ and may be neglected for heavy molecules. To the lowest order in A, there is no mixing of the different electronic states, that is, in the adiabatic corrections the total molecular wave function can be written as

$$\psi(r,R) = \psi_n(R)\varphi_n(r,R). \qquad (1.22)$$

The nonadiabatic corrections $(-\sum_{m\neq n} A_{nm}\psi_m(R))$ mix different electronic states, so that the total molecular wave function cannot be expressed as a simple product of the electronic and nuclear wave function.

Bunker [22,23] studied the effect of both adiabatic and nonadiabatic corrections on the effective vibration-rotation Hamiltonian for the ground electronic states of diatomic molecules. For considering the non-adiabatic corrections, he wrote the radial Schrödinger equation in the following form

$$\left\{-\frac{\hbar^2}{2\mu_v}\frac{d^2}{dr^2}+\left[W(r)+\Delta W(r)+\frac{\hbar^2 J(J+1)}{2\mu_r r^2}-E_{v,J}\right]\right\}\chi(r)=0, \quad (1.23)$$

where $-\frac{\hbar^2}{2\mu_v}\frac{d^2}{dr^2}$ and $-\frac{\hbar^2 J(J+1)}{2\mu_r r^2}$ are the vibrational and rotational kinetic energy operator respectively, $W(r)$ is the relativistically and adiabatically corrected internuclear potential, and $E_{v,J}$ are vibration-rotation eigenvalues.

As a result of non-adiabatic lag of electrons behind the nuclear motion, it is more reasonable to use μ_v and μ_r [22,23] rather than nuclear reduced mass μ and atomic reduced mass μ_{atomic} where

$$\mu < \mu_v < \mu_{atomic}, \; \mu < \mu_r < \mu_{atomic}.$$

A least-squares optimization of μ_v and μ_r was performed [22,23] by fitting the eigenvalues of Eq. (1.23) to the experimental energies. Satisfactory fits were achieved when $\mu_r = \mu$ and $\mu_v = \mu(1+\Delta)$, where $\Delta = \frac{\alpha}{2\mu}$. For HF the parameter α is about 2.537×10^{-4} , and $\mu = .95705545 a.m.u.$.

1.3. Electric Dipole Moment and Transition Matrix Elements

In our present work, we are also interested in the dipole moment of HF as a function of the internuclear distance. The knowledge of this quantity is necessary for many physical applications (such as transition probability). It may be determined either by empirical or theoretical methods.

In the latter approach, the electronic wave functions at a particular electronic state need to be known. Techniques such as Hartree-Fock (H-F), configuration interaction (CI), and multi-configuration self consistent (MCSCF) are commonly used to form these electronic wave functions with a high degree of accuracy. Typical works on dipole moment of HF are those performed by Sileo and Coal [26], Lee [27], and Meyer [28]. In this approach, one considers the electric dipole moment operator defined as

$$\underline{M}(\vec{r}_i, \vec{R}_\alpha) = -\sum_i e\vec{r}_i + \sum_\alpha e z_\alpha \vec{R}_\alpha, \tag{1.24}$$

where e is the electronic charge, z_α is the atomic number of the α^{th} nucleus, and $\vec{r}_i$ and $\vec{R}_\alpha$ are the center-of- mass coordinates of the i^{th} electron and α^{th} nucleus, respectively.

The dipole moment function is then determined by the expectation value of the projection of the above dipole moment operator on the internuclear axis.

In the empirical method, one needs to obtain the ro-vibrational wave functions satisfying the radial Schrödinger Eq. (1.2) and the experimentally deduced transition matrix elements.

The electronic transition probability between two molecular states $N = (n, v, J)$ and $N' = (n', v', J')$ is proportioned to the square of the matrix element $\mu_{NN'}$:

$$P_{NN'} = |\mu_{N,N'}|^2 = |\int \psi_N^* \underline{M} \psi_{N'} \, dr|^2. \tag{1.25}$$

With the Born Oppenheimer wave function given by Eq. (1.1) the integration over rotational eigenfunctions may be performed independently, producing a factor $S_{J,J'}$, called the Hönl-London factor. The integration over electronic eigenfunctions produces a quantity $\underline{M}^{(el)}_{nn'}(R)$ [5,6]. Hence, Eq. (1.25) can be written as

$$P_{NN'} = S_{J,J'} \left| \int \psi^{*(vib)}_{N} \underline{M}^{(el)}_{nn'} \psi^{(vib)}_{N'} \, dR \right|^2, \qquad (1.26)$$

where

$$S_{J,J'} = J \text{ for the } P \text{ branch,}$$
$$\text{and} \quad S_{J,J'} = J + 1 \text{ for the } R \text{ branch.}$$

If the two vibrational levels employed correspond to different electronic states (i.e., $n \neq n'$), and if we assume that the R dependence of $\underline{M}^{(el)}_{nn'}(R)$ is small [6], then we can write Eq. (1.26) as

$$P_{NN'} = S_{J,J'} |\overline{\underline{M}}^{(el)}_{nn'}|^2 q_{vv'}, \qquad (1.27)$$

where $\overline{\underline{M}}^{(el)}_{nn'}$ is the average value of $\underline{M}^{(el)}_{nn'}$, and $q_{vv'} = |\int \psi^{*(vib)}_{N'} \psi^{(vib)}_{N} \, dR|^2$ is known as the Franck-Condon-Factor (FCF). Theoretically, the FCF is just the overlap between the vibrational wave functions corresponding to two different electronic states.

If the two vibrational levels employed correspond to the same electronic states (i.e., $n = n'$), the R dependence of $\underline{M}^{(el)}_{nn'}(R)$ may not be small enough to be taken out of the integral in Eq. (1.26) [38]. In this case, if the internuclear axis is along the z axis, Eq. (1.26) can be written as

$$P_{NN'} = S_{JJ'} |\langle vJ | \{M(R) | v' J' \rangle|^2, \qquad (1.28)$$

where $M(R) \equiv \underline{M}^{(el)}_{nn}$ is also referred to as the "electric dipole moment function." The square of the ro-vibrational matrix element $\langle vJ | M(R) | v' J' \rangle$

may be related to the square of the rotationless matrix element $\langle v|M(R)|v'\rangle$ in the following manner:

$$|\langle vJ|M(R)|v'J'\rangle|^2 = F_{v,J}^{v',J'}(m)|\langle v|M(R)|v'\rangle|^2, \tag{1.29}$$

where $F_{v,J}^{v',J'}(m)$ is called the Herman-Wallis factor (HWF) representing the rotation-vibration interaction and where $F_{v,J}^{v',J'}(0) = 1$. The behavior of the HWF was studied by Herman, Rothery and Rubin [42] for different internuclear potentials. The results of their calculations were summarized in Ref. [42].

Robert E. Meredith and Frederick G. Smith [36] studied the effects of the internuclear potential functions on the vibrational matrix elements and concluded that the matrix elements involving small v were affected very little by the potential. However, for large v, the influence of the potential is more pronounced.

From vibrational intensity data, one can calculate the squares of matrix elements $\langle v|M(R)|v'\rangle$, from which the parameters of the electric dipole moment function can be determined.

The relationship between various modified Dunham coefficients and the PMO parameters are given in Chapter II. Chapter III presents a technique from which a PMO potential with correct asymptotic behavior can be obtained. In Chapter IV, we determine the dipole moment functions of HF as cubic polynomials in variables u, y, and z, respectively. Chapter IV shows how to construct a dipole moment function of HF with correct asymptotic behavior at both small and large r. Concluding remarks on the

PMO potential and dipole moment function are made in Chapter V.

Appendix A gives formulas for finding coefficients e_n, f_n, and g_n in terms of d_n. In Appendix B, we discuss the convergence of the $M(y)$, $M(u)$, and $M(z)$ series; and different infinite series used in Chapters III and V are discussed in Appendix C. The Numerov method used in Chapters III and V is derived in Appendix D. Appendix E gives the relationship between coefficients of the three expansions of a function of r

CHAPTER II

CALCULATION OF THE MODIFIED DUNHAM COEFFICIENTS $Y_{jk}^{(2l)}$ IN TERMS OF PMO PARAMETERS

2.1. Purely Vibrational Case ($J = 0$)

Following Dunham [12] the WKB energy condition may be written [10] in the dimensionless form

$$\sigma \oint (f-w)^{\frac{1}{2}}\left(\frac{\rho}{w'}\right) dw - \frac{1}{32\sigma} \oint \left(\frac{w'}{\rho}\right)(f-w)^{-\frac{5}{2}}\, dw -$$

$$\frac{1}{2048\sigma^3} \oint \left[49\left(\frac{w'}{\rho}\right)^3 (f-w)^{-\frac{11}{2}} - 16\frac{w'''}{\rho^3}(f-w)^{-\frac{7}{2}}\right] dw + \cdots$$

$$= 2\pi\left(v+\frac{1}{2}\right), \tag{2.1}$$

where $\rho = ar_e,$

$$w = \frac{V(r)}{hc\tau} = \frac{U}{\rho^2} = y^2\left(1+\sum_{n=2} b_n y^n\right),$$

$$f = \frac{E_{v,0}}{hc\tau} = \frac{F}{\rho^2},$$

$$\sigma = (2hc\mu\tau)^{\frac{1}{2}}/a\hbar = \frac{S}{\rho^2}.$$

$\frac{\rho}{w'}$, $\frac{w'}{\rho}$, $(\frac{w'}{\rho})^3$, and $\frac{w'''}{\rho^3}$ have the series expansions [10]

$$\frac{\rho}{w'} = \frac{1}{2}w^{-\frac{1}{2}} \sum_{n=0}^{\infty} d_n w^{\frac{n}{2}}, \tag{2.2a}$$

$$\frac{w'}{\rho} = 2w^{\frac{1}{2}} \sum_{n=0}^{\infty} e_n w^{\frac{n}{2}}, \tag{2.2b}$$

$$(\frac{w'}{\rho})^3 = 8w^{\frac{3}{2}} \sum_{n=0}^{\infty} f_n w^{\frac{n}{2}}, \tag{2.2c}$$

$$\frac{w'''}{\rho^3} = 2w^{-\frac{1}{2}} \sum_{n=0}^{\infty} g_n w^{\frac{n}{2}}. \tag{2.2d}$$

Since the integration path in Eq. (2.1) may be deformed such that $|w| > |f|$ everywhere on the path, we can use the binomial theorem to expand the half-integral powers of $(f - w)$, and then evaluate the integrals. The binomial theorem can be written in the following form

$$(f - w)^{\frac{n}{2}} = i^n w^{\frac{n}{2}}[1 + \frac{n}{2}\frac{f}{w} + \cdots]. \tag{2.3}$$

Substituting Eqs. (2.2) and (2.3) into Eq. (2.1) and using the following integral

$$\int w^p \, dw = 4\pi i \delta_{-1,p},$$

we obtain

$$\begin{aligned}&\frac{4\pi\sigma}{4}[fd_0 + \frac{1}{4}d_2 f^2 + \frac{1}{8}d_4 f^3 + \frac{5}{64}d_6 f^4 + \frac{7}{128}d_8 f^5 + \cdots] \\ &- \frac{4\pi}{16\sigma}[e_2 + \frac{5}{2}fe_4 + \frac{35}{8}f^2 e_6 + \frac{105}{16}f^3 e_8 + \frac{1155}{128}f^4 e_{10} + \cdots] \\ &+ \frac{4\pi}{2048\sigma^3}\{8 \times 49[f_6 + \frac{11}{2}ff_8 + \frac{143}{8}ff_{10} + \cdots] \\ &- 2 \times 16[g_6 + \frac{7}{2}fg_8 + \frac{63}{8}fg_{10} + \cdots]\} = 2\pi(v + \frac{1}{2}).\end{aligned} \tag{2.4}$$

After dividing Eq. (2.4) by $2\pi\sigma$ and collecting terms, we obtain an equation of the form

$$\begin{gathered}
[\frac{1}{2}d_0 - \frac{5}{16\sigma^2}e_4 + \frac{7}{256\sigma^4}(77f_8 - 4g_8) + \cdots]f + \\
\frac{1}{4}[\frac{1}{2}d_2 - \frac{35}{16\sigma^2}e_6 + \frac{7}{256\sigma^4}(1001f_{10} - 36g_{10}) + \cdots]f^2 + \\
\frac{1}{8}[\frac{1}{2}d_4 - \frac{105}{16\sigma^2}e_8 + \cdots]f^3 + \\
\frac{5}{64}[\frac{1}{2}d_6 - \frac{231}{16\sigma^2}e_{10} + \cdots]f^4 + \\
[\frac{7}{256}d_8 + \cdots]f^5 + \\
[\frac{21}{1024}d_{10} + \cdots]f^6 = \frac{(v+\frac{1}{2})}{\sigma} + \frac{1}{8\sigma^2}e_2 - \frac{1}{128\sigma^4}(49f_6 - 4g_6). \qquad (2.5a)
\end{gathered}$$

The above equation can be written in the form

$$y = \sum_{n=1}^{\infty} a_n f^n, \qquad (2.5b)$$

where y and the coefficients a_n may be written in terms of powers of $S = \sigma^{-1}$ as follows:

$$y = (v + \frac{1}{2})S + q_0 S^2 - r_0 S^4 + \cdots \qquad (2.6a)$$

$$a_n = p_n - q_n S^2 + r_n S^4. \qquad (2.6b)$$

The quantities p_n, q_n and r_n are defined in terms of D_n, F_n, E_n, and G_n [10,20] as follows:

$$p_n = D_n d_2(n-1)/2^n, \qquad (2.7a)$$

$$q_n = E_n e_2(n+1)/2^{n+3}, \qquad (2.7b)$$

$$r_n = [49F_n f_2(n+3) - 4G_n g_2(n+3)]/2^{n+7}. \qquad (2.7c)$$

The coefficients D_n, E_n, F_n, and G_n introduced in Eq. (2.7) may be calculated iteratively from initial values $D_1 = 1$, $E_0 = F_0 = G_0 = 1$ [10,20] by

$$D_n = (2n-3)D_{n-1}/n, \tag{2.8a}$$

$$E_n = (2n+3)E_{n-1}/n, \tag{2.8b}$$

$$F_n = (2n+9)F_{n-1}/n, \tag{2.8c}$$

$$G_n = (2n+5)G_{n-1}/n. \tag{2.8d}$$

The coefficients e_n, f_n, and g_n introduced in Eq. (2.2) can be calculated from the coefficients d_n by the following relations (Appendix A)

$$e_0 = d_0^{-1}, \; e_n = -d_0^{-1} \sum_{j=0}^{n-1} d_j \, d_{n-j} \quad \text{for } n \geq 1, \tag{2.9a}$$

$$f_n = \sum_{j=0}^{n} \sum_{k=0}^{n-j} e_j e_k e_{n-j-k}, \tag{2.9b}$$

$$g_n = \sum_{j=0}^{n} \sum_{k=0}^{n-j} (j+1)(j+k) e_j e_k e_{n-j-k}. \tag{2.9c}$$

The coefficients d_n, which depend on the particular potential function parameters, may be obtained by the following method [10,20]. We start with Sandeman's parameterization [40]

$$\xi = \sum_{n=0} C_n \left(\frac{U}{a_0}\right)^{(n+1)/2}. \tag{2.10}$$

Differentiating with respect to ξ, we obtain

$$1 = [\sum_{n=0} \frac{(n+1)}{2} C_n (\frac{U}{a_0})^{(n-1)/2}] \frac{U'}{a_0}, \tag{2.11a}$$

$$\frac{1}{U'} = \frac{1}{2\sqrt{a_0 U}} \sum_{n=0} (n+1) C_n (\frac{U}{a_0})^{\frac{n}{2}}, \tag{2.11b}$$

where

$$a_0 = \tau\rho^2 \tag{2.12a}$$

$$U = \tau w = \tau(y^2 + \sum_{n=4} b_n y^n). \tag{2.12b}$$

Multiplying Eq. (2.11b) by $\tau\rho$ and using Eq. (2.12), we obtain

$$\frac{\rho}{w'} = \frac{1}{2\sqrt{w}} \sum_{n=0} \frac{(n+1)}{\rho^n} C_n w^{\frac{n}{2}}, \tag{2.13}$$

which is equivalent to Eq. (2.2a) when we make the identification

$$d_n = \frac{(n+1)C_n}{\rho^n}. \tag{2.14}$$

In order to relate the PMO parameters to the Sandeman parameters, we need to express ξ in terms of y by

$$\xi = \frac{aq}{\rho} = -\ln(1-y)/\rho. \tag{2.15}$$

Following Lagrange series method [11] we can express the series coefficients C_n and then d_n in terms of the PMO parameters:

$$x = y, \tag{2.16a}$$

$$X = w^{\frac{1}{2}} = y(1 + \sum_{n=4} b_n y^n)^{\frac{1}{2}},$$

$$x = X(1+\sum_{n=4} b_n y^n)^{-\frac{1}{2}}, \tag{2.16b}$$

$$f(x) = (1+\sum_{n=4} b_n y^n)^{-\frac{1}{2}}, \tag{2.16c}$$

$$g(y) = \rho\xi = \rho U^{\frac{1}{2}}(1+\sum_{n} C_n U^{\frac{n}{2}}) = -\ln(1-y), \tag{2.16d}$$

$$g' = \rho\frac{d\xi}{dy} = \frac{1}{1-y} = \sum_{n=0} y^n, \tag{2.16e}$$

from which we obtain

$$d_n = (n+1)p_{n+1},$$

$$= 1+\sum_{l=0}^{n}\sum_{m=1}^{n}\binom{-\frac{1}{2}(n+1)}{m}\Omega_{lm}(b), \tag{2.17}$$

where $\binom{-\frac{1}{2}(n+1)}{m}$ is a binomial coefficient defined inductively by

$$\binom{p}{1} = p,\ \binom{p}{m} = [(p+1-m)/m]\binom{p}{m-1}, \tag{2.18a}$$

and where $\Omega_{n1}(b) = b_n,$ (2.18b)

$$\Omega_{nm}(b) = \sum_{l=0}^{n} b_l\Omega_{n-l,m-1}(b). \tag{2.18c}$$

It is easy to show that for a Morse oscillator all coefficients d_n are equal to 1 [10].

2.2. Inclusion of Rotational Effects ($J\neq 0$)

If the molecule has nonzero rotational kinetic energy, $E_R = h^2 J(J+1)/2\mu r^2$, this term must be added to $U(r)$ to find the effective vibrational potential. The potential energy function is now

$$U(r) = [y^2 + \sum_{n=4} b_n y^n] + \frac{\hbar^2 J(J+1)}{2\mu r^2}. \tag{2.19}$$

Huffaker showed [14,20] that E_R can be expanded as the Taylor series

$$E_R = \kappa \sum_{m=0} \varphi_n(\rho) y^n, \tag{2.20}$$

where $\kappa = \frac{J(J+1)}{\sigma^2 \rho^2}$ and the polynomial $\varphi_n(\rho)$ can be written in the form

$$\varphi_n(\rho) = \rho^{-n} \sum_{m=0}^{n-1} (-1)^{n+m} C_{nm} \rho^m, \tag{2.21}$$

and where the numerical coefficients C_{nm} may be defined inductively by

$$C_{1m} = 2\delta_{m,0}, \tag{2.22a}$$

$$C_{nm} = [(n-1)C_{n-1,m-1+(n-m+1)}C_{n-1,m}]/n. \tag{2.22b}$$

Thus we can write the dimensionless effective potential $U(y)$ in the form

$$U(y) = y^2 + \sum_{n=4} b_n y^n + \kappa \sum_{n=0} \varphi_n y^n = \sum_{n=0} A_n y^n, \tag{2.23}$$

with $A_0 = \kappa$, $A_1 = \kappa\varphi_1$, $A_2 = 1 + \kappa\varphi_2$, $A_3 = \kappa\varphi_3$, and $A_n = b_n + \kappa\varphi_n$, $n \geq 4$.

We consider a change of variable to $z = 1 - e^{-a(r-r_e)+\Delta(\kappa)}$, where $\Delta(\kappa)$ is to be chosen so that the resulting series in z will have the form

$$U(z) = c(\kappa) + \sum_{n=2} b_n(\kappa) z^n. \tag{2.24}$$

$$y = 1 - e^{-a(r-r_e)} = 1 - e^{-\Delta(\kappa)+\Delta(\kappa)-a(r-r_e)} = (z - 1 + e^{\Delta(\kappa)})e^{-\Delta(\kappa)},$$

and defining

$$e^{\Delta(k)} - 1 = \delta(\kappa),\ y = e^{-\Delta}(z + \delta), \tag{2.25}$$

we then try to obtain explicit expressions for $\delta(\kappa)$, $c(\kappa)$, and $b_n(\kappa)$ as power series in k, defined by

$$\delta(\kappa) = \sum_{m=1} \delta_m \kappa^m, \tag{2.26a}$$

$$c(\kappa) = \sum_{m=1} c_m \kappa^m, \tag{2.26b}$$

$$b_n(\kappa) = \sum_{m=0} b_n^{(m)} \kappa^m, \quad n \geq 2, \tag{2.26c}$$

where powers up through κ^3 have been included. By substituting y from Eq. (2.25) into Eq. (2.23), gathering the coefficients of various powers of z and comparing with Eq. (2.24), Huffaker was able to find the coefficients of the $\delta(k)$, $c(k)$, and $b_n(k)$ series [21]:

$$\delta_1 = -\frac{1}{2}\varphi_1 = \frac{1}{\rho}, \tag{2.27a}$$

$$\delta_2 = \frac{1}{4}\varphi_1(\varphi_1 + 2\varphi_2) = (2\rho - 3)/\rho^3, \tag{2.27b}$$

$$\begin{aligned} \delta_3 &= -\frac{1}{8}\varphi_1[\varphi_1(\varphi_1 + 2\varphi_2 + 3\varphi_3) + 2\varphi_2(\varphi_1 + 2\varphi_2)] + \frac{1}{4}b_4\varphi_1^3, \\ &= \frac{1}{2}(10\rho^2 - 33\rho + 30 - 4b_4\rho^2)/\rho^5, \end{aligned} \tag{2.27c}$$

$$b_1^{(0)} = 0,\ b_2^{(0)} = 1,\ b_3^{(0)} = 0,\ b_n^{(0)} = b_n, \text{ for } n \geq 4, \tag{2.28a}$$

$$b_n^{(1)} = \varphi_n - \frac{1}{2}\varphi_1[(n+1)b_{n+1} - nb_n], \tag{2.28b}$$

$$\begin{aligned} b_n^{(2)} = &-\frac{1}{2}\varphi_1[(n+1)\varphi_{n+1} - n\varphi_n] + (n+2)(n+1)\varphi_1^2 b_{n+2}/8 \\ &+ (n+1)\varphi_1(2\varphi_2 - n\varphi_1)b_{n+1}/4 \\ &- n\varphi_1[4\varphi_2 - (n-1)\varphi_1]b_n/8, \end{aligned} \tag{2.28c}$$

$$\begin{aligned} b_n^{(3)} = {} & (n+2)(n+1)\varphi_1^2\varphi_{n+2}/8 + (n+1)\varphi_1(2\varphi_2 - n\varphi_1)\varphi_{n+1}/4 \\ & - n\varphi[4\varphi_2 - (n-1)\varphi_1]\varphi_n/8 - (n+3)(n+2)(n+1)\varphi_1^3 b_{n+3}/48 \\ & - (n+2)(n+1)\varphi_1^2(4\varphi_2 - n\varphi_1)b_{n+2}/16 - (n+1)\varphi_1\{\varphi_1[6\varphi_3 \\ & - 8n\varphi_2 + n(n-1)\varphi_1] + 8\varphi_2^2 - 2\varphi_1^2 b_4\}b_{n+1}/16 + n\varphi_1\{\varphi_1 \\ & [18\varphi_3 - 12(n-1)\varphi_2 + (n-1)(n-2)\varphi_1] \\ & + 24\varphi_2^2 - 12\varphi_1^2 b_4\}b_n/48 \end{aligned} \tag{2.28d}$$

$$c_1 = 1, \tag{2.29a}$$

$$c_2 = [\varphi_1\delta_1 + \delta_1^2], \tag{2.29b}$$

$$c_3 = [\varphi_2\delta_1^2 + \varphi_1(\delta_2 - \delta_1^2) + (2\delta_1\delta_2 - 2\delta_1^3)]. \tag{2.29c}$$

Coefficients d_n have been found for the case of $J = 0$ in Eq. (2.17). We now modify the coefficients d_n so that they depend on the rotational states. For this purpose, we express the quantities d_n of Eq. (2.17) in the form [10]

$$d_n = d_n^{(0)} + {}_n^{(1)} + \kappa^2 d_n^{(2)} + \kappa^3 d_n^{(3)} + \cdots, \tag{2.30}$$

where $d_n^{(0)}$ contains non-rotational contribution and $d_n^{(1)}$, $d_n^{(2)}$, ... contain rotational contribution. Eqs. (2.17) and (2.18) should also be modified to

$$d_n^{(k)} = \sum_{m=1}^{n} \left[{-\tfrac{1}{2}(n+1) \atop m} \right] \sum_{l=0}^{n} \Omega_{lm}^{(k)}(b) + \delta_{k,0} \tag{2.31a}$$

$$\Omega_{nl}^{(k)}(b) = b_n^{(k)}, \tag{2.31b}$$

$$\Omega_{nm}^{(k)}(b) = \sum_{j=0}^{k} \sum_{l=0}^{n} b_l^{(j)} \Omega_{n-l,m-1}^{(k-j)}(b). \tag{2.31c}$$

2.3. Formulas for Modified Dunham Coefficients $Y_{jk}^{(2l)}$

We now perform a reversion of series of Eq. (2.5b) to obtain an expression for f as a power series in y (a general formula for reversion of series is given in reference [11]):

$$y = \sum_{n=1}^{\infty} a_{n-1} x^n, \tag{2.32a}$$

$$x = \sum_{n=1}^{\infty} A_{n-1} y^n. \tag{2.32b}$$

Coefficients A_{n-1} are given by

$$A_0 = a_0^{-1},\; A_n = -a_0^{-(2n+1)} \sum_{m=1}^{n} b(n,m) a_0^{n-m} \Omega_{nm}(a), \tag{2.32c}$$

where $a(n,m)$ are defined inductively by

$$b(n,1) = 1,\; b(n,m) = -(n+m)b(n,m-1)/m. \tag{2.32d}$$

Performing the reversion of series using Eq. (2.32), one obtains

$$f = \sum_{n=1}^{\infty} A_n y^n, \tag{2.33}$$

where

$$\begin{aligned} y &= (v + \frac{1}{2})S + q_0 S^2 - r_0 S^4 + \cdots, \\ A_n &= n - q_n S^2 + r_n S^4 + \cdots, \\ f &= \frac{E_{v,J}}{hc\tau} - c(k), \end{aligned}$$

and p_n, q_n, and r_n are defined as in Eq. (2.7). We then express the reversion of series in the form

$$f = \sum_{n=1}^{\infty} B_n (1 - qS^2 + rS^4 + \cdots)^{-(2n-1)} y^n, \tag{2.34}$$

where

$$p = p_1,\ q = q_1/p,\ r = r_1/p,$$

$$B_n = B_n^{(0)} + B_n^{(2)} S^2 + B_n^{(4)} S^4 + \cdots.$$

The coefficients B_n can then be calculated from a_n by comparing Eq. (2.34) and Eq. (2.33). Using Eq. (2.32) we can write

$$A_1 = \frac{1}{a_1} = \frac{1}{p_1 - q_1 S^2 + r_1 S^4} = \frac{1}{p}(1 - qS^2 + rS^4)^{-1},$$

where $B_1^{(0)} = \frac{1}{p}$, $B_1^{(2)} = 0$ and $B_1^{(4)} = 0$,

$$A_2 = -\frac{a_2}{a_1^3} = -\frac{(p_2 - q_2 S^2 + r_2 S^4)}{(p_1 - q_1 S^2 + r_1 S^4)^3},$$

$$= (-\frac{p_2}{p^3} + \frac{q_2}{p^3} S^2 - \frac{r_2}{p^3} S^4)(1 - qS^2 + rS^4)^{-3},$$

where $B_2^{(0)} = -\frac{p_2}{p^3}$, $B_2^{(2)} = \frac{q_2}{p^3}$ *and* $B_2^{(4)} = -\frac{r_2}{p^3}$,

$$A_3 = \frac{2a_2^2 - a_1 a_3}{a_1^5},$$

$$= \frac{2(p_2 - q_2 S^2 + r_2 S^4)^2 - (p_1 - q_1 S^2 + r_1 S^4)(p_3 - q_3 S^2 + r_3 S^4)}{(p_1 - q_1 s^2 + r_1 s^4)^5}$$

$$= \frac{1}{p_5}[2(p_2 - q_2 S^2 + r_s S^4)^2 - (p - qS^2 + rS^4)(p_3 - q_3 S^2 + r_3 S^4)] \\ (1 - qS^2 + rS^4)^{-5},$$

$$= [\frac{2p_2^2 - pp_3}{p^5} + \frac{(-p_2 q_2 + qp_3 + pq_3)S^2}{p^5} + \frac{(2q_2^2 - qq_3)S^4}{p^5}] \\ (1 - qS^2 + rS^4)^{-5},$$

where $B_3^{(0)} = \frac{2p_2^2 - pp_3}{p^5}$, $B_3^{(2)} = -\frac{4p_2 q_2 + qp_3 + pq_3}{p^5}$,

$$and\ B_3^{(4)} = \frac{(2q_2^2 - qq_3)}{p^5},$$

and so on.

General formulas were given in Ref. [20] for $B_n^{(0)}$, $B_n^{(2)}$, and $B_n^{(4)}$. In particular,

$$B_1^{(0)} = p_1^{-1},\ B_n^{(0)} = -p_1^{-(2n-1)} \sum_{m=1}^{n-1} a(n-1,m) p_1^{n-m-1} \Omega_{n-1,m}(p_{l+1}),$$

where $a(n,m)$ and Ω_{nm} are defined in Eqs. (2.31) and (2.32). The quantities $B_n^{(2)}$ and $B_n^{(4)}$ have a similar structure and can be derived by some change in $B_n^{(0)}$ [20].

Expanding Eq. (2.33), solving for $E_{v,J}$, using Eq. (1.3), and equating the coefficients of different powers of $v+\frac{1}{2}$and$J(J+1)$, we find that the Dunham coefficients which may be expressed in the form [10]

$$Y_{jk} = Y_{jk}^{(0)} + Y_{jk}^{(2)} + Y_{jk}^{(4)} + \cdots, \qquad (2.35a)$$

where the quantities Yjk(2l),which are called modified Dunham coefficients, are given by

$$Y_{jk}^{(2l)} = \frac{\tau}{\sigma^{j+2k+2l}\rho^{2k}} K_k[z_j^{(2l)}], \qquad (2.35b)$$

where the operator K_k is defined by

$$p_k = K_k(p_0 + kp_1 + \kappa^2 p_2 + \cdots \kappa^k p_k + \cdots),$$

and where $z_n^{(0)}$, $z_n^{(2)}$, and $z_n^{(4)}$ are defined [10,20] as follows:

$$z_j^{(0)} = B_j^{(0)} \text{ for } j \geq 1,$$

$$
\begin{aligned}
z_j^{(2)} &= (j+1)q_0 B_{j+1}^{(0)} + (2j-1)qB_j^{(0)} + B_j^{(2)} \text{ for } j \geq 1, \\
z_j^{(4)} &= \frac{1}{2}(n+1)(n+2)q_0^2 B_{n-2}^{(0)} + (n+1)[(2n+1)q_0 q - r_0]B_{n+1}^{(0)} \\
&+ (2n-1)(nq^2 - r)B_n^{(0)} + (n+1)q_0 B_{n+1}^{(2)} \\
&+ (2n-1)qB_n^{(2)} + B_n^{(4)}.
\end{aligned}
$$

Bunker [22,23] concluded that the nonadiabatic corrections due to the breakdown of Born-Oppenheimer approximation could be taken into account by introducing vibrational and rotational reduced mass μ_v and μ_r, where $\mu_v = \frac{\mu}{1-\Delta}$ and $\mu_r = \mu$. Rewriting Eq. (2.35a) in the following form using Eq. (2.35b)

$$
Y_{jk} = \frac{\tau}{\sigma^{j+2k}\rho^{2k}} K_k [z_j^{(0)} + \frac{1}{\sigma^2} z_j^{(2)} + \frac{1}{\sigma^4} z_j^{(4)} + \cdots \frac{1}{\sigma^{2l}} z_j^{(2l)} + \cdots]. \quad (2.36)
$$

Using $\kappa = \frac{J(J+1)}{\rho^2}(\frac{1}{\sigma^2})$, we see that k in Eq. (2.36) can be interpreted as rotational quantum number. From Eq. (1.2) it is easy to see that j and l are vibrational quantum numbers. With the above piece of information and the relationship between σ and μ, one can split σ in Eq. (2.35) into σ_v and σ_r as follows:

$$
\sigma^{(j+2k+2l)} = \sigma_v^{(j+2l)} \sigma_r^{(2k)} = (\frac{\sigma}{1-.5\Delta})^{(j+2l)} \sigma^{(2k)},
$$

$$
\text{and } Y_{jk}^{(2l)} = \frac{\tau(1-.5\Delta)^{(j+2l)}}{\sigma^{j+2k+2l}\rho^{2k}} K_k [z_j^{(2l)}]. \quad (2.37)
$$

By comparing Eq. (2.35) and Eq. (2.37) we see that the nonadiabatic corrections have been taken into account by introducing a factor $(1 - .5\Delta)^{j+2l}$ in Eq. (2.35). The parameter Δ then is considered as a free parameter which may be varied in the process of reproducing experimental data. A computer program was written by Huffaker [46] for evaluating modified Dunham coefficients in terms of PMO parameters.

CHAPTER III

ANALYTICAL PMO POTENTIAL FUNCTIONS WITH CORRECT ASYMPTOTIC BEHAVIOR

3.1. Introduction

The main objective of this chapter is to find a PMO potential function satisfying the following asymptotic property

$$V(r=\infty)=\tau\left(1+\sum_{n=1}^{\infty} b_n\right)=D_e, \tag{3.1}$$

where D_e is the dissociation energy of the diatomic molecule.

Because of the finite number of spectroscopic data G_v, B_v, and D_v, only a finite number of independent PMO parameters b_n can be determined. We note that the convergence of the series in Eq. (3.1) requires that

$$b_n \rightarrow 0 \quad \text{as} \quad n \rightarrow \infty, \tag{3.2}$$

i.e., the higher-order PMO coefficients b_n become increasingly small as n increases. Therefore, it is possible to approximate higher-order PMO coefficients so that their effect may be included in the determination of the PMO potential function by expressing them as some suitable function decreasing with n and satisfying Eq. (3.2). In this case, the PMO potential function can be written as

$$V(r) = \tau(y^2 + \sum_{n=4}^{N} b_n y^n + \sum_{n=N+1}^{\infty} b_n^* y^n), \tag{3.3}$$

where b_n^* are generated higher-order PMO coefficients, and N should be less than the number of available spectroscopic data.

We express the functional form for b_n^* in terms of n and a set of parameters designated as c_1, c_2, ..., c_M, and B:

$$b_n^* = F(c_1, c_2, \ldots, c_M, B). \tag{3.4}$$

The modified PMO potential function (3.3) is also subject to the asymptotic condition (3.1), which now can be written as

$$\tau(1 + \sum_{n=4}^{N} b_n + \sum_{n=N+1}^{\infty} b_n^*) = D_e, \tag{3.5}$$

and which may be satisfied by adjusting one parameter (the one denoted by B) . The PMO parameters (including Δ and asymptotic parameters c_1, c_2, ..., c_M) are determined numerically by a minimization routine [43] using experimental data.

3.2. Functional Forms for Asymptotic b_n^*

Theoretically, it is possible to introduce an infinite number of different functions of the parameters c_1, ..., c_M ,and B, which satisfy the asymptotic condition (3.5) and also fit spectroscopic constants G_v, B_v, and D_v. However, we are interested in those functions that are well-behaved and contain a reasonable number of parameters, so that our problem can be easily treated numerically or analytically.

A suitable set of functional forms was introduced by Tran and Huffaker[37,38] for use in connection with dipole functions,we applied them to potential functions

$$b_n^{*1} = (c_1 + c_2/n + c_3 n)B^n, \tag{3.6a}$$

$$b_n^{*2} = (c_1 + c_2/n + c_3/n(n+1))B^n, \tag{3.6b}$$

$$b_n^{*3} = \begin{cases} (c_1 + c_2/n + c_3/n(n-1))B^n & n > 1, \\ (c_1 + c_2)B & n = 1, \end{cases} \tag{3.6c}$$

$$b_n^{*4} = (c_1 + c_2/n + c_3 n + c_4/n(n+1))B^n, \tag{3.6d}$$

$$b_n^{*5} = \begin{cases} (c_1 + c_2/n + c_3/n(n-1) + c_4/n(n+1))B^n & n > 1, \\ (c_1 + c_2 + 0.5c_4)B & n = 1. \end{cases} \tag{3.6e}$$

We must require the parameter B to have values only between 0 and 1, and this is equivalent to expressing $B = e^{-\beta}$ where $0 < \beta < \infty$.

Using the ratio test, it is easy to verify that all five functions above produce convergent series:

$$\lim_{n\to\infty} \frac{b_{n+1}^*}{b_n^*} = \lim\left[\frac{(n+1)^k B^{n+1}}{n^k B^n}\right] = \lim_{n\to\infty} [(1+\frac{1}{n})^k B] < 1, \tag{3.7}$$

which is a sufficient condition for the convergence of the b_n^* series.

In addition, these functional forms for b_n^* given in Eq. (3.6) produce PMO potentials in closed forms. Using the following relations derived by Tran and Huffaker[37,38](derivations included in Appendix C):

$$\sum_{n=1}^{\infty}(By)^n = \frac{By}{1-By}, \tag{3.8a}$$

$$\sum_{n=1}^{\infty}\frac{(By)^n}{n} = -\ln(1-By), \tag{3.8b}$$

$$\sum_{n=1}^{\infty}n(By)^n = \frac{By}{(1-By)^2}, \tag{3.8c}$$

$$\sum_{n=1}^{\infty}\frac{(By)^n}{n(n+1)} = (\frac{1-By}{By})\ln(1-By)+1, \tag{3.8d}$$

$$\sum_{n=2}^{\infty}\frac{(By)^n}{n(n-1)} = (1-By)\ln(1-By)+By, \tag{3.8e}$$

we can write the PMO potential (3.3) in a relatively simple form:

$$V^1_{PMO}(y) = \tau[\sum_{n=1}^{N}\gamma_n y^n + \frac{c_1 By}{1-By} - c_2\ln(1-By) + \frac{c_3 By}{(1-By)^2}], \tag{3.9a}$$

$$\begin{aligned} V^2_{PMO}(y) = \tau[&\sum_{n=1}^{N}\gamma_n y^n + \frac{c_1 By}{1-By} - c_2\ln(1-By) + \\ &c_3\big(1+\frac{1-By}{By}\ln(1-By)\big)], \end{aligned} \tag{3.9b}$$

$$\begin{aligned} V^3_{PMO}(y) = \tau[&\sum_{n=1}^{N}\gamma_n y^n + \frac{c_1 By}{1-By} - c_2\ln(1-By) + \\ &c_3\big(By+(1-By)\ln(1-By)\big)], \end{aligned} \tag{3.9c}$$

$$\begin{aligned} V^4_{PMO}(y) = \tau[&\sum_{n=1}^{N}\gamma_n y^n + \frac{c_1 By}{1-By} - c_2\ln(1-By) + \\ &c_3\big(1+\frac{1-By}{By}\ln(1-By)\big) + \frac{c_4 By}{(1-By)^2}], \end{aligned} \tag{3.9d}$$

$$V_{PMO}^{5}(y) = \tau[\sum_{n=1}^{N} \gamma_n y^n + \frac{c_1 By}{1-By} - c_2 \ln(1-By) +$$
$$c_3(By + (1-By)\ln(1-By)) + c_4(1 + \frac{1-By}{By}\ln(1-By))],$$

where

$$\gamma_1 = -b_1^*,\ \gamma_2 = 1 - b_2^*,\ \gamma_3 = -b_3^*,$$

and

$$\gamma_n = b_n - b_n^* \text{ for } n \geq 4.$$

The asymptotic condition (3.5) can also be written in a compact form using the same procedure (or by putting $y = 1$ and $V_{PMO}^{\alpha}(y) = D_e$ in Eq. (3.9)):

$$D_e^1 = \tau[\sum_{n=1}^{N} \gamma_n + \frac{c_1 B}{1-B} - c_2 \ln(1-B) + \frac{c_3 B}{(1-B)^2}], \qquad (3.10a)$$

$$D_e^2 = \tau[\sum_{n=1}^{N} \gamma_n + \frac{c_1 B}{1-B} - c_2 \ln(1-B)$$
$$+ c_3\left|1 + \frac{(1-B)}{B}\right|\ln(1-B)], \qquad (3.10b)$$

$$D_e^3 = \tau[\sum_{n=1}^{N} \gamma_n + \frac{c_1 B}{1-B} - c_2 \ln(1-B)$$
$$+ c_3(B + (1-B)\ln(1-B))], \qquad (3.10c)$$

$$D_e^4 = \tau[\sum_{n=1}^{N} \gamma_n + \frac{c_1 B}{1-B} - c_2 \ln(1-B),$$
$$+ c_3(1 + \frac{(1-B)}{B})\ln(1-B)) + \frac{c_4 B}{(1-B)^2}], \qquad (3.10d)$$

$$D_e^5 = \tau[\sum_{n=1}^{N} \gamma_n + \frac{c_1 B}{1-B} - c_2 \ln(1-B) +$$

$$c_3(B+(1-B)\ln(1-B))+c_4(1+\frac{(1-B)}{B}\ln(1-B))]. \quad (3.10e)$$

3.3. Procedure for Determination of PMO Potential Function

Since G_v, B_v, and D_v are functions of Dunham coefficients which in turn are functions of PMO parameters ρ, σ, τ, Δ, $b_4, \ldots b_{12}$, $c_1, \ldots c_M$, and B, they are also functions of these parameters:

$$\begin{aligned} G_v^{cal} &= \sum_{j=1} Y_{j0}(v+\frac{1}{2})^j - G_0^{cal}, \\ &= F_1(\rho,\sigma,\tau,\Delta,b_4,\ldots,b_{12},c_1,\ldots,c_M,B) - G_0^{cal}, \end{aligned} \quad (3.11a)$$

$$B_v^{cal} = \sum_{j=0} Y_{j1}(v+\frac{1}{2})^j = F_2(\rho,\sigma,\tau,\Delta,b_4,\ldots,b_{12},c_1,\ldots,c_M,B), (3.11b)$$

$$D_v^{cal} = \sum_{j=0} Y_{j2}(v+\frac{1}{2})^j = F_3(\rho,\sigma,\tau,\Delta,b_4,\ldots,b_{12},c_1,\ldots,c_M,B), (3.11c)$$

where G_0^{cal} is the calculated term value at the $v = 0$ level. We consider B as a dependent parameter and determine the other ones by fitting the above expressions directly to the experimental spectroscopic constants, G_v^{ex}, B_v^{ex}, and D_v^{ex}. After each minimization the dissociation energy of the molecule is reconstructed and the asymptotic condition (3.5) is checked. If it is not satisfied, a new value of B is given and the minimization procedure is repeated until the desired accuracy is achieved. In our program, new values of B were approximated using Newton's method [25].

The accuracy of the resulting PMO function for the considered diatomic molecule is determined by the agreement between the eigenvalues and spectroscopic constants it predicts and those experimentally deduced [30,31]. We calculated the spectroscopic constants by a computer program developed by Cashion and Cooley [30,31] for solving the radial Schrödinger equation using the Numerov method [30,35]. A short description of this numerical technique is presented in Appendix D.

The rotational constant B_v is defined as: $B_v = \frac{h}{8\pi^2 c\mu} \langle \psi_v | r^{-2} | \psi_v \rangle$, where ψ_v is vibrational wave function, B_v is in cm^{-1} units. From Eq. (1.8), one can easily see the correlation between B_v and the shape of the diatomic molecule potential function. If calculated values of B_v are greater or smaller than observed values, we could infer that the corresponding potential function has tilted toward the left or the right with respect to the true potential curve. The rotational constant D_v is a measure of the width [5] of the potential curve and is related to B_v by $D_v \simeq \frac{4B_v}{w_e^2}$. Of course, as shown by their definitions, B_v and D_v can be evaluated by integration using vibrational eigenfunctions. An alternative way employed by us is to differentiate the Dunham expression for vibrational-rotational eigenenergies with respect to $J(J+1)$, which is considered as a continuous variable.

From the relation

$$\begin{aligned} E(v,J) &= \sum_{j,k} Y_{jk}(v+\frac{1}{2})^j [J(J+1)]^k, \\ &= Y_{00} + G_v + B_v[J(J+1)] + D_v[J(J+1)]^2 + \cdots, \end{aligned}$$

we see that

$$\begin{aligned} B_v &= \left[\frac{\partial E(v,J)}{\partial[J(J+1)]}\right]_{J=0} = \frac{\partial E(v,\alpha)}{\partial\alpha}\Big|_{\alpha=0}, \\ D_v &= \left[\frac{\partial^2 E(v,J)}{\partial[J(J+1)]^2}\right]_{J=0} = \frac{\partial^2 E(v,\alpha)}{\partial\alpha^2}\Big|_{\alpha=0}, \end{aligned}$$

where $\alpha = J(J+1)$. For numerical computation of B_v and D_v, we used the first and second central differences to approximate $\frac{\partial E(v,\alpha)}{\partial\alpha}$ and $\frac{\partial^2 E(v,\alpha)}{\partial\alpha^2}$ as

$$\frac{\partial E(v,\alpha)}{\partial\alpha} = \frac{E(v,\alpha-2\Delta\alpha)-8E(v,\alpha-\Delta\alpha)}{12\Delta\alpha} + \frac{8E(v,\alpha+\Delta\alpha)-E(v,\alpha+2\Delta\alpha)}{12\Delta\alpha}, \tag{3.12a}$$

$$\frac{\partial^2 E(v,\alpha)}{\partial\alpha^2} = \frac{E(v,\alpha-2\Delta\alpha)+16E(v,\alpha-\Delta\alpha)-30E(v,\alpha)}{12(\Delta\alpha)^2} \frac{+16E(v,\alpha+\Delta\alpha)-E(v,\alpha+2\Delta\alpha)}{12(\Delta\alpha)^2}, \tag{3.12b}$$

where $\Delta\alpha$ is a small increment in $J(J+1)$. Theoretically, computed values of B_v^{cal} and D_v^{cal} are more accurate if $\Delta\alpha$ is smaller. However, using a computer, one cannot guarantee a continuous improvement in accuracy by decreasing $\Delta\alpha$ indefinitely. As $\Delta\alpha$ decreases, the buildup of round-off error will eventually offset the error reduction which arises from using the 2nd-order differences in approximating the first and second derivatives. Therefore, the accuracy would approach a highest degree as $\Delta\alpha$ decreases toward an optimum value, which we found to be about 1×10^{-3}. For each vibrational level v, eigenenergies $E(v,\alpha+n\Delta\alpha)$ where $n = -2, -1, 1$, and 2 were computed for $\Delta\alpha = 1 \times 10^{-3}$ using the Cashion-Cooley program in which the effective potential energy included the rotational term $\frac{\hbar^2 J(J+1)}{2\mu r^2}$. The results were substituted in Eq. (3.12) to yield B_v and D_v.

Bunker [22,23] showed that the non-adiabatic corrections could be achieved if the vibrational reduced mass μ_v of the vibrational kinetic energy in the effective vibration-rotation Hamiltonian,

$$\{-\frac{\hbar^2}{2\mu_v}\frac{d^2}{dr^2}+[W(r)+\frac{\hbar^2 J(J+1)}{2\mu_r r^2}-E_{(}v,J)]\}\chi(r)=0,$$

(where $W(r)$ is the adiabatically corrected internuclear potential function) is replaced by

$$\mu_v = \mu(1+2\Delta),$$

$$\text{where for } HF \;\; \Delta = 1.325\times 10^{-4},$$

and Δ is the Born-Oppenheimer vibrational parameter. This would imply an increase in the vibrational reduced mass ,which in turn leads to an energy decrease as a result of the non-adiabatic correction.

3.4. Zero-Order Approximation of $c_1, c_2, \ldots, c_M$, and B

Since approximate initial values of parameters $c_1, \ldots, c_M$, and B are needed as input to the minimization routine, we develop a method of finding good starting values for these parameters, which essentially is the zero-order approximation. From Eq. (3.9), we have

$$w_1(y_1) = q_{11}(y_1)c_1 + q_{12}(y_1)c_2 + q_{13}(y_1)c_3 + q_{14}(y_1)c_4,$$

$$w_2(y_2) = q_{21}(y_2)c_1 + q_{22}(y_2)c_2 + q_{23}(y_2)c_3 + q_{24}(y_2)c_4,$$

$$w_3(y_3) = q_{31}(y_3)c_1 + q_{32}(y_3)c_2 + q_{33}(y_3)c_3 + q_{34}(y_3)c_4,$$

$$w_4(y_4) = q_{41}(y_4)c_1 + q_{42}(y_4)c_2 + q_{43}(y_4)c_3 + q_{44}(y_4)c_4,$$

where

$$w_i(y_i) = \frac{V(y_i)}{\tau} - y_i^2 - \sum_{n=4}^{N} b_n y_i^n,$$

$$q_{ij}(y_i) = \varphi_j(y_i) - s_j(y_i),$$

$$\varphi_1(y_i) = \frac{By_i}{1-By_i}, \ \varphi_2(y_i) = -\ln(1-By_i), \ \varphi_3(y_i) = \frac{By_i}{(1-By_i)^2},$$

$$\varphi_4(y_i) = \left(\frac{1-By_i}{By_i}\right)\ln(1-By_i) + 1,$$

$$s_1(y_i) = \sum_{n=1}^{N} (By_i)^n, \ s_2(y_i) = \sum_{n=1}^{N} \frac{(By_i)^n}{n}, \ s_3(y_i) = \sum_{n=2}^{N} n(By_i)^n,$$

$$s_4(y_i) = \sum_{n=1}^{N} \frac{(By_i)^n}{n(n+1)}.$$

The coefficients c_1, c_2, c_3 and c_4 then can be determined simply by solving a set of four linear inhomogeneous equations, which can be written as:

$$w_i = \sum_{j=1}^{4} q_{ij} c_j,$$

where initial values of PMO parameters b_n needed here were taken from Ref. [44] and w_i were approximately evaluated from data of Ref. [32].

3.5. Further Correction of PMO Potential Function

Calculations as described in Chapter III would determine a set of PMO parameters (ρ, σ, τ, Δ, b_4, ..., b_{12}, c_1, ..., c_M, B) from which a series of vibrational eigenenergies G_v^{cal} and rotational constants B_v^{cal} can be evaluated and compared with experimental data G_v^{ex} and B_v^{ex}. Unfortunately, the PMO potential function obtained by this approach for

HF in particular produces values of G_v^{cal} and B_v^{cal} which deviate considerably from G_v^{ex} and B_v^{ex}. In order to reduce these discrepancies to obtain a more accurate PMO potential, we need to improve the above PMO parameters further; the following approach was adopted for this purpose.

The PMO parameters values which produce G_v^{cal} and B_v^{cal} should not differ very much from those values that would produce G_v^{ex} and B_v^{ex}. Then considering G_v^{cal} and B_v^{cal} both denoted by f_v, as functions of some or all of the PMO parameters, designated as x_1, x_2, ..., x_μ, we can expand them as a multivariable Taylor series about values $x_{10}, x_{20}, \ldots, x_{\mu 0}$, which would correspond to G_v^{ex} and B_v^{ex}, using the general formula [24]

$$f_v(x_1, x_2, \ldots, x_\mu) = \sum_{n=0}^{\infty} \frac{t^n}{n!} (\sum_{i=1}^{\mu} \alpha_i \frac{\partial}{\partial x_i})^n f_v(x_k)\Big|_{x_k = x_{k0}}, \qquad (3.12)$$

where $t_{\alpha_i} = x_i - x_{i0}$. We think that most of the contributions to $G_v^{cal} - G_v^{ex}$ and $B_v^{cal} - B_v^{ex}$ come from the linear terms, so we expand the summations and keep terms up to linear ones in $\frac{\partial}{\partial x_i}$:

$$\begin{aligned} \Delta f_v &= f_v(x_1, x_2, \ldots, x_\mu) - f_v(x_{10}, x_{20}, \ldots, x_{\mu 0}) \\ &= \sum_{i=u_1}^{u_2} (x_i - x_{i0}) \frac{\partial f_v(x_k)}{\partial x_i}\Big|_{x_k = x_{k0}}. \end{aligned} \qquad (3.13)$$

For each level v, we may write the above equations in the more convenient form

$$\Delta f_v = \sum_{i=u_1}^{u_2} (x_i - x_{i0}) \frac{\partial f_v}{\partial x_i} = \sum_{i=u_1}^{\mu_2} \beta_i f_{iv}, \qquad (3.14)$$

where $\beta_i = x_i - x_{i0}$ is the change in the corresponding PMO parameter, and $f_{iv} = \frac{\partial f_v}{\partial x_i}$.

The coefficients β_i then can be determined simply by fitting functions Δf_j directly to g_j defined below. For this purpose, we form the quantity S that needs to be minimized:

$$S = \sum_{j=1}^{N} [w_j (\sum_{i=u_1}^{u_2} \beta_i f_{ij} - g_j)]^2,$$

where $N = 40$, $u = u_2 - u_1$ is the number of parameters, $f_{ij} = \frac{\partial G_j^{cal}}{\partial b_i}$ and $g_j = G_j^{cal} - G_j^{ex}$ for $j \leq 20$, and $f_{ij} = \frac{\partial B_{j-20}^{cal}}{\partial b_i}$ and $g_j = B_{j-20}^{cal} - B_{j-20}^{ex}$ for $j > 20$. The function S now can be minimized with respect to β_k [25] by setting

$$\frac{\partial S}{\partial \beta_k} = 0 \quad \text{for} \quad k = 1, 2, \ldots, u,$$

from which

$$\sum_{j=1}^{N} w_j^2 f_{jk} (\sum_{i=u_1}^{u_2} \beta_i f_{ij} - g_j) = 0,$$

or

$$\sum_{i=u_1}^{u_2} \beta_i P_{ik} = R_k, \tag{3.15}$$

$$\text{where } P_{ik} = \sum_{j=1}^{N} w_j^2 f_{jk} f_{ji},$$

$$\text{and } R_k = \sum_{j=1}^{N} w_j^2 f_{jk} g_j.$$

From Eq. (3.15) we see that the minimization is reduced to solving a set of linear inhomogeneous equations.

We found that only the parameters $(b_8, \ldots, b_{12}, c_1, \ldots, c_4)$ needed to be improved because G_v and B_v at high v are more sensitive to their change. Solving Eq. (3.15) for β_i, we obtain a new set of PMO parameter values given by

$$b'_i = b_i - \Delta b_i,$$

$$\text{and} \quad c'_i = c_i - \Delta c_i.$$

Using these new values and the Cashion-Cooley program we solve for the new G_v^{cal} and B_v^{cal} and compare with G_v^{ex} and B_v^{ex}. If the differences are not reduced enough, further improvement may be made by varying Δb_i and Δc_i by a small amount from their initial values and solving the problem again. This process may be repeated until the differences $G_v^{cal} - G_v^{ex}$ and $B_v^{cal} - B_v^{ex}$ become adequately small. It should be noted that, at the end of each process, since we have changed PMO parameters b_i and c_i, we must find a new value for the parameter B so that the asymptotic condition for the potential function is satisfied.

3.5. Numerical Results and Discussion

Approximate values of internuclear potential $V(r)$ as a function of internuclear distances r and initial values of PMO parameters are needed as input to the zero-order approximation program. These values are taken from Ref. [10,32] and are listed in Tables 3.1 and 3.2. Carrying out the zero-order approximation for different functional forms of b_n^*, initial values of $c_1, \ldots, c_M$, and B are found and listed in Table 3.4.

These starting values together with those of PMO parameters (including the Born-Oppenheimer violation parameter Δ) then are used in another program which minimizes the quantity

$$\sum_{n=1}^{3} \sum_{v=1}^{20} (G_{n,v}^{cal} - G_{n,v}^{cx}) W_{n,v},$$

where $G_{1,v} = G_v$, $G_{2,v} = B_v$, $G_{3,v} = D_v$, and $W_{n,v}$ is a weighting factor. Since $W_{n,v}$ is the inverse of the standard deviation, which is a measure of the accuracy of the $G_{n,v}$, and since the PMO model is less accurate for higher values of v, we used a weighting function $W_{n,v} = \frac{\alpha_n}{(v+\beta_n)}$ ($\alpha_1 = 5 \times 10^3$, $\alpha_2 = 5 \times 10^4$, $\alpha_3 = 2 \times 10^5$, $\beta_1 = 5$, $\beta_2 = 5$, $\beta_3 = 5$). This weighting factor makes absolute errors for large v less important than those for small v. It can be shown that the highest- order PMO parameter contributing to $Y_{jk}^{(2l)}$ is $b_{2j+k+2l}$ [14]. Theoretically, we can include as many PMO parameters as we need for constructing $Y_{jk}^{(2l)}$ or Y_{jk}, but because the series representing G_v^{cal}, B_v^{cal}, and D_v^{cal} then will diverge, we choose $2j + k + 2l = 20$ to be the upper limit.

The fitting procedure was carried out up to $v \leq \frac{1}{2}\sigma \simeq 10$ and the results for different functional forms of b_n^* are presented in Table 3.5.

Our calculations involve two types of series whose convergence needs some careful attention. The first one is the series of Eq. (2.35a), which is formed from the terms $Y_{jk}^{(0)}$, $Y_{jk}^{(2)}$, and $Y_{jk}^{(4)}$ (abbreviated as WKB series). We can see from Table 3.6 that the WKB series converges fairly well up to $j = 10$. So we decided to keep modified Dunham coefficients $Y_{jk}^{(2l)}$ for $j \leq 10$, $k \leq 3$, and $l \leq 2$.

On the other hand, the series expansions for G_v^{cal}, B_v^{cal}, and D_v^{cal} [Eqs. (1.12)] converge less rapidly with increasing v. It is expected that D_v would diverge as v approaches the dissociation limit [21]. An approximate way to check for the convergence of these series is to find v such that

$Y_{jk}(v+\frac{1}{2})^j$ is equal to the leading term of the series [21]. If v found by this approximation turns out to be greater than $\sigma = 19$ for HF, then the series would converge; otherwise it would diverge. From Table 3.7, we see that in order to make the $j = 10$ term have the same value as the leading term $[Y_{10}(v+\frac{1}{2}), Y_{01}$, and $Y_{02}]$, we would need v to be about 26, 20, and 14, respectively. This suggests that the series for G_v and B_v are convergent but the series for D_v is divergent.

We tested the Cashion-Cooley program by applying it to the equivalent Morse potential for HF [i.e., the leading term in PMO potential] for which energy eigenvalues are exactly known [13]. The results of this part are listed in Table 3.8. We then checked the effects of the number of integration cells N_c on the errors $G_v^{cal} - G_v^{Morse}$ and found out that the optimum case occurred for $N_c = 4000$.

The spectroscopic data G_v^{ex}, B_v^{ex}, D_v^{ex}, and the PMO parameters are listed in Tables 3.3 and 3.1. They were fed into a program using Cashion-Cooley routine so that the quantities G_v^{cal}, B_v^{cal}, D_v^{cal}, $G_v^{cal} - G_v^{ex}$, $B_v^{cal} - B_v^{ex}$, and $D_v^{cal} - D_v^{ex}$ could be calculated. Results are presented in Tables (3.9-3.13).

By comparison, we found that the PMO potential function using the functional form $b_n^{*5} = (c_1 + c_2/n + c_3/n(n-1) + c_4/n(n+1))B^n$ with four parameters offered more accuracy than the other ones. Therefore, the process as described in § 3.5 was applied to this potential function only; and due to the complexity of the numerical approach to the problem, it was carried out in two steps. The differences $G_v^{cal} - G_v^{ex}$ and $B_v^{cal} - B_v^{ex}$ were first minimized with respect to the changes Δc_1, Δc_2, Δc_3, and Δc_4 in the asymptotic parameters, being subject to the asymptotic condition (3.5) from which B was determined. New values of these differences then were minimized with respect to Δb_9, Δb_9, ..., and Δb_{12}, being subject to the same asymptotic condition. The whole process was repeated twice so that desired results were obtained as shown in Table 3.14 and 3.15.

In this work, we have shown how to determine a highly accurate PMO potential function for a diatomic molecule ($X^1\Sigma^+$ state of HF) with correct asymptotic behavior. Another important feature of our calculations is that they also include the higher-order WKB terms and non-adiabatic corrections due to the Born-Oppenheimer approximation.

Our PMO potential with 17 parameters has a very good behavior about the equilibrium point and the dissociation limit. We think that by including the dipole-dipole interaction into our calculations, it may be possible to have a potential function which is accurate over the whole range of internuclear distance [20].

The numerical solution to the radial Schrödinger equation by Cashion-Cooley procedure [30,31] provides a method of testing potential functions. Its usefulness, however, is not limited to testing potential. It can generate eigenvalues and eigenfunctions, from which many other properties of the molecule such as B_v, D_v, ... may be calculated.

Fig. 3.1 shows our PMO potential function based on the model

b_n^{*5} and the potential curve obtained by the RKR method from Ref. [32]. Numerical values of these two potentials are also listed in Table 3.16. A comparison of our PMO potential function with the RKR method is made in Figure 3.2, where the quantity $(V^{PMO}\text{-}V^{RKR})/D_e$ is plotted against r. The agreement is so good that at $v = 19$ vibrational level, where V/hc=49017.71 cm^{-1}, the discrepancy between our PMO and the RKR analysis is only about 8.6 cm^{-1}. However, we think that our PMO potential may be a better representation than the RKR counterpart because it includes higher-order WKB terms while the RKR potential does not.

Table 3.1. Initial Values of PMO Parameters [10]

ρ	2.251542
σ	19.48903
τ	40036.03
b_4	0.0981267
b_5	0.0729912
b_6	0.0429170
b_7	-0.0048765
b_8	0.0277501
b_9	0.0178745
b_{10}	0.0030899
b_{11}	0.0192811
b_{12}	0.0105170

Table 3.2. Approximate $V(r)$ for HF at Some Values of r [32]

r(Å)	$V(r)$(cm^{-1})
30	49380
2.86	49026
2.56	48328
2.37	47325
2.01	42884

Table 3.3. Molecular Constants of $X^1\Sigma^+$ State of HF (cm^{-1}) [32]

v	$G_0(v)$	B_v	$D_v \cdot 10^3$
0	0.0	20.5596	2.117
1	3 961.418	19.7872	2.059
2	7 750.814	19.0328	1.98
3	11 372.807	18.2995	1.940
4	14 831.622	17.5829	1.908
5	18 130.966	16.8792	1.864
6	21 273.69	16.8792	1.838
7	24 262.18	15.5033	1.796
8	27 097.87	14.8266	1.776
9	29 781.33	14.1497	1.756
10	32 311.79	13.4729	1.773
11	34 687.32	12.7800	1.773
12	36 903.88	12.0696	1.804
13	38 995.56	11.3280	1.859
14	40 833.40	10.5428	1.972
15	42 525.06	9.6869	2.104
16	44 013.22	8.7396	2.396
17	45 274.57	7.6528	2.899
18	46 277.52	6.344	3.80
19	46 975.55	4.619	5.68

Table 3.4. Initial Values of c_1, c_2, …, c_4, and B for Different Models

Functional Form	c_1	c_2	c_3	c_4	B
$(c_1 + \frac{c_2}{n} + c_3 n)B^n$	0.36510	-2.5406	-0.011741	0	0.90
$(c_1 + \frac{c_2}{n} + \frac{c_3}{n(n+1)})B^n$	-0.7352	27.734	-261.0529	0	0.90
$(c_1 + \frac{c_2}{n} + \frac{c_3}{n(n-1)})B^n$	-0.33777	6.20835	0.03149	0	0.90
$(c_1 + \frac{c_2}{n} + c_3 n + \frac{c_4}{n(n+1)})B^n$	5.0931	-0.0622	-132.629	1121.7329	0.90
$(c_1 + \frac{c_2}{n} + \frac{c_3}{n(n-1)} + \frac{c_4}{n(n+1)})B^n$	-0.3379	6.208	0.0314	0	0.90

Table 3.5. Results for PMO Parameters for Different Function Forms (8 level fit)

	Functional Model				
PMO param.	F^1	F^2	F^3	F^4	F^5
ρ	2.251279	2.251613	2.251517	2.250645	2.252030
σ	19.48794	19.48101	19.48285	19.49836	19.47409
τ	40334.59	40318.69	40322.80	40355.39	40305.05
Δ	1.3254E-4	1.3254E-4	1.3254E-4	1.3254E-4	1.3254E-4
b_4	9.890209E-2	0.1016067	0.1013802	9.985423	0.101470
b_5	6.849766E-2	6.437817E-2	6.295135E-2	6.071794E-2	6.445854E-2
b_6	4.100268E-2	3.605764E-2	3.776866E-2	5.070443E-2	3.676537E-2
b_7	—6.16674E-3	9.873132E-3	2.420457E-3	2.405137E-2	2.026553E-2
b_8	2.658403E-2	3.051210E-3	1.996225E-2	—1.638818E-2	2.381092E-2
b_9	5.904186E-2	5.426649E-3	1.683443E-2	3.084916E-2	2.238828E-2
b_{10}	8.977636E-3	6.933938E-3	2.044549E-2	4.487353E-2	1.541780E-2
b_{11}	1.066200E-2	—4.986487E-3	1.226160E-2	3.013573E-3	9.372035E-3
b_{12}	9.804577E-3	—1.432905E-3	7.448849E-3	2.223751E-2	8.000742E-3
c_1	0.253478	—0.6865282	—0.28	5.977427	—0.249230
c_2	—3.009061	28.63210	4.893776	—129.5724	6.199259
c_3	—7.269434	—290.1074	—10.25408	—0.108818	—20.00091
c_4	0.0	0.0	0.0	1000.038	—15.38407
B	0.9904194	0.9142407	0.8811524	0.8295132	0.8970642

E-2 stands for 10^{-2}

Table 3.6. Modified Dunham Coefficients $Y^{2l}_{j,k}$
Using Model F^5

k	l	$j = 0$	$j = 6$	$j = 10$
0	0	0	—0.234348D-3	0.4163077D-9
0	1	0.40421D01	—0.342078D-5	—0.365456D-9
0	2	0.10536D-01	0.5551282D-7	0.000
1	0	0.20966D02	0.178391D-6	—0.112063D-10
1	1	—0.29902D-03	0.182532D-7	0.000
1	2	0.12963D-04	0.127372D-8	0.000
2	0	—0.21482D-02	0.225377D-9	0.100101D-13
2	1	—0.47657D-06	0.526572D-11	0.000
2	2	—0.56678D-08	—0.192202D-11	0.000
3	0	0.164722D-06	—0.240094D-12	0.161612D-16
3	1	0.121755D-10	—0.292984D-13	0.000
3	2	0.506585D-11	—0.934395D-15	0.000

D-11 stands for 10^{-11}

Table 3.7. Dunham Coefficients Y_{jk} Using Model F^5

j k	0	1	2	3
0	0.405268D1	0.20955111D2	—0.214872540D-2	0.16473925D-6
1	0.413844D4	—0.79701129	0.60314973D-4	—0.27285395D-8
2	—0.9003521D2	0.12686943D-1	—0.20260698D-5	—0.75638776D-9
3	0.97957502	—0.608038f1D-3	0.12234252D-6	0.12597387D-9
4	—0.3180475D-1	0.46196443D-4	—0.74160057D-8	—0.26201486D-10
5	0.2180949D-2	—0.44423369D-5	—0.13511795D-8	0.29415273D-11
6	—0.2375248D-3	0.19776136D-6	0.22853895D-9	—0.27011291D-12
7	0.1406806D-4	—0.45415666D-8	0.30070862D-10	0.17849023D-13
8	—0.7830740D-6	—0.75926349D-9	0.28875834D-11	—0.59837803D-15
9	0.2812817D-7	0.12447778D-9	—0.21892145D-12	—0.78186633D-16
10	0.5078359D-10	—0.11191527D-10	0.99969034D-14	0.16139831D-16

D-2 stands for 10^{-2}

Table 3.8. G_v^{cal} and B_v^{cal} Calculated by The Cashion-Cooley program Using the Morse Oscillator Potential

v	G_v^{cal}	$G_v^{cal} - G_v^{Morse}$	B_v^{cal}	$B_v^{cal} - B_v^{Morse}$
0	2043.341254	0.0	20.5557	—0.3817D-2
1	5970.591896	0.0	19.7477	—0.3941D-1
2	9685.266715	—0.000001	18.9283	—0.1044
3	13187.365711	—0.000001	18.0968	—0.2026
4	16476.888883	—0.000002	17.2528	—0.3300
5	19553.836233	—0.000004	16.3954	—0.4837
6	22418.207759	—0.000006	15.5237	—0.6629
7	25070.003461	—0.000009	14.6366	—0.8666
8	27509.223339	—0.000014	13.7327	—0.1093D1
9	29735.867391	—0.000022	12.8102	—0.1330D1
10	31749.935618	—0.000033	11.8668	—0.1606D1
11	33551.428019	—0.000047	10.8998	—0.1880D1
12	35140.344595	—0.000063	9.9053	—0.2164D1
13	36516.685350	—0.000077	8.8780	—0.2449D1
14	37680.450287	—0.000087	7.8106	—0.2732D1
15	38631.639409	—0.000090	6.6919	—0.2994D1
16	39370.252720	—0.000079	5.5034	—0.3236D1
17	39896.302414	0.012136	4.2109	—0.3441D1
18	40216.975954	7.224020	2.9727	—0.3371D1

D1 stands for 10^1

Table 3.9. G_v^{cal}, B_v^{cal} and D_v^{cal} Calculated from the Cashion-Cooley program along with the Differences $G_v^{cal} - G_v^{ex}$, $B_v^{cal} - B_v^{ex}$, and $D_v^{cal} - D_v^{ex}$, Using Model F[1]

v	G_v^{cal}	$G_v^{cal} - G_v^{ex}$	B_v^{cal}	$B_v^{cal} - B_v^{ex}$	D_v^{cal}	$D - v^{cal} - D_v^{ex}$
0	2050.8697	— 0.001893	0.205595D2	—0.5970D-4	0.201464D-2	—0.102355D-3
1	6012.2396	0.001922	0.197864D2	—0.733D-3	0.218703D-2	0.128031D-3
2	9801.6670	0.002340	0.190338D2	0.1099D-2	0.196390D-2	—0.160977D-4
3	13423.6782	— 0.003473	0.182996D2	0.1237D-3	0.193176D-2	—0.823325D-5
4	16882.4600	— 0.071677	0.175817D2	—0.1178D-2	0.187719D-2	—0.308029D-4
5	2-181.4776	— 0.343985	0.168777D2	—0.1474D-2	0.189114D-2	0.271426D-4
6	23323.3051	— 1.256527	0.161842D2	—0.2443D-2	0.181656D-2	—0.214359D-4
7	26309.4164	— 3.625200	0.154969D2	—0.6310D-2	0.176866D-2	—0.273359D-4
8	29140.0342	— 8.707394	0.148107D2	—0.1582D-1	0.174380D-2	—0.321954D-4
9	32814.0383	— 18.143297	0.141197D2	—0.2991D-1	0.180686D-2	0.508628D-4
10	34328.9156	— 33.775980	0.134175D2	—0.5530D-1	0.183232D-2	0.593286D-4
11	36680.7252	— 57.456414	0.126971D2	—0.8287D-1	0.185294D-2	0.799438D-4
12	38864.0552	— 90.726432	0.119505D2	—0.1190D-1	0.182384D-2	0.198400D-4
13	40871.9580	—134.453623	0.111688D2	—0.1591D-1	0.189174D-2	0.327489D-4
14	42695.8640	—188.407614	0.103415D2	—0.2012	0.200816D-2	0.361654D-4
15	44325.5002	—250.431477	0.945615D1	—0.2307	0.217308D-2	0.690860D-4
16	45748.8921	—315.199568	0.849759D1	—0.2420	0.234770D-2	—0.482910D-4
17	46952.6395	—372.802172	0.744813D1	—0.2046	0.261934D-2	—0.279655D-3
18	48647.6412	319.249527	0.4199977D1	—0.13442D1	0.357977D-2	—0.220228D-3
19	49121.7119	95.290252	0.357088D1	—0.10481D1	0.443348D-2	—0.124651D-2

D-4 stands for 10^{-4}

Table 3.10. G_v^{cal}, B_v^{cal}, and D_v^{cal} Calculated from the Cashion-Cooley program along with the Differences $G_v^{cal} - G_v^{ex}$, $B_v^{cal} - B_v^{ex}$, and $D_v^{cal} - D_v^{ex}$, Using Model F^2

v	G_v^{cal}	$G_v^{cal} - G_v^{ex}$	B_v^{cal}	$B_v^{cal} - B_v^{ex}$	D_v^{cal}	$D_v^{cal} - D_v^{ex}$
0	2050.8722	0.0005	0.205597D2	0.103186D-3	0.210222D-2	—0.147787D-4
1	6012.2936	0.0059	0.197862D2	—0.922161D-3	0.199725D-2	—0.617496D-4
2	9801.6738	0.0091	0.190336D2	0.861528D-3	0.201483D-2	0.348339D-4
3	13423.6877	0.0061	0.18299702	0.206693D-3	0.202756D-2	0.875668D-4
4	16882.4988	— 0.0328	0.175820D2	—0.822497D-3	0.184506D-2	—0.629394D-4
5	20181.6308	— 0.1908	0.168780D2	—0.115356D-2	0.186021D-2	—0.378016D-5
6	23323.9334	— 0.6282	0.16184702	—0.197767D-2	0.179776D-2	—0.402321D-4
7	26311.6522	— 1.3894	0.154993D2	—0.393784D-2	0.17775D-2	—0.188473D-4
8	29146.5416	— 2.2000	0.148195D2	—0.709524D-2	0.163153D-2	—0.144366D-3
9	31829.9252	— 2.256	0.141427D2	—0.691909D-2	0.162011D-2	—0.135886D-3
10	34362.6102	— 0.0814	0.134663D2	—0.653300D-2	0.170742D-2	—0.655752D-4
11	36744.5893	6.4076	0.127861D2	0.614160D-2	0.162981D-2	—0.143185D-3
12	38974.5038	19.7221	0.120956D2	0.260411D-1	0.162981D-2	—0.174185D-3
13	41048.8670	42.4554	0.113848D2	0.568286D-1	0.162011D-2	—0.238886D-3
14	42961.0323	76.7606	0.106384D2	0.956273D-1	0.167832D-2	—0.293679D-3
15	44699.7855	123.8539	0.983302D1	0.1461252	0.179473D-2	—0.309263D-3
16	46247.1863	183.0946	0.893083D1	0.19123307	0.2056670D-2	—0.339329D-3
17	47574.6046	249.1629	0.786357D1	0.2107718	0.254173D-2	—0.357265D-3
18	4633.5382	305.1466	0.647785D1	0.1338503	0.368648D-2	—0.113514D-3
19	49321.6753	295.2536	0.406908D1	—0.549915	0.158324D-1	0.101524D-2

D-3 stands for 10^{-3}

Table 3.11. G_v^{cal}, B_v^{cal}, and D_v^{cal} Calculated From the Cashion-Cooley program along with the Differences $G_v^{cal} - G_v^{ex}$, $B_v^{cal} - B_v^{ex}$, and $D_v^{cal} - D_v^{ex}$, Using Model F^3

v	G_v^{cal}	$G_v^{cal} - G_v^{ex}$	B_v^{cal}	$B_v^{cal} - B_v^{ex}$	D_v^{cal}	$D_v^{cal} - D_v^{ex}$
0	2050.8745	0.0029	0.205596D2	0.972047D-4	0.193157D-2	—0.185422D-3
1	6012.2900	0.0024	0.197863D2	—0.870465D-3	0.214519D-2	0.861948D-4
2	9801.6646	— 0.00006	0.190337D2	0.982836D-3	0.202514D-2	0.451415D-4
3	13423.6818	0.0001	0.182997D2	0.293593D-3	0.197906D-2	0.390604D-4
4	16882.5192	— 0.0124	0.175821D2	—0.728373D-3	0.192812D-2	0.201287D-4
5	20181.7925	— 0.0291	0.168785D2	—0.671163D-3	0.188265D-2	0.186540D-4
6	23324.4259	— 0.1357	0.161860D2	—0.677763D-3	0.182444D-2	—0.135536D-4
7	26312.4749	— 0.5667	0.155011D2	—0.215840D-2	0.178295D-2	0.769527D-4
8	29146.9252	— 1.8164	0.148195D2	—0.704833D-2	0.179170D-2	0.157045D-4
9	31827.4878	— 4.6938	0.141359D2	—0.137301D-1	0.177230D-2	0.163020D-4
10	34352.3976	— 10.2940	0.134440D2	—0.288515D-1	0.180625D-2	0.332564D-4
11	36718.2158	— 19.9658	0.127362D2	—0.437898D-1	0.175593D-2	—0.170688D-4
12	38919.6251	— 35.1564	0.120033D2	—0.662109D-1	0.175593D-2	—0.480688D-4
13	40949.2051	— 57.2065	0.112346D2	—0.933825D-1	0.192085D-2	0.618528D-4
14	42797.1735	— 87.0981	0.104164D2	—0.1263985	0.196935D-2	—0.264080D-5
15	44451.1018	—124.8299	0.953183D1	—0.155062	0.214398D-2	0.399821D-4
16	45895.6619	—168.4297	0.855981D1	—0.180089	0.248352D-2	0.875268D-4
17	47112.6171	—212.8245	0.747254D1	—0.1802500	0.269695D-2	—0.202045D-3
18	48081.6804	—246.7111	0.623936D1	—0.104633	0.325962D-2	—0.540370D-3
19	49210.9385	184.5168	0.325516D1	—0.136383D1	0.484093D-2	—0.839062D-3

D-3 stands for 10^{-3}

Table 3.12. G_v^{cal}, B_v^{cal}, and D_v^{cal} Calculated From the Cashion-Cooley Routine Along with the Differences $G_v^{cal} - G_v^{ex}$, $B_v^{cal} - B_v^{ex}$, and $D_v^{cal} - D_v^{ex}$, Using Model F^4

v	G_v^{cal}	$G_v^{cal} - G_v^{ex}$	B_v^{cal}	$B_v^{cal} - B_v^{ex}$	D_v^{cal}	$D_v^{cal} - D_v^{ex}$
0	2050.8714	— 0.00020	0.205596D2	0.403397D-4	0.209574D-2	—0.212589D-4
1	6012.2903	0.00271	0.197863D2	—0.849668D-3	0.210032D-2	0.413264D-4
2	9801.6676	0.00298	0.190338D2	0.102163D-2	0.206030D-2	0.803083D-4
3	13423.6816	0.02047	0.182998D-2	0.320792D-3	0.203969D-2	0.996934D-4
4	16882.5316	0.06171	0.175821D2	—0.777203D-3	0.198633D-2	0.783364D-4
5	20182.0698	0.24814	0.168781D2	—0.109977D-2	0.201968D-2	0.155684D-3
6	23325.2012	0.63955	0.161843D2	—0.230901D-2	0.215125D-2	0.313258D-3
7	26314.1074	1.0658	0.154967D2	—0.656961D-2	0.272774D-2	0.631744D-3
8	29149.6556	0.91400	0.148099D2	—0.166593D-1	0.227009D-2	0.494098D-3
9	31831.2021	— 0.97957	0.141180D2	—0.316922D-1	0.238893D-2	0.632939D-3
10	34356.3988	— 6.2928	0.134141D2	—0.587496D-1	0.238590D-2	0.612970D-2
11	36721.0581	— 17.1234	0.126908D2	—0.891950D-1	0.252233D-2	0.749331D-3
12	38919.0562	— 35.7253	0.119394D2	—0.13301225	0.259994D-2	0.795942D-3
13	40942.2578	— 64.1538	0.111504D2	—0.177548	0.270665D-2	0.847656D-3
14	42780.4608	—103.8108	0.103123D2	—0.230436	0.281337D-2	0.841370D-3
15	44421.3917	—154.5399	0.941171D1	—0.275187	0.301709D-2	0.913097D-3
16	45840.8532	—213.2384	0.843248D1	—0.307111	0.324992D-2	0.853927D-3
17	47053.2644	—272.1772	0.735638D1	—0.296417	0.363797D-2	0.738978D-3
18	48013.1007	—315.2903	0.6116446D1	—0.179530	0.412304D-2	0.323042D-3
19	49165.2117	138.7900	0.3338405D1	—0.123494D1	0.571405D-2	0.340520D-4

D-3 stands for 10^{-3}

Table 3.13. G_v^{cal}, B_v^{cal}, and D_v^{cal} Calculated From the Cashion-Cooley program along with the Differences $G_v^{cal} - G_v^{ex}$, $B_v^{cal} - B_v^{ex}$, and $D_v^{cal} - D_v^{ex}$, Using Model F^5

v	G_v^{cal}	$G_v^{cal} - G_v^{ex}$	B_v^{cal}	$B_v^{cal} - B_v^{ex}$	D_v^{cal}	$D_v^{cal} - D_v^{ex}$
0	2050.8864	0.01478	0.205596D2	0.674461D-4	0.216387D-2	0.468773D-4
1	6012.3032	0.0155	0.197862D2	—0.927256D-3	0.210578D-2	0.467833D-4
2	9801.6783	0.0136	0.190338D2	0.100201D-2	0.198754D-2	0.754908D-5
3	13423.6970	0.0153	0.182998D2	0.379919D-3	0.196693D-2	0.269338D-4
4	16882.5380	0.0063	0.175822D2	—0.640802D-3	0.187780D-2	0.301966D-4
5	20181.8294	0.0078	0.168785D2	—0.652325D-3	0.183839D-2	—0.256080D-4
6	23324.5485	— 0.0131	0.161859D2	—0.714986D-3	0.184263D-2	0.463626D-5
7	26312.8799	— 0.1617	0.155012D2	0.204248D-2	0.175229D-2	—0.437068D-4
8	29148.0455	— 0.6961	0.148203D2	0.626235D-2	0.179898D-2	0.229805D-4
9	31830.1127	— 2.0689	0.141383D2	—0.113707D-1	0.173713D-2	—0.188651D-4
10	34357.7834	— 4.9082	0.134492D2	—0.236073D-1	0.179958D-2	0.265368D-4
11	36728.1587	— 10.0229	0.127460D2	—0.339936D-1	0.173652D-2	0.364714D-4
12	38936.4683	— 18.3133	0.120196D2	—0.499885D-1	0.175593D-2	—0.480688D-4
13	40975.7427	— 30.6689	0.112590D2	—0.689494D-1	0.184324D-2	—0.157574D-4
14	42836.4014	— 47.8701	0.104501D2	—0.9926260D-1	0.194995D-2	—0.220433D-4
15	44505.7251	— 70.2065	0.957431D1	—0.112580	0.203726D-2	—0.667318D-4
16	45967.1949	— 96.8966	0.860609D1	—0.133501	0.225069D-2	—0.145303D-3
17	47199.7870	—125.6546	0.751018D1	—0.142610	0.268725D-2	—0.211746D-3
18	48177.7292	—150.6623	0.623798D1	—0.106014	0.328873D-2	—0.511267D-3
19	48872.8450	—153.5765	0.473048D1	0.111485	0.429766D-2	—0.138233D-2

D-3 stands for 10^{-3}

Table 3.14. Results for 7 Parameters of the Best HF Potential Function Using Model F^5 and Additional Correction

Symbol	PMO Parameters	Symbol	Improved PMO Parameters
ρ	2.2520300	ρ	2.2520300
σ	19.474095	σ	19.474095
τ	40305.041	τ	40305.041
Δ	1.325D-4	Δ	1.325D-4
b_4	0.10147098	b_4	0.10147098
b_5	6.4458544D-2	b_5	6.4458544D-2
b_6	3.6765372D-2	b_6	3.6765372D-2
b_7	2.0265535D-2	b_7	2.0265535D-2
b_8	2.3810927D-2	$b_8 + \Delta b_8$	0.24062879D-1
b_9	2.2388284D-2	$b_9 + \Delta b_9$	0.31662496D-1
b_{10}	1.5417809D-2	$b_{10} + \Delta b_{10}$	0.90408234D-2
b_{11}	9.3720353D-3	$b_{11} + \Delta b_{11}$	0.42494011D-1
b_{12}	8.0007428D-3	$b_{12} + \Delta b_{12}$	0.10058756D-1
c_1	—0.24923032	$c_1 + \Delta c_1$	—0.15010326
c_2	6.1992591	$c_2 + \Delta c_2$	4.7076628
c_3	—20.000915	$c_3 + \Delta c_3$	—19.961683
c_4	—15.384071	$c_4 + \Delta c_4$	—15.349504
B	0.98706427	$B + \Delta B$	0.92185016

D-3 stands for 10^{-3}

Table 3.15. G_v^{cal}, B_v^{cal}, and D_v^{cal} Calculated From the Cashion-Cooley program along with the Differences $G_v^{cal} - G_v^{ex}$, $B_v^{cal} - B_v^{ex}$, and $D_v^{cal} - D_v^{ex}$, using the Best Data from Table 3.16

v	G_v^{cal}	$G_v^{cal} - G_v^{ex}$	B_v^{cal}	$B_v^{cal} - B_v^{ex}$	D_v^{cal}	$D_v^{cal} - D_v^{ex}$
0	2050.8794	0.0077	0.205597D2	0.111374D-3	0.216694D-2	0.499469D-4
1	6012.2706	—0.0170	0.197865D2	—0.658130D-3	0.205545D-2	—0.354197D-5
2	2801.6089	—0.0557	0.190346D2	0.189439D-2	0.203787D-2	0.578744D-4
3	13423.6109	—0.0707	0.183019D2	0.246150D-2	0.194328D-2	0.328701D-5
4	16882.4850	—0.0466	0.175861D2	0.321716D-2	0.192327D-2	0.152781D-4
5	20181.8723	0.0506	0.168846D2	0.548510D-2	0.184566D-2	—0.183320D-4
6	23324.7656	0.2040	0.161948D2	0.812865D-2	0.176805D-2	—0.699422D-4
7	26313.4182	0.3766	0.155132D2	0.998603D-2	0.179837D-2	0.237419D-5
8	29149.2392	0.4975	0.148362D2	0.969228D-2	0.17715D-2	0.115264D-5
9	31832.6641	0.4824	0.141594D2	0.974647D-2	0.173228D-2	—0.237157D-4
10	34362.9845	0.2928	0.134774D2	0.459416D-2	0.181292D-2	0.399261D-4
11	36738.1180	—0.0636	0.127839D2	0.399228D-2	0.176563D-2	—0.736761D-5
12	38954.953	—0.4863	0.120707D2	0.119974D-2	0.173652D-2	—0.674714D-4
13	41005.6327	—0.7789	0.113272D2	—0.710984D-2	0.188204D-2	0.230477D-4
14	42883.5342	—0.7371	0.105390D2	—0.373981D-2	0.193055D-2	—0.414459D-4
15	44575.8285	—0.1031	0.968573D1	—0.116747D-2	0.208577D-2	—0.182254D-4
16	46065.4682	1.3765	0.873681D1	—0.278340D-2	0.2228960D-2	—0.106498D-3
17	47328.4811	3.0394	0.764352D1	—0.927988D-2	0.271635D-2	—0.182642D-3
18	48330.6997	2.3080	0.632091D1	—0.230829D-1	0.353126D-2	—0.268735D-3
19	49023.4050	—3.0166	0.460826D1	—0.107328D-1	0.523868D-2	—0.441310D-3

D-4 stands for 10^{-4}

Table 3.16 Comparison Between RKR Potential Energies and our Best PMO Values for the $X^1\Sigma^+$ State of HF

r_{min}(Å)	Our Best PMO Potential (cm^{-1})	r_{max}(Å)	Our Best PMO potential (cm^{-1})	RKR potential (cm—1)
0.8342	2049.98	1.0206	2052.80	2050.76
0.7845	6017.06	1.1131	6012.78	6012.18
0.7548	9808.25	1.1869	9802.27	9801.58
0.7331	13425.79	1.2541	13428.33	13423.56
0.7159	16888.31	1.3181	16887.57	16882.39
0.7018	20169.83	1.3807	20189.76	20181.72
0.6898	23309.58	1.4429	23336.27	23324.52
0.6795	26281.08	1.5054	26326.84	26313.03
0.6705	29102.59	1.5688	29161.41	29148.72
0.6626	31764.16	1.6339	31848.01	31832.11
0.6556	34276.35	1.7011	34374.60	34362.58
0.6494	36629.75	1.7715	36750.00	36738.08
0.6439	38824.62	1.8460	38964.79	38954.72
0.6390	40870.19	1.9261	41014.78	41006.39
0.6347	42739.61	2.0139	42891.03	42884.20
0.6310	44407.19	2.1129	44584.65	44575.74
0.6278	45896.03	2.2286	46075.64	46063.97
0.6261	47187.71	2.3711	47336.14	47325.53
0.6231	48166.47	2.5625	48330.56	48328.10
0.6220	48713.06	2.8692	49017.71	49026.38

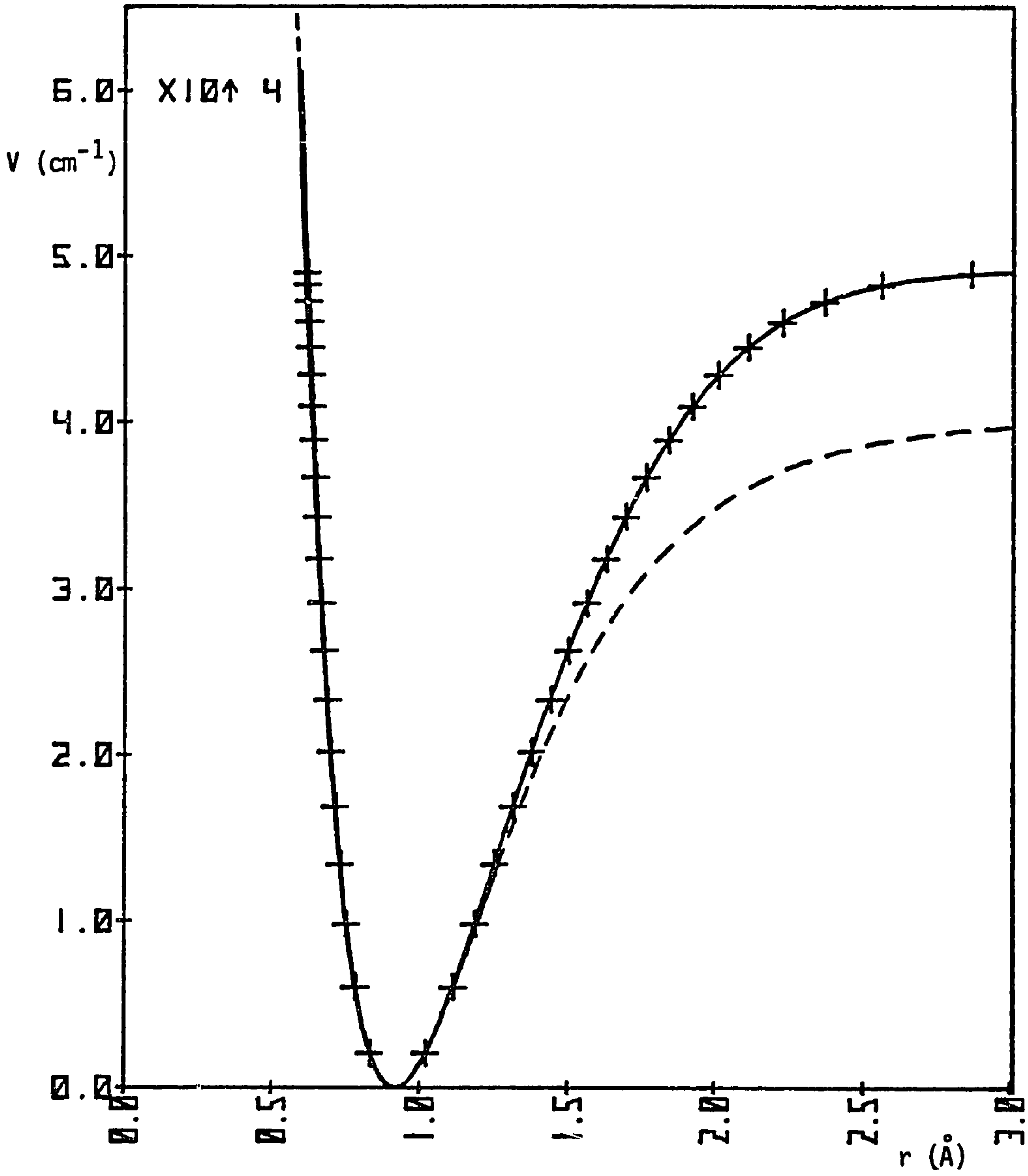

Fig. 3.1. Plots of internuclear potential functions of HF.

———— : Our best potential function.

\+ + + + + : RKR potential function.

— — — — — : Equivalent Morse potential function.

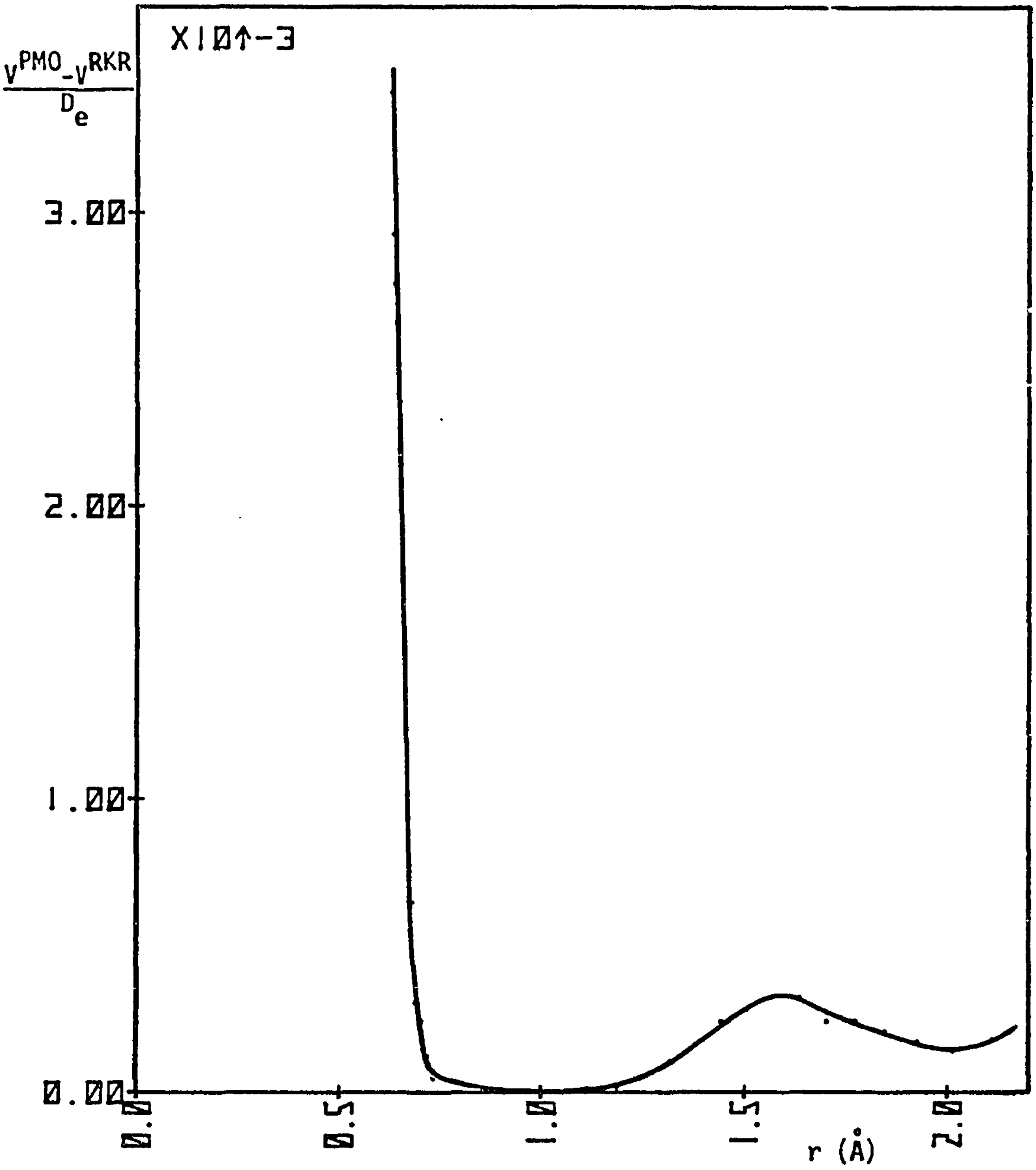

Fig. 3.2. Comparison of our PMO and RKR potential function for HF.

CHAPTER IV

ELECTRIC DIPOLE MOMENT FUNCTION OF $X^1\Sigma^+$ STATE OF HF

4.1. Introduction

In a homonuclear diatomic molecule the electronic charge distribution is symmetric with respect to a plane perpendicular to its internuclear axis at the mid-point, and therefore the molecule has a zero dipole moment. However, in the case of a heteronuclear diatomic molecule such as HF, the electronic charge distribution does not possess this kind of symmetry and hence may produce an electric dipole moment. The general shape of the dipole moment of a diatomic molecule as a function of r is shown in Fig. (4.1). The dipole moment of molecules such as CO changes sign at small r while that of HF does not [33,34].

In Chapter I we defined the electric dipole moment vector of a diatomic molecule and showed that its expectation value $M(r)$ on the internuclear axis was a function of the internuclear distance r. Therefore, the dipole moment is usually expanded as a Taylor series in terms of r. It can also be expressed in terms of the variables y and z defined below, and we can write in general:

$$M(q) = q_0 + \sum_{n=1}^{\infty} m_n q^n, \tag{4.1}$$

where q is one of the following variables

$$u = r - r_e, \tag{4.2}$$

$$y = 1 - e^{-a(r-r_e)}, \tag{4.3}$$

$$z = -1 + e^{a(r-r_e)}. \tag{4.4}$$

The first term q_0, which is called the permanent dipole moment, and the coefficients m_n are defined as follows:

$$\begin{aligned} q_0 &= M(q_e) = M(r_e) \\ m_n &= \frac{1}{n!}\left[\frac{d^n M(q)}{dq^n}\right]_{q=q_e}. \end{aligned} \tag{4.5}$$

If r is expressed in units of cm and electric charge in units of esu, then $M(r)$ has the unit of esu·cm. Another unit which is also commonly used for electric dipole moment is Debye (abbreviated as D) where $1\text{D}=10^{-18}$ esu-cm.

A great deal of effort has been made to obtain highly accurate intensity data for the $X^1\Sigma^+$ state of HF from which the transition matrix elements were determined [26,27,28]. These data are presented in Tables (4.1) and (4.4). Only the uncertainties on μ_{01},μ_{02},and μ_{03} are listed in Table 4.1. They were determined based on reported informations[26]that $\frac{\Delta\rho^2}{\rho^2} = .15$,where ρ is the ratio of two transition matrix elements.

The accuracy with which one determines dipole moment matrix elements depends in particular on the accuracy of the vibrational wave functions. This in turn depends upon the extent to which the internuclear potential function used in the radial Schrödinger equation truly represents the potential of the molecule. With the technique described in Chapter III, we have obtained for the ground electronic state of HF a highly accurate PMO internuclear potential function (within the framework of the Born-Oppenheimer approximation). Our next task is to solve the radial Schrödinger equation for the vibrational wavefunctions using this PMO potential. There are two approaches to this problem.

i) Matrix diagonalization: The PMO wave functions are expanded in terms of a set of basis functions (for example Morse basis functions). For this purpose, it is necessary to neglect the continuum of the Morse oscillator and retain a certain number M of bound states in order to have a finite and discrete matrix representation. The coefficients of the expansion and hence the PMO wave functions then can be found by matrix diagonalization. This approach is very suitable and efficient for molecules with many bound states. Tran [37,38] applied this method to CO, which has about 77 bound states, and got excellent results. We also applied it to the HF molecule with about 20 bound states. As we predicted, the results are not satisfactory, due to the small number of HF bound states. We therefore decided to solve the problem entirely by numerical method.

ii) Numerical calculations: The Cashion-Cooley routine was used to solve the radial Schrödinger equation, Eq. (1.2), for vibrational eigenfunctions of HF. Their numerical procedure may be summarized below.

The Schrödinger equation is first written in the form

$$\frac{d^2\psi}{dr^2} + [E - V(r)]\psi(r) = 0, \qquad (4.6)$$

where $\psi(r)$ is the radial eigenfunction multiplied by r, and $V(r)$ is the effective potential energy. In the above equation, length is measured in the Bohr radius a0=0.529172 Å, and energy is measured in unit of $\frac{hN_0}{(8\pi^2 C a_0^2 \mu_A)}$ wavenumbers, where N_0 is the Avagadro,s number and μ_A is the reduced mass in atomic mass unit (a.m.u). The numerical value of this factor is $60.2198/\mu_A$. Values of $\psi(r)$ are obtained obtained by the Numerov method [Appendix D] which is characterized by the following relations:

$$Y_{i+1} + Y_{i-1} - 2Y_i = h^2(V_i - E)\psi_i, \qquad (4.7a)$$

$$Y_i = [1 - (\frac{h^2}{12})(V_i - E)]\psi_i, \qquad (4.7b)$$

where h is the step size and E is a trial eigenvalue. For any E, there are two values of r (classical turning points r_1 and r_2) such that

$$V_i(r) - E = 0. \qquad (4.8)$$

$\psi(r)$ has increasing exponential behavior for $0 < r < r_1$, oscillatory behavior for $r_1 < r < r_2$, and decreasing exponential behavior for $r > r_2$. This method is a three point method, i.e., ψ_{i+1} can be found by knowing

ψ_i and ψ_{i-1} (the values of $(V - E)$ are known). The Numerov method is of sixth order and produces less roundoff error than lower-order methods such as the Runge-Kutta method (which is of fourth order). For using the Numerov method, we require the value of ψ_{i+1} if ψ_i be known. Using the WKB method ψ_i can be found in terms of ψ_{i+1} as

$$\psi_i = \psi_{i+1} \exp[r_{i+1}(V_{i+1} - E)^{\frac{1}{2}} - r_i(V_i - E)^{\frac{1}{2}}]. \qquad (4.8)$$

Next a correction to E is determined from the variational method:

$$D(E) = \frac{[(-Y_{m-1} + 2Y_m - Y_{m+1})h^{-2} + (V_m - E)\psi_m]}{\sum_{i=1}^{n} \psi_i^2} \qquad (4.9)$$

The process is repeated until successive values of E differ by a specified small number. Finally the resulting values of ψ_i can be normalized.

The relative phase of the various wave functions are arbitrary. In analogy to the case of wavefunctions of the Morse oscillator [38], we may divide the PMO wave functions into two categories called Class I and Class II. All class I wavefunctions are positive for very large r, while class II wavefunctions are negative for very large r. These two classes are related by

$$\psi_v^{(I)} = (-1)^v \psi_v^{(II)}. \qquad (4.10)$$

This means that eigenfunctions of the two classes are the same for even values of v and have the opposite sign for its odd values. The difference in the wavefunction signs results in the difference in the matrix elements signs. Using the relation (4.10), one obtains for the matrix elements of a function $M(r)$:

$$\langle \psi_v^{(I)} | M(r) | \psi_{v'}^{(I)} \rangle = (-1)^{v+v'} \langle \psi_v^{(II)} | M(r) | \psi_{v'}^{(II)} \rangle. \tag{4.11}$$

The wave functions generated by the Cashion-Cooley routine are found to be class I.

In solving the radial Schrödinger equation by the above numerical method, the highly accurate PMO potential function obtained in Chapter III was employed. A two dimensional array is needed to store vibrational wavefunction values for many vibrational levels, which then were used in computing various PMO matrix elements by numerical integration using the Simpson rule. The range of internuclear distance was chosen from r_{min}=0.60137 Å to r_{max}=4.37508 Å, and was divided into 2000 equal integration steps for obtaining adequately accurate results for HF. Double precision was employed throughout our calculations providing accuracy up to 16 significant digits.

4.2. HF Dipole Moment Functions as Cubic Polynomials

Highly accurate intensity data were obtained for the (0 — 0) band, fundamental (0 — 1) band, and the first two overtone (0 — 2 and 0 — 3) bands of HF ($X^1\Sigma^+$) [27], from which reliable absolute values for the corresponding rotationless matrix elements were deduced. These empirical data are listed in Table (4.1). Data for other transitions of HF are not so accurate and reliable.

This insufficiency of good experimental data usually limits the number of terms that one can retain in a Taylor series expansion of the dipole moment. For this reason, we keep up to the cubic term only in the Taylor expansion, and write in terms of the variables u, y, and z:

$$M(u) = m_0 + m_1 u + m_2 u^2 + m_3 u^3, \; 0 \leq r \leq 1.833 \tag{4.12a}$$

$$M(y) = M_0 + M_1 y + M_2 y^2 + M_3 y^3, \; 0.634 \leq r \leq \infty \tag{4.12b}$$

$$M(z) = T_0 + T_1 z + T_2 z^2 + T_3 z^3, \; -\infty < r < 1.199. \tag{4.12c}$$

where the inequality following each cubic polynomial shows the range of convergence of the corresponding infinite series [Appendix B].

With the few experimental data listed in Table (4.1) and with accurate PMO eigenfunctions available, our next task is to solve for the coefficients of the cubic dipole moment functions in variables u, y, and z. The coefficients m_0, m_1, $\cdots$, m_3, M_0, M_1, $\cdots$, M_3 and T_0, T_1, $\cdots$, T_3 can be determined simply by solving a set of four linear inhomogeneous equations which can be written in the matrix form:

$$\begin{bmatrix} \delta_{00} & q_{01} & q_{02} & q_{03} \\ \delta_{01} & q_{11} & q_{12} & q_{13} \\ \delta_{02} & q_{21} & q_{22} & q_{23} \\ \delta_{03} & q_{31} & q_{32} & q_{33} \end{bmatrix} \begin{bmatrix} c_1 \\ c_2 \\ c_3 \\ c_4 \end{bmatrix} = \begin{bmatrix} \mu_{00} \\ \mu_{01} \\ \mu_{02} \\ \mu_{03} \end{bmatrix} \tag{4.13}$$

where $\delta_{0n} = \langle 0|n\rangle$, $q_{np} = \langle 0|u^p|n\rangle$, or $\langle 0|y^p|n\rangle$, or $\langle 0|z^p|n\rangle$.

Cubic polynomial representations of HF dipole moment are obtained as follows:

$$M(u) = 1.795 + 1.5232u - 0.0907u^2 - 1.4129u^3, \tag{4.13a}$$

$$M(y) = 1.795 + 0.6213y + 0.2949y^2 + 0.0743y^3, \tag{4.13b}$$

$$M(z) = 1.795 + 0.6215z - 0.3203z^2 + 0.0944z^3. \tag{4.13c}$$

Coefficients of these polynomials are also listed in Table (4.2), and their graph versus r are plotted in Fig. (4.2).

Our cubic polynomials in u are in excellent agreement with that obtained by Meredith and Smith [29] using the RKR potential: $M(u) = 1.7965 + 1.5229u - 0.0806u^2 - 1.4077u^3$. We also see that the first terms (permanent dipole moment) of the three cubic polynomials are practically the same, and from Fig. (4.2) these functions coincide over a small range of r about the equilibrium r_e. This feature is of course necessary and provides a way to check the correctness and consistency of the various dipole moment functions for the same molecule.

4.3. Analytical Dipole Moment Functions with Correct Asymptotic Behavior

At present, most theoretical and experimental treatments of the dipole moment can give information about it only over a limited range of r about the equilibrium r_e, and none provides a detailed picture of the dipole moment over the whole range of r. Theoretically, the dipole moment function of diatomic molecules such as HF should have the following general behavior:

$$M(r) = 0 \quad \text{for} \quad r = 0 \quad \text{and} \quad r = \infty. \tag{4.14}$$

The large r behavior of the dipole moment function can be explained by the fact that at large r, the diatomic molecule would dissociate into two neutral atoms, and therefore must have a zero dipole moment [36]. In the limit of $r = 0$, if the molecule is considered to be transformed into a single atom, then its dipole moment should also vanish. However, very much less information can be found for the small r behavior of the dipole moment in the literature; James *et al.* [44] suggested that $M(r)$ should go to zero as r^3.

The main objective of the present chapter is to approximately evaluate values of unknown coefficients of the infinite series $M(y)$ from a limited number of intensity data, in such a way that the asymptotic property $M(r = \infty) = 0$ is satisfied or

$$M_0 + \sum_{n=1}^{\infty} M_n = 0 \tag{4.15}$$

For this purpose, we assume a functional form for M_n, i.e., we express

$$M_n = F(n, c_1, c_2, \ldots, c_M, B), \tag{4.16}$$

where F is a function of the index n and the parameter $c_1, \ldots, c_M$ and B, and we require that

$$M_0 + \sum_{n=1}^{\infty} F(n, c_1, c_2, \ldots, c_M, B) = 0. \tag{4.17a}$$

Thus, the series generated by the function F must be convergent and satisfy a necessary condition:

$$\lim_{n \to \infty} F(n, c_1, c_2, \ldots, c_M, B) = 0. \tag{4.17b}$$

Tran and Huffaker[37,38]introduced suitable functions for F. Note that the mathematical treatment of the asymptotic behavior of the dipole moment is similar to what we have carried out previously for the PMO potential function of HF. Of the five functional forms we used in that case,we found that only two worked for HF dipole moment. For the others, underflow or overflow occurred and B went out of its range. These two functional forms are:

$$M_n^1 = F^1(n, c_1, c_2, c_3, c_4, B)$$

$$= \begin{cases} (c_1 + c_2/n + c_3/n(n-1) + c_4/n(n+1))B^n & , n > 1 \\ (c_1 + c_2 + \frac{1}{2}c_4)B & , n = 1 \end{cases} \qquad (4.18a)$$

$$M_n^2 \; = \; F^2(n, c_1, c_2, B) \; = \; (c_1 + \frac{c_2}{n})B^n \qquad (4.18b)$$

where $0 < B < 1$.

The corresponding dipole moment functions then can be written in a compact form:

$$M^1(y) = M_0 + \sum_{n=1}^{\infty} M_n^1 y^n = M_0 + c_1 \frac{By}{1 - By} - c_2 \ln(1 - By)$$

$$+ c_3[By + (1 - By)\ln(1 - By)]$$

$$+ c_4[1 + (\frac{1 - By}{By})\ln(1 - By)], \qquad (4.19a)$$

$$M^2(y) = M_0 + \sum_{n=1}^{\infty} M_n^2 y^n = M_0 + \frac{c_1 By}{1 - By} - c_2 \ln(1 - By), \quad (4.19b)$$

as we have done in Chapter III.

The asymptotic conditions (4.15) can also be written in a similar form by letting $y = 1$ and $M^{\alpha}(y) = 0$ in Eq. (4.19)

$$M^1(1) = 0 = M_0 + \frac{c_1 B}{1-B} - c_2 \ln(1-B) + c_3[B + (1-B)\ln(1-B)]$$

$$+ c_4[1 + (\frac{1-B}{B})\ln(1-B)] \qquad (4.20a)$$

$$M^2(1) = 0 = M_0 + \frac{c_1 B}{1-B} - c_2 \ln(1-B). \qquad (4.20b)$$

Using equations (4.19a) and (4.19b), we can write the matrix elements of $M^1(y)$ and $M^2(y)$ as

$$\mu_{vv'} = \langle v|M^1(y)|v'\rangle$$

$$= M_0 \delta_{vv'} + c_1 \langle v|\frac{By}{1-By}|v'\rangle - c_2\langle v|\ln(1-By)|v'\rangle,$$

$$c_3\langle v|[By + (1-By)\ln(1-By)]|v'\rangle$$

$$+ c_4\langle v|[1 + (\frac{1-By}{By})\ln(1-By)]|v'\rangle,$$

$$= M_0 \delta_{vv'} + c_1 \varphi^{v}_{v'1} + c_2 \varphi^{v}_{v'2} + c_3 \varphi^{v}_{v'3} + c_4 \varphi^{v}_{v'4}, \qquad (4.21a)$$

$$\mu_{vv'} = \langle v|M^2(y)|v'\rangle$$

$$= M_0 \delta_{vv'} + c_1 \langle v|\frac{By}{1-By}|v'\rangle - c_2\langle v|\ln(1-By)|v'\rangle,$$

$$= M_0 \delta_{vv'} + c_1 \varphi^{v}_{v'1} + c_2 \varphi^{v}_{v'2}, \qquad (4.21b)$$

where $\varphi^{v}_{v'1} = \langle v|\frac{By}{1-By}|v'\rangle$, $\varphi^{v}_{v'2} = -\langle v|\ln(1-By)|v'\rangle$,

$$\varphi^{v}_{v'3} = \langle v|[By + (1-By)\ln(1-By)]|v'\rangle,$$

$$\varphi^{v}_{v'4} = \langle v|[1 + (\frac{1-By}{By})\ln(1-By)]|v'\rangle.$$

All the matrix elements in the right hand side of Eq. (4.21) can be evaluated by numerical integration using Simpson's rule and different vibrational eigenfunction values produced by the Cashion-Cooley program.

Since equations (4.21a) and (4.21b) are linear in M_0, c_1, $c, \ldots, c_M$ and non-linear in B, we can use the linear minimization iteration method developed in § (III.5) to determine parameters $c_1, c_2, \ldots, c_M$. Parameter B is an iterative parameter and varies in the process of minimization until the asymptotic condition (4.20) is satisfied within a desired degree of accuracy.

The linear minimization approach is much easier to understand and work with than the general minimization routine which was used for finding PMO parameters [43]. If the number of experimental transition matrix elements $\mu_{vv'}$ are equal to the number of parameters in $M^{\alpha}(y)$, the least-squares fitting for determining parameters $M_0, c_1, \ldots, c_M$ is reduced to a set of linear inhomogeneous equations written in the form

$$\varphi_{ij}^{k} c_j = \mu_i^k , \tag{4.22}$$

φ_{ij}^{k} are defined in Eq. (4.21) and μ_i^k are experimental transition matrix elements.

4.4. Results and Discussion

4.4.a. Dipole Moment Function with Correct Large-r Behavior

We first fit the matrix elements $\langle v|M^1(y)|v'\rangle$ and $\langle v|M^2(y)|v'\rangle$ directly to the empirical matrix elements $\mu_{vv'}$ whose values are given in Table (4.1). The parameter B is iterated until the asymptotic condition is satisfied within the desired accuracy. Final values obtained for the set of parameters $\{M_0, c_1, c_2, \ldots, c_m, B\}$ of the functional models M_n^1 and M_n^2

are listed in Table 4.3. Using these parameters the dipole moment functions $M^1(y)$ and $M^2(y)$ were plotted in Figs. (4.3) and (4.4).

4.4.b. Dipole Moment Functions with Correct Large and Small-r Behavior

Although the dipole moment functions $M^1(y)$ and $M^2(y)$ obtained above as an infinite power series in y have the correct large-r property, they are not convergent for $0 < r < 1.833$ Å in case of HF and therefore display a wrong general behavior at small-r. In order to force these dipole moment curves to pass through the origin we can add to them an extra term which is $M_c y(1 - y)$, where M_c is an additional adjustable parameter to be determined by iteration. This term was first used by Tran and Huffaker [37,38] in achieving the correct small-r behavior of CO dipole moment. Equations (4.19) then are modified as

$$\begin{aligned} M^1(y) = M_0 &+ \frac{c_1 By}{1 - By} - c_2 \ln(1 - By) \\ &+ c_3[By + (1 - By)\ln(1 - By)] \\ &+ c_4[1 + (\frac{1 - By}{By})\ln(1 - By)] + M_c y(1 - y), \end{aligned} \tag{4.23a}$$

$$M^2(y) = M_0 + \frac{c_1 By}{1 - By} - c_2 \ln(1 - By) + M_c y(1 - y). \tag{4.23b}$$

For each trial value of M_c the whole process of calculations carried out above for the large-r behavior was repeated. The parameter M_c was varied until the dipole moment function vanishes at $r = 0$. Results thus obtained for all parameters (including M_c) are listed in Table 4.5 and plots of the corresponding dipole moment functions are shown in Figs. 4.6 and

4.7. We see that while both functions go to zero as r goes to 0 or ∞, the dipole moment function $M^1(y)$ does not behave in a physically acceptable manner, exhibiting a peculiar hump in the small-r range $0 < r < r_e$. The cause of this second maximum can be explained by plotting each factor of c_1, c_2, c_3 and c_4 of $M^1(y)$ separately in Fig. 4.5. As shown, the third term $[By + (1 + By)\ln(1 - By)]$ (which is due to $B^n y^n / n(n-1)$) in the M_n^1 model may be responsible for the occurrence of this misbehavior, because it changes much more rapidly than the other terms as r decreases to zero. We removed the third term and repeated the calculations. The resulting dipole moment function, however, still did not behave satisfactorily at small-r range. Therefore, we decided to remove both the third and the fourth term to obtain the second model $M^2(y)$, which as expected and shown in Fig 4.4 has only one maximum and decreases monotonically to zero as r approaches zero. For comparison we plot $M^2(y)$ in Fig. 4.9 together with the HF *ab initio* dipole moment obtained by Lie [27], the HF experimental dipole moment listed in this reference, and our cubic polynomials (4.13a). Agreement between the two curves is excellent about the equilibrium distance but rather poor at large r.

For the dipole moment function $M^1(y)$ we use only the most accurate transition matrix elements in Table 4.1 in the fitting; since $M^2(y)$ was the most suitable function to best represent HF dipole moments, we fitted it to all available matrix element data (empirical or semi-empirical) recorded in Table (4.4).

One problem one usually faces is an ambiguity in the sign of the dipole moment matrix elements which arises from the fact that the experimental intensity data depend on the square of the dipole moment matrix elements and therefore determine only the magnitude, and not the sign of the matrix elements. One way to remove this sign ambiguity is to reconstruct the matrix elements using the dipole moment function $M^2(y)$ with parameters found by minimization [45]. A rule for determining the sign of the dipole moment matrix elements of HF was predicted by Cashion [26] and developed by Sileo and Cool [26]. According to this rule, the sign of the matrix element $\langle v|M^{(2)}(y)|v'\rangle$ is positive (negative) if $v - v'$ is odd (even). The rule was confirmed as we applied it to the results [Table 4.4] which are reconstructed vibrational matrix elements calculated by the HF dipole moment function $M^2(y)$. The matrix elements generated by the ab initio dipole moment function(model 1)and our best dipole moment function(model 2)were compared with the experimental data in Table 4.4. For transitions between the lower vibrational levels both models compare well with the experimental data. However,for transitions between the higher vibrational levels model 2 agrees more closely with the experimental data than model 1.

4.4.c. Equivalent Infinite Series Representing Dipole Moment Function of HF

With the parameters c_1, c_2 and B, one can calculate all the coefficients of the infinite power series in y, which is an analytical continuation of the dipole moment function $M^2(y)$ (our best form). Values of a number of these coefficients M_n are listed in Table 4.6 and plotted against the index n in Fig. 4.8. We then write out the dipole moment in y explicitly to the cubic term:

$$M(y) = 1.7979 + 0.6317y + 0.2051y^2 + 0.6883y^3 + \cdots \tag{4.24}$$

In previous § 4.2 we have determined HF cubic dipole moment function in y as

$$M(y) = 1.795 + 0.6213y + 0.2949y^2 + 0.07432y^3. \tag{4.25}$$

Comparing Eq. (4.24) and Eq. (4.25), we see that the corresponding coefficients do not differ very considerably, showing that truncation of the power series to the cubic term would not drastically affect the retained dipole moment coefficients.

The function $M^2(y)$ can also be expanded as an infinite power series in u as

$$M(u) = m_0 + \sum_{n=1}^{\infty} m_n u^n, \tag{4.26}$$

which actually is a Taylor series. Since this series is of practical interest, it is worthwhile to determine its coefficients from the coefficients M_n by a relationship derived in Appendix E.

We list the results in Table 4.7 and write the power series in u explicitly up to cubic term:

$$M^{*}(u) = 1.7979 + 1.5516u - 0.6661u^2 - 0.4642u^3 + \cdots (4.28)$$

Comparing these first few terms to the cubic polynomial obtained previously

$$M(u) = 1.795 + 1.5232u - 0.0807u^2 - 1.4129u^3$$

shows that the truncation and the inclusion of a large number of the transition matrix elements in the minimization would affect the linear term only slightly. This is also the reason why cubic polynomials in u or y have been widely used to represent the dipole moment of the diatomic molecules.

To conclude this chapter, we may say that the functional form $M^1(y)$ is the most suitable to represent the dipole moment that changes sign as in the case of CO [33,34,37,38] while $M^2(y)$ (so far being the only choice) should be used to represent the dipole moment which does not change signs as in our case.

Table 4.1. Most Reliable Experimental Vibrational Matrix Elements $\mu_{vv'}$ (units of debye)

μ_{00}	μ_{01}	μ_{02}	μ_{03}
1.819	9.850D-2	—1.253D-2	1.628D-3
Ref [23]	∓.370D-2	∓.047D-2	∓.061D-3
μ_{12}	μ_{13}	μ_{23}	
1.374D-1	—1.909D-2	1.392D-1	
Ref [25]	Ref [26]	Ref [26]	

D-2 stands for 10^{-2}

Table 4.2. Coefficients of Various Cubic Polynomials in Variables u, y, and z as HF Dipole Moment

	P_0	P_1	P_2	P_3
$M(u)$	1.7958	1.523	—8.065D-2	—1.412
$M(y)$	1.7958	6.213D-1	2.949D-1	7.432D-2
$M(z)$	1.7958	6.215D-1	—3.203D-1	9.439D-2

D-2 stands for 10^{-2}

Table 4.3. Coefficients in the Dipole Moment Functions $M^1(y)$ and $M^2(y)$ with Correct Large-r Behavior

	M_0	C_1	C_2	C_3	C_4	B
$M^1(y)$	1.790488	—45.017124	225.40443	—12.419533	—358.40518	0.5552209
$M^2(y)$	1.797887	—0.21179768	0.87378465	0	0	0.95514959

Table 4.4. Comparison of the matrix elements generated by various models with those obtained experimentally

i i'	Model 1: ab initio dipole		Model 2: our best dipole		Experimental data
	$\mu_{ii'}^{(1)}$	Δ_2	$\mu_{ii'}^{(2)}$	Δ_3	$\mu_{ii'}^{exp}$
0 0	1.823	-0.404D-2	1.819	0.0	1.819
0 1	0.439D-1	0.545D-1	0.993D-1	-0.008D-1	0.985D-1
0 2	-0.723D-2	-0.546D-2	-0.155D-1	0.028D-1	-0.127D-1
0 3	0.136D-2	0.510D-3	0.307D-2	-0.12D-2	0.187D-2
0 4	-0.326D-3	-0.335D-4	-0.804D-3	0.444D-3	-0.36D-3
0 5	0.944D-4	-0.128D-4	0.254D-3	-0.172D-3	0.816D-4
0 6	-0.314D-4	0.962D-5	-0.919D-4	-0.701D-4	-0.218D-4
1 2	0.0603	0.776D-1	0.137	0.001	0.138
1 3	-0.126D-1	-0.064D-1	-0.271D-1	0.043D-1	-0.228D-1
1 4	0.275D-2	0.114D-2	0.614D-2	-0.224D-2	0.389D-2
1 5	-0.737D-3	-0.124D-3	-0.178D-2	0.682D-2	-0.862D-3
1 6	0.233D-3	-0.132D-4	0.613D-3	-0.393D-3	0.22D-3
1 7	-0.838D-4	0.205D-4	-0.238D-3	1.75D-4	0.633D-4
2 3	0.713D-1	0.094	0.164	0.002	0.166
2 4	-0.179D-1	-0.154D-1	-0.384D-1	0.05D-1	-0.334D-1
2 5	0.440D-2	0.199D-2	0.972D-2	-0.332D-2	0.64D-2
2 6	-0.129D-2	-0.028D-2	-0.306D-3	0.148D-2	-0.158D-2
2 7	0.441D-3	0.002D-3	0.113D-2	-0.069D-2	0.444D-3
2 8	-0.169D-3	0.03D-3	-0.470D-3	0.331D-3	-0.139D-3
3 4	0.789D-1	0.108	0.183	0.004	0.187
3 5	-0.233D-1	-0.213D-1	-0.499D-1	0.052D-1	-0.447D-1
3 6	0.630D-2	0.311D-2	0.137D-1	-0.043D-1	0.942D-2
3 7	-0.200D-2	-0.56D-2	-0.466D-2	0.209D-2	-0.257D-2

Table 4.4 (Continued)

	Model 1: ab initio dipole		Model 2: our best dipole		Experimental data
i i'	$\mu^{(1)}_{ii'}$	Δ_2	$\mu^{(2)}_{ii'}$	Δ_3	$\mu^{exp}_{ii'}$
3 8	0.730D-3	0.049D-3	0.183D-2	-1.0D-3	0.780D-3
3 9	-0.298D-3	0.038D-3	-0.805D-3	0.546D-3	-0.259D-3
4 5	0.839D-1	1.18D-1	0.197	-0.005	0.202
4 6	-0.286D-1	-0.282D-1	-0.615D-1	0.0460D-1	-0.569D-1
4 7	0.084D-1	0.044D-1	0.183D-1	-0.054D-1	0.129D-1
4 8	-0.287D-2	-0.095D-2	-0.658D-2	0.275D-2	-0.383D-2
4 9	0.111D02	0.014D-2	0.273D-2	-0.147D-2	0.126D-2
5 6	0.866D-1	0.125	0.207	-0.005	0.212
5 7	-0.340D-1	-0.360D-1	-0.731D-1	0.030D-1	-0.701D-1
5 8	0.108D-1	0.061D-1	0.233D-1	-0.063D-1	0.170D-1
5 9	-0.393D-2	-0.149D-2	-0.885D-2	0.34D-2	-0.543D-2
6 7	0.871D-1	1.27D-1	0.211D-1	-0.014D-1	0.215D-1
6 8	-0.393D-1	-0.454D-1	-0.849D-1	0.001D-1	-0.848D-1
6 9	0.135D-1	0.080D-1	0.289D-1	-0.074D-1	0.215D-1
7 8	0.853D-1	0.125	0.212	-0.001	0.211
7 9	-0.044	-0.056	-0.097	0.004	-0.101
8 9	0.081	0.116	0.207	-0.009	0.198
	Δ^1_{rms} = 0.52D-1		Δ^2_{rms} = 0.72D-2		

note 1: $\Delta_j = \mu^{exp}_{ii'} - \mu^{(j)}_{ii'}$

note 2: Δ^j_{rms} is the root mean squre error between model j and experimental data.

note 3: 1.D-1 stands for 10^{-1}

Table 4.5. Values of the Parameters M_0, c_1, c_2, c_3, c_4, B, and M_c For the Generating Functions M_n^1 and M_n^2

Functional Form	M_0	c_1	c_2	c_3	c_4	B	M_c
M_n^1	1.790	—50.865	266.63	—26.731	—425.24	0.55047	—1.0750
M_n^2	1.7979	—0.21118	0.87231	0	0	0.955249	0.7062 D-3

4.6. Comparison Between our HF Dipole Moment Function with Correct Asymptotic Behavior at Both Small and Large r, $M^2(y)$ and those determined theoretically and experimentally by other authors

r(Å)	$M^{cal^{(1)}}$ (Debye)	$M^{exp^{(1)}}$ (Debye)	our best $M^2(y)$
0.0	*	*	0.0
0.100	*	*	0.230
0.200	*	*	0.449
0.300	*	*	0.659
0.400	*	*	0.862
0.500	*	*	1.060
0.662	1.446	1.422	1.364
0.688	1.485	1.457	1.412
0.741	1.563	1.532	1.506
0.794	1.640	1.609	1.597
0.847	1.719	1.689	1.686
0.917	1.816	1.797	1.798
1.005	1.917	1.929	1.930
1.058	1.969	2.005	2.003
1.164	2.031	2.143	2.134
1.323	2.004	2.298	2.283
1.587	1.641	2.332	2.373
2.117	0.600	0.997	1.838
2.646	0.155	-3.250	0.871
3.704	0.012	*	0.085
5.292	0.002	*	0.002

(1) from Ref. (27)

(*) not listed in this Ref.

Table 4.7. Coefficients of the HF Dipole Moment as an Infinite Power Series in y Given by the Model $M_n^2 = (c_1 + c_2/n)B^n$ and coefficients m_n^* of the equivalent infinite power series in u

Coefficients of the y Series		Coefficients of the equivalent u Series	
M_n	value	m_n^*	value
M_0	+1.79790	m_n^*	+1.79
M_1	+0.63165	m_1^*	+1.55155
M_2	+0.20542	m_2^*	—0.66612
M_3	+0.68828E-1	m_3^*	—0.46417
M_4	+0.52203E-2	m_4^*	—0.16422
M_5	—0.29705E-1	m_5^*	—0.18061E-1
M_6	—0.50468E-1	m_6^*	+0.64834E-1
M_7	—0.63284E-1	m_7^*	+0.30882E-1
M_8	—0.71252E-1	m_8^*	—0.20909E-1
M_9	—0.76087E-1	m_9^*	—0.40876E-2
M_{10}	—0.78814E-1	m_{10}^*	—0.37228E-2
M_{11}	—0.80080E-1	m_{11}^*	—0.45489E-2
M_{12}	—0.80311E-1	m_{12}^*	—0.10325E-2
M_{13}	—0.79801E-1	m_{13}^*	+0.59331E-4
M_{14}	—0.78755E-1	m_{14}^*	+0.60910E-3
M_{15}	—0.77321E-1	m_{15}^*	+0.30590E-3

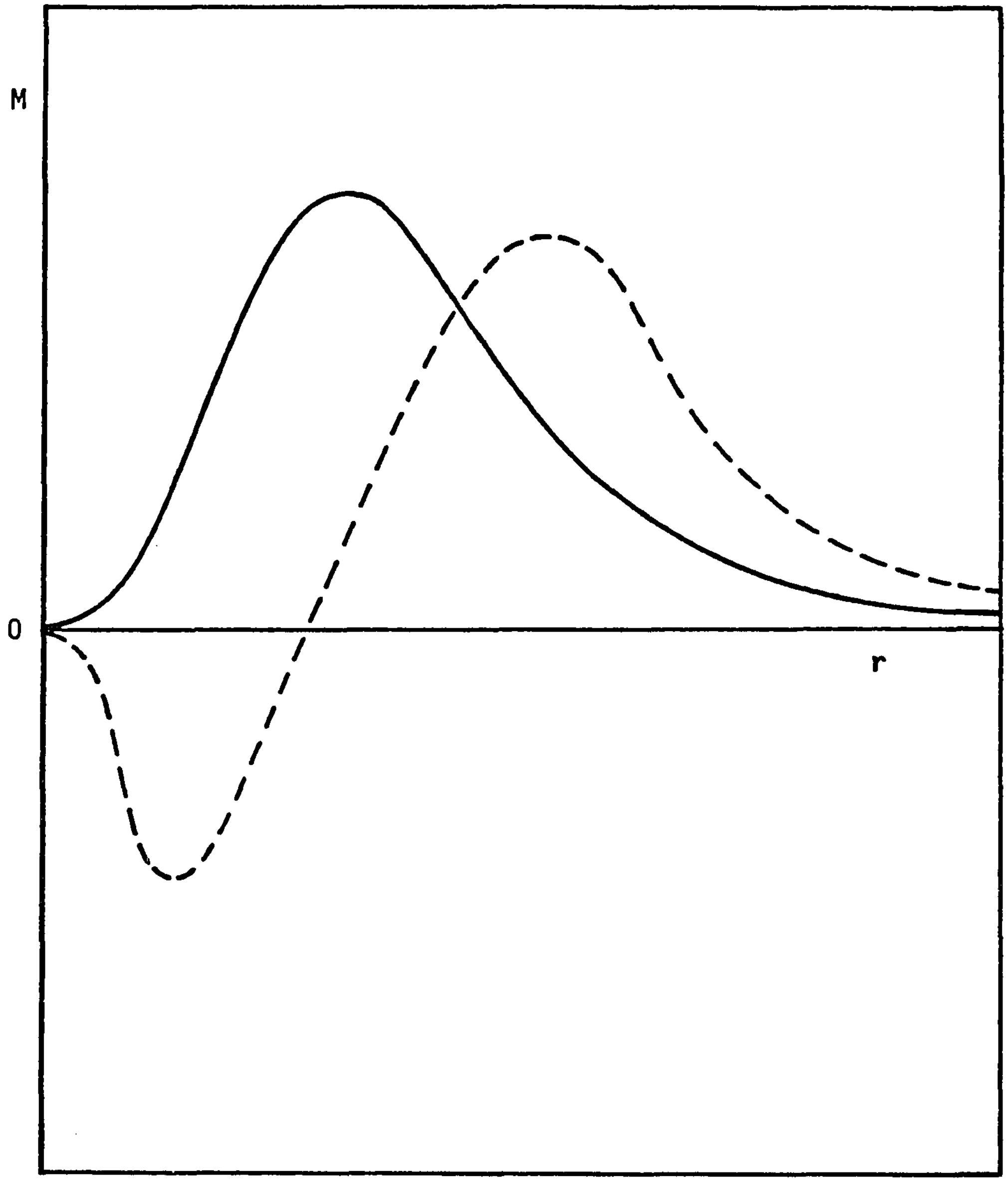

Fig. 4.1. General shape of the dipole moment of diatomic molecules as a function of the internuclear distance.

——— : Dipole moment with unique polarity.

– – – – – : Dipole moment with reversal of polarity.

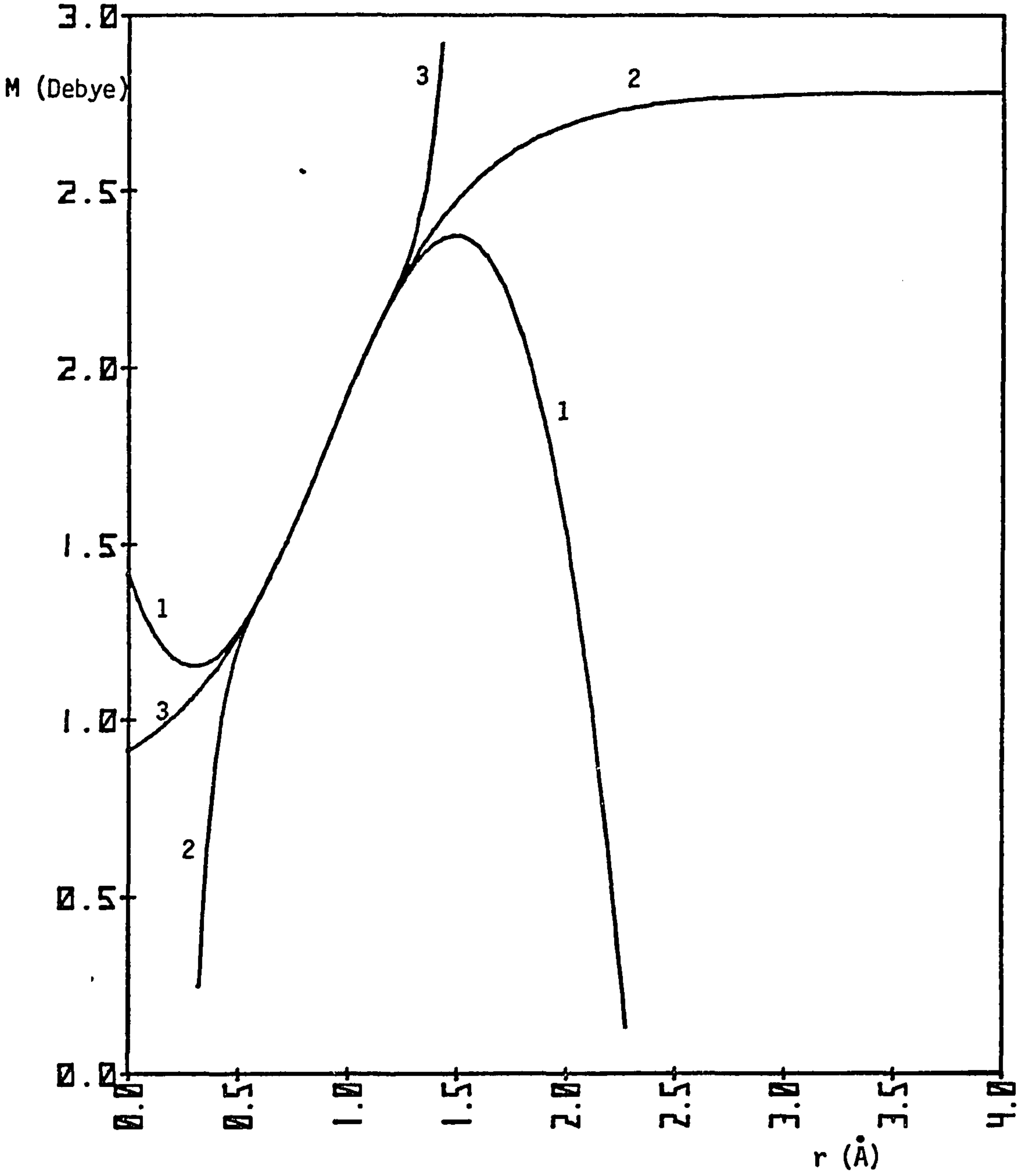

Fig. 4.2. Dipole moment of HF as a cubic polynomial in u (curve 1), in y (curve 2), and in z (curve 3).

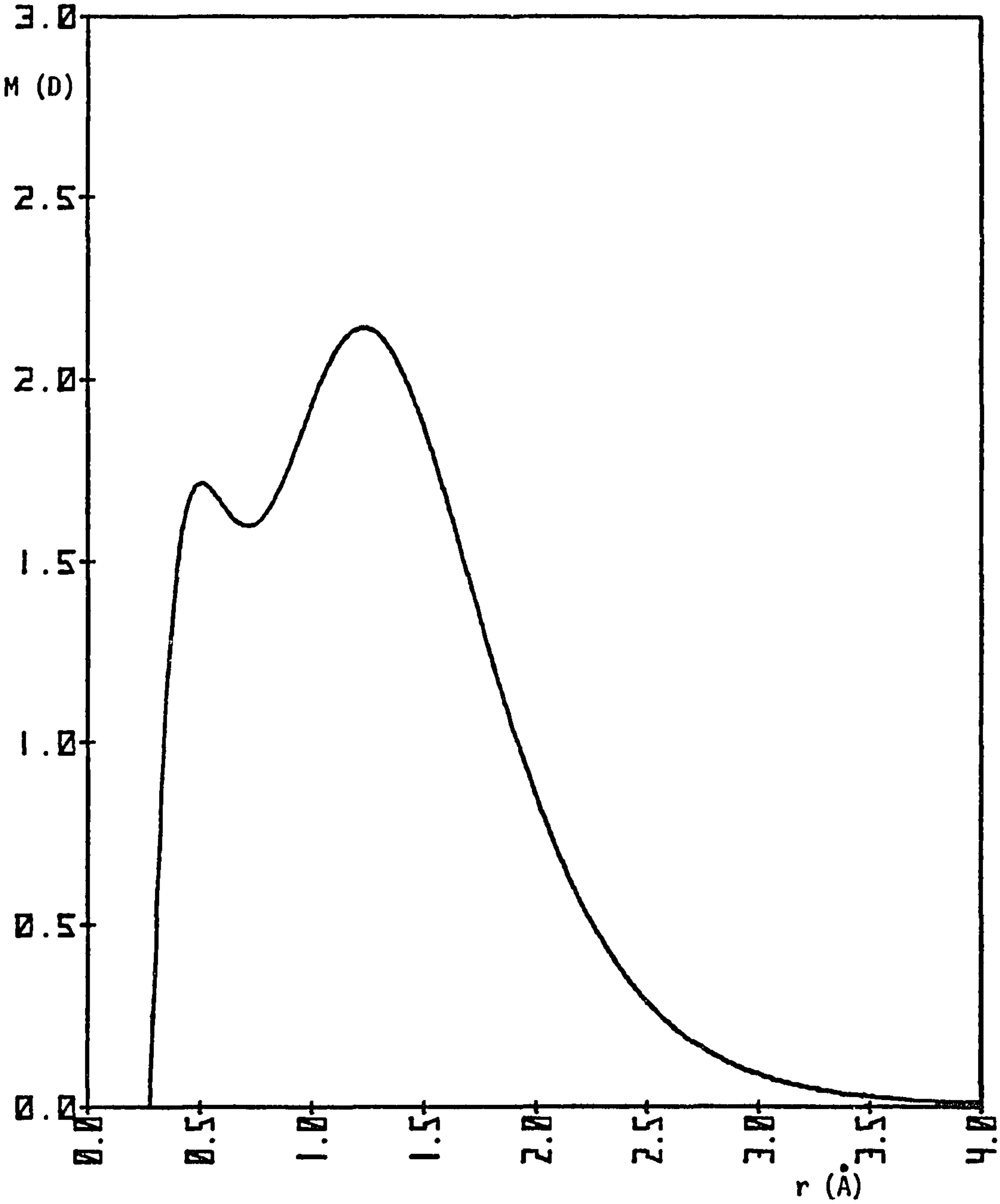

Fig. 4.3. HF dipole moment function $M^1(y)$ with correct large-r behavior, obtained by minimization using a small number of experimental transition matrix elements.

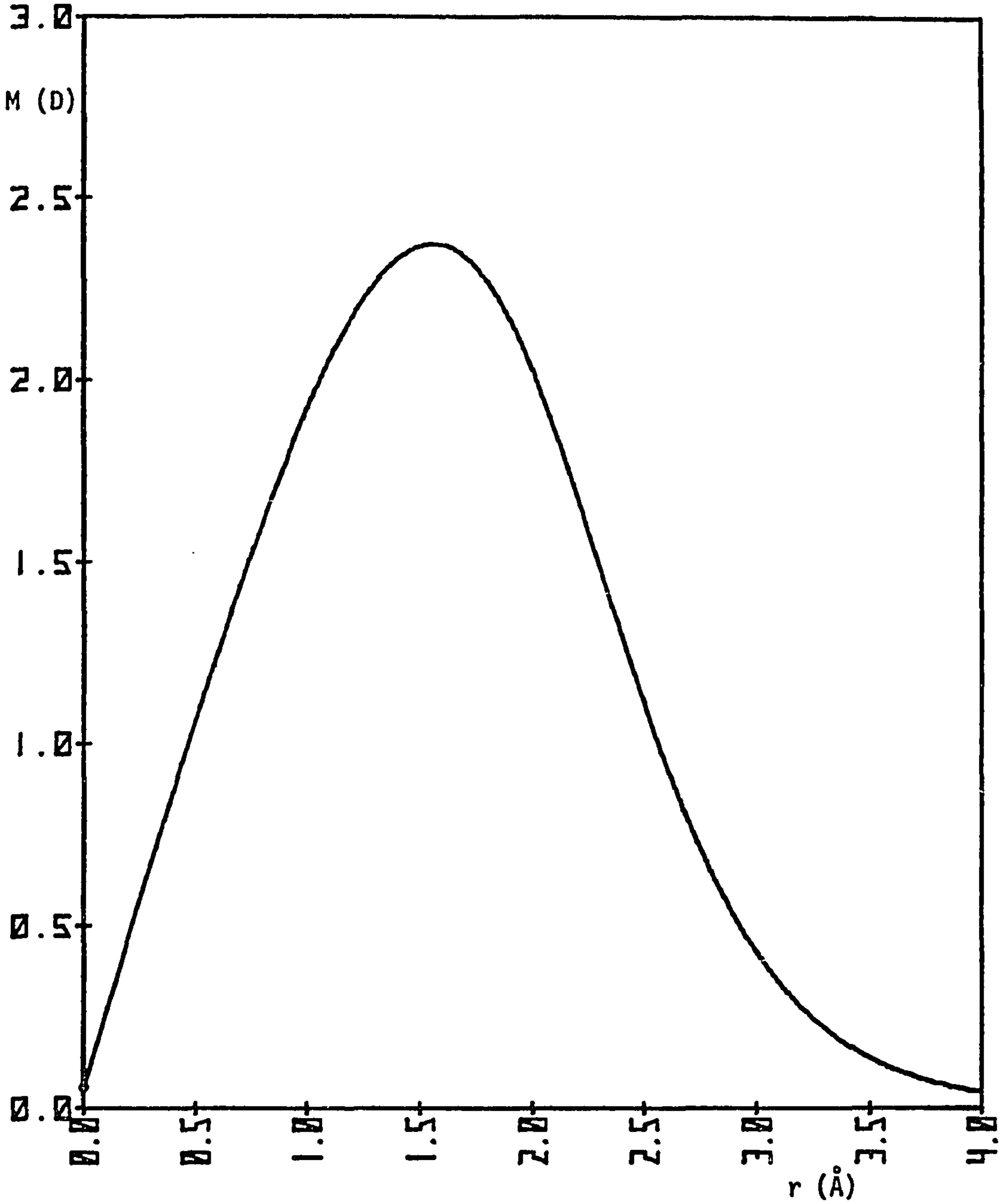

Fig. 4.4. HF dipole moment function $M^2(y)$ with correct large-r behavior, obtained by minimization using a large number of experimental transition matrix elements.

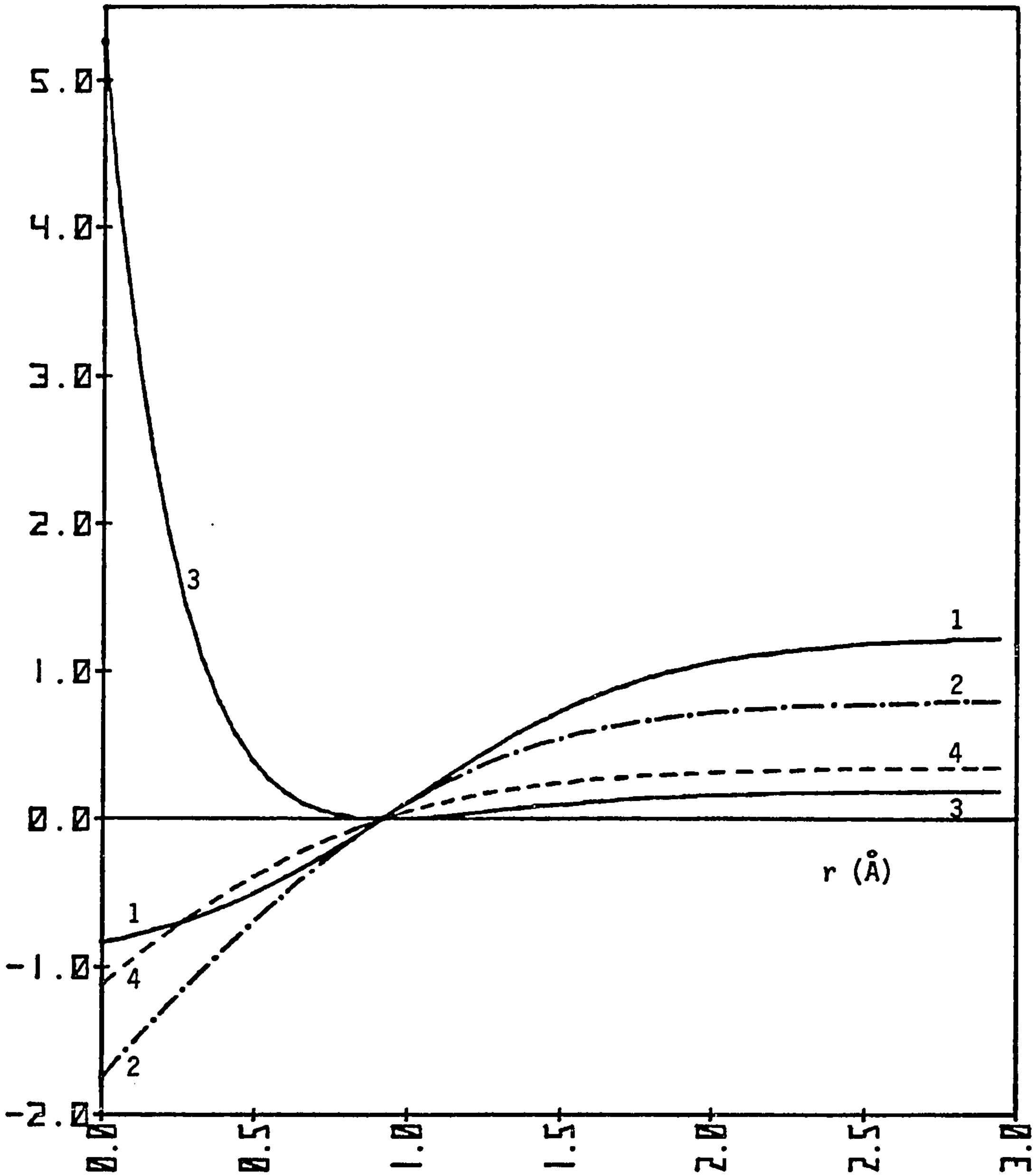

Fig. 4.5. Variation with r of the factors of c_1, c_2, c_3, and c_4 in the dipole moment function $M^1(y)$.

Curve 1: By/(1-By) ; Curve 2: -ln(1-By) ;

Curve 3: By + (1-By)ln(1-By) ; Curve 4: 1 + (1-By)ln(1-By)/By.

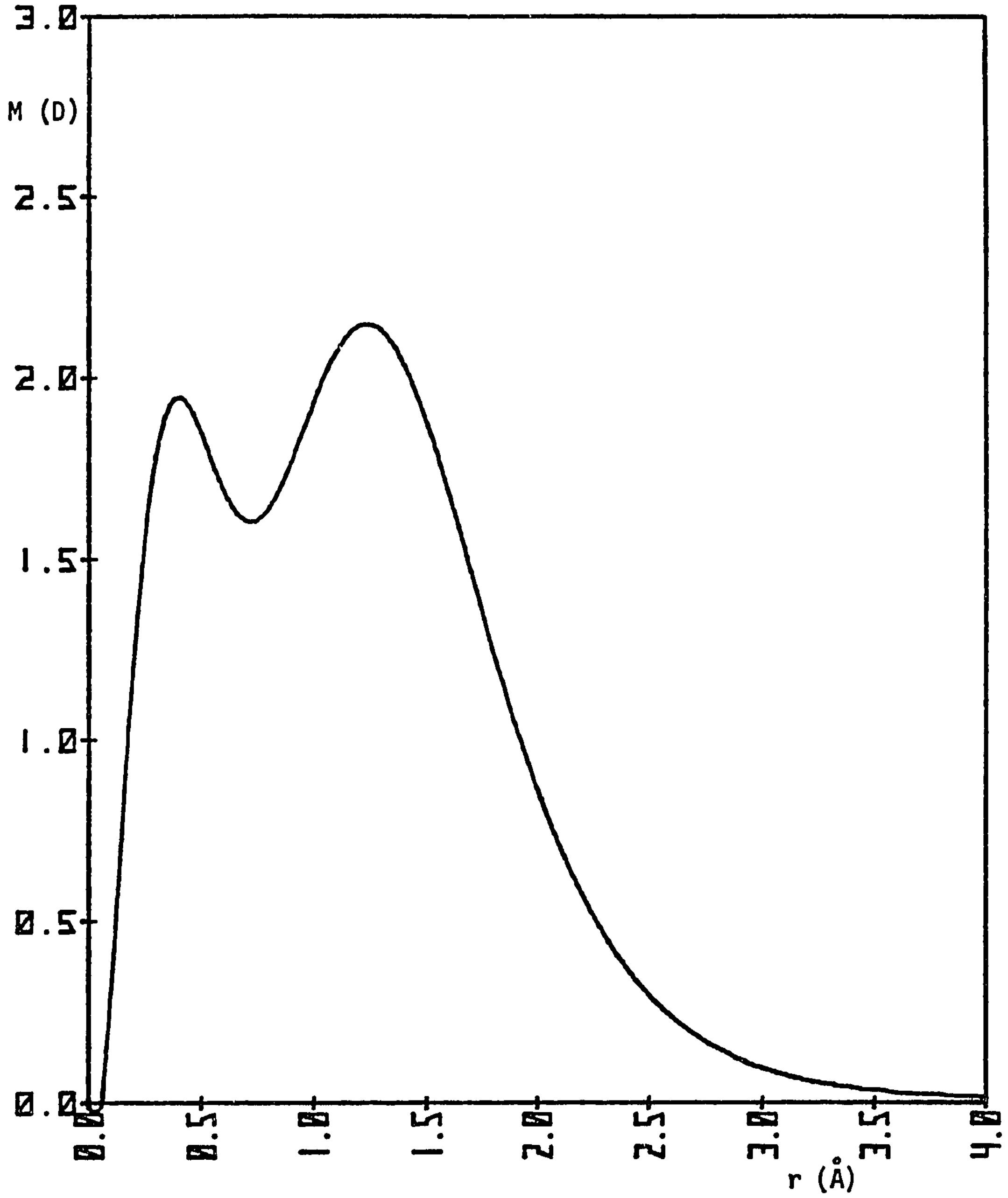

Fig. 4.6. HF dipole moment function $M^1(y)$ with correct large-r and small-r behavior, obtained by minimization using a small number of experimental transition matrix elements.

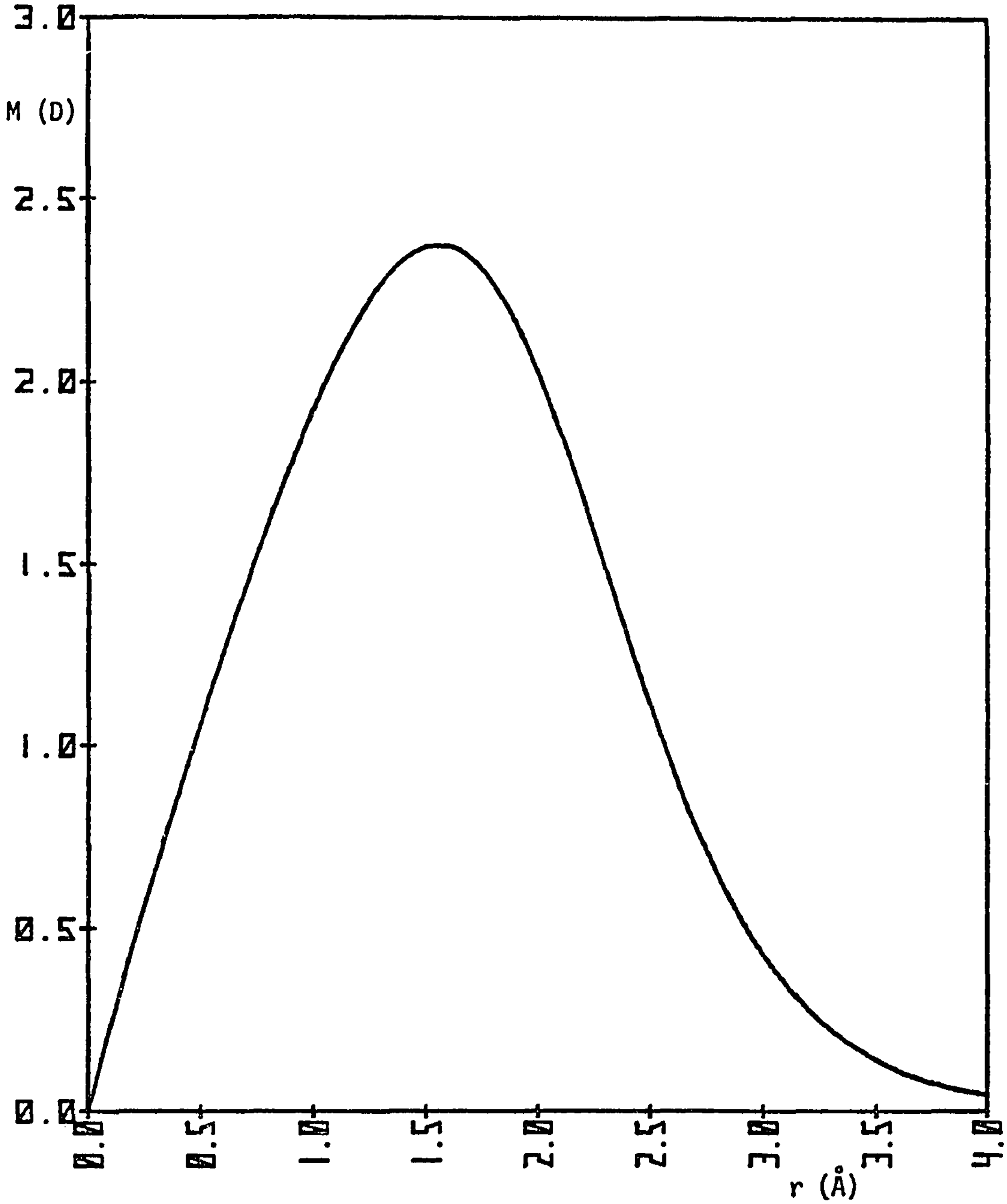

Fig. 4.7. HF dipole moment function $M^2(y)$ with correct large-r and small-r behavior, obtained by minimization using a large number of experimental transition matrix elements.

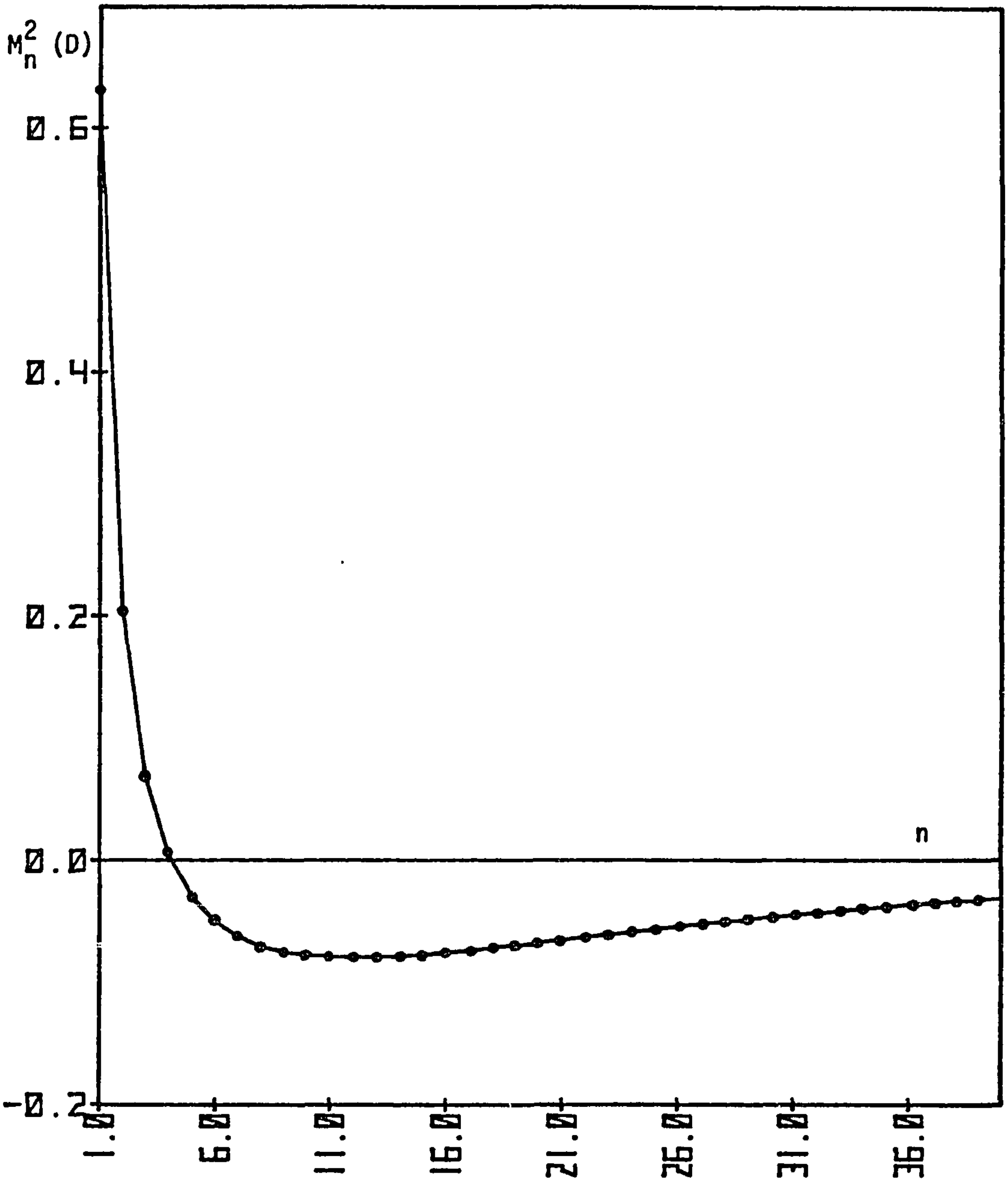

Fig. 4.8. Plot of the generating function $M_n^2 = (c_1 + c_2)B^n$ versus the index n.

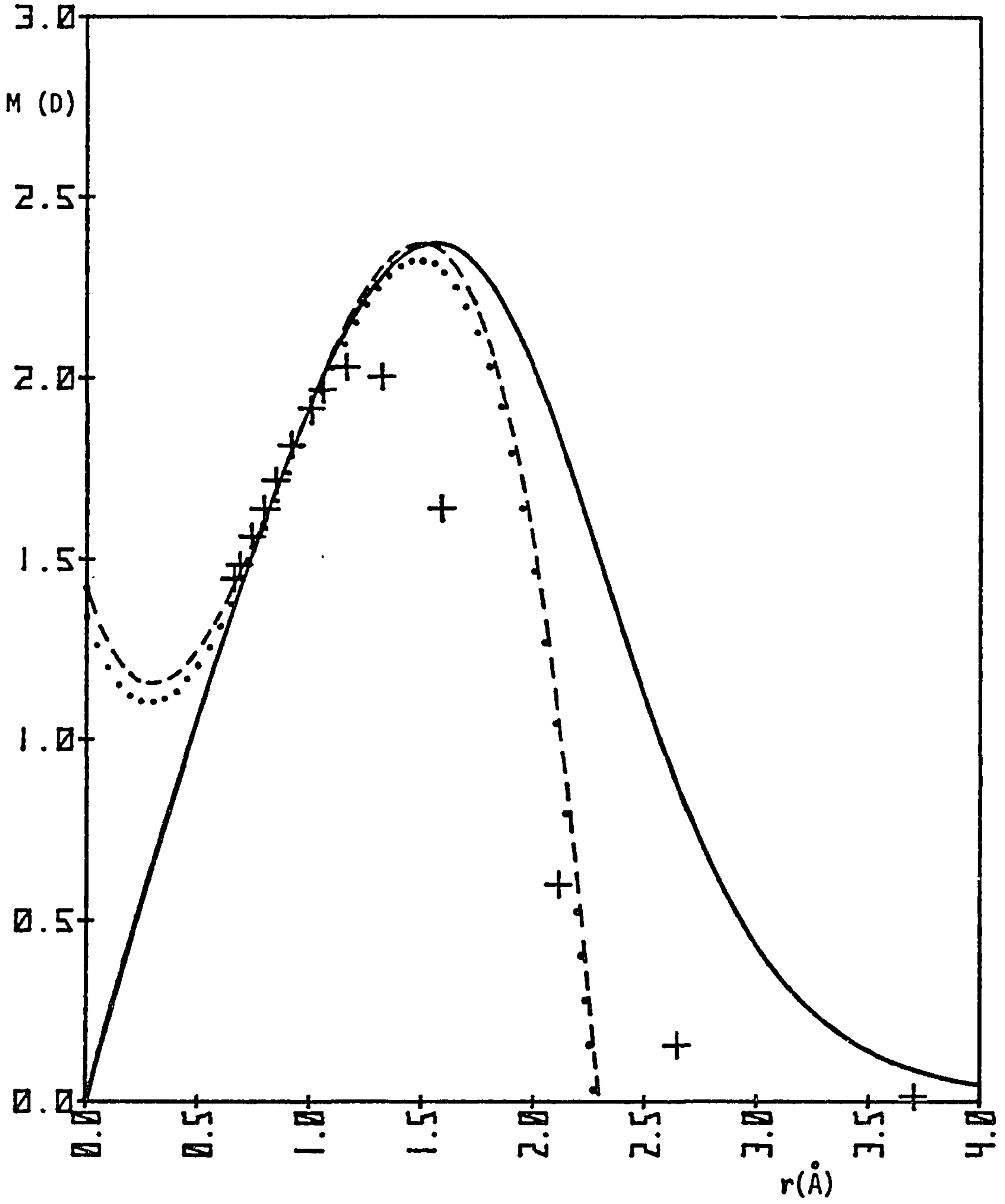

Fig. 4.9. Comparison of various dipole moment functions for HF.

———— : Our best dipole moment function $M^2(y)$.

– – – – – : Our cubic dipole moment function M(u).

• • • • • : Cubic dipole moment function from Ref.(29).

+ + + + + : Ab initio dipole moment by Lie (Ref.(27)).

CHAPTER V

CONCLUSIONS

In this work we have shown that the infinite series in powers of y is a very useful representation of many quantities of a diatomic molecule, as we have applied it to determine the internuclear potential energy and the dipole moment of HF. In case of a heavy molecules such as CO, a truncated version of this series is sufficient to represent its internuclear potential for many bound-state levels. However, for lighter molecules like HF, the truncated series still can be used, but the breakdown of the Born-Oppenheimer approximation should be accomodated in the modified Dunham's coefficients.

We have gone further by developing a method to determine the HF internuclear potential function which has the correct asymptotic behavior and at the same time is capable of reproducing not only accurate vibrational eigenenergies but also accurate term values and rotational constants. For this purpose, we have expressed higher-order PMO parameters b_n with $n > 12$ as a function of n, which goes to zero as n approaches infinity. Several functional forms have been tested, and the one giving the best results is found to be $(c_1 + c_2/n + c_3/n(n-1) + c_4/n(n+1))B^n$. In this way the potential is represented by an infinite power series in y, which however can be cast in a finite analytical form containing a reasonable number of parameters. These parameters then have been determined by a least-squares fitting of experimental spectroscopic data. Our PMO potential function thus obtained is at least as accurate as the RKR counterpart but obviously offers a lot more of convenience and economy.

The same idea has been applied to obtain the dipole moment of HF with correct large-r asymptotic property, to which a suitable corrective term has been added so that its correct small-r behavior can also be attained. Among the various functional forms proposed, we have found that only the model $M_n = (c_1 + c_2/n)B^n$ works best for HF whose dipole moment has unique polarity. The calculation of this dipole moment function has been performed numerically, using the highly accurate PMO potential obtained previously to solve for the vibrational eigenfunctions, and a large number of available transition matrix elements (experimentally deduced) in the process of minimization.

The dipole moment functions of HF as cubic polynomials in u, y and z have also been determined because they are of practical interest and besides their calculation is rather easy and straightforward.

APPENDIX A

CALCULATION OF e_n, f_n AND g_n IN TERMS OF d_n

1. Calculation of e_n

Multiplying Eq. (2.2a) and Eq. (2.2b) by each other, we obtain [10]

$$1 = \sum_{m,n=0} d_n e_m w^{(n+m)/2}. \qquad (A.1)$$

Since the coefficients of every power of w except w^0 must vanish in Eq. (A.1), we have the following:

$$1 = d_0 e_0; \quad e_0 = d_0^{-1}$$

$$e_0 d_1 + e_1 d_0 = 0; \quad e_1 = -\frac{d_1 e_0}{d_0};$$

$$e_0 d_2 + e_1 d_1 + e_2 d_0 = 0; \quad e_2 = -\frac{e_1 d_1 + e_0 d_2}{d_0};$$

$$e_2 d_1 + e_1 d_2 + e_0 d_3 + e_3 d_0 = 0; \quad e_3 = -\frac{e_2 d_1 + e_1 d_2 + e_0 d_3}{d_0};$$

$$\cdots$$

$$e_0 d_N + e_1 d_N + \cdots, + e_N d_0 = 0; \quad e_N = -\frac{1}{d_0} \sum_{n=0}^{N-1} e_n d_{N-n}. \qquad (A.2)$$

2. Calculation of f_n

Raising Eq. (2.2b) to the third power, we obtain

$$(\frac{w'}{\rho})^3 = 8w^{\frac{3}{2}} \sum_{k,l,m=0}^{\infty} e_k e_l e_m w^{\frac{k+l+m}{2}} = 8w^{\frac{3}{2}} \sum_{n=0}^{\infty} f_n w^{\frac{n}{2}},$$

and equating coefficients of $w^{\frac{n}{2}}$, we get

$$f_n = \sum_{k=0}^{n} \sum_{l=0}^{n-k} e_k e_l e_{n-k-l}. \qquad (A.3)$$

3. Calculation of g_n

Differentiating Eq. (2.2b) with respect to ξ, (ξ is defined in Eq. (2.10)), we have

$$\begin{aligned} \frac{w''}{\rho^2} &= \sum_{n=0} (n+1) e_n e^{(n-1)/2} \frac{w'}{\rho}, \\ &= 2 \sum_{\substack{n=0 \\ m=0}} (n+1) e_n e_m w^{(n+m)/2}, \end{aligned}$$

where $w' = \frac{dw}{d\xi}$.

Differentiating again and dividing again by ρ yields

$$\begin{aligned} \frac{w'''}{\rho^3} &= \sum_{\substack{n=0 \\ m=0}} (n+1)(n+m) e_n e_m w^{\frac{(n+m-2)}{2}} \frac{w'}{\rho}, \\ &= \frac{2}{\sqrt{w}} \sum_{m,n,l} (n+1)(n+m) e_n e_m e_l w^{(n+m+l)/2}, \\ &= \frac{2}{\sqrt{w}} \sum_{j=0} g_j w^{\frac{j}{2}}. \end{aligned}$$

Equating coefficients of $w^{\frac{j}{2}}$, we find

$$g_j = \sum_{m=0}^{n} \sum_{n=0}^{j-m} (n+1)(n+m) e_n e_m e_{j-n-m}. \qquad (A.4)$$

APPENDIX B

CONVERGENCE OF THE INFINITE POWER SERIES $M(u)$, $M(y)$ AND $M(z)$

Given an infinite power series in variable q in the form

$$M(q) = M_0 + \sum_{n=1}^{\infty} M_n q^n. \tag{B.1}$$

This series will be convergent if the following condition is satisfied

$$\lim_{n\to\infty} \left|\frac{M_{n+1} q^{n+1}}{M_n q^n}\right| = \lim_{n\to\infty} \left|\frac{M_{n+1}}{M_n} q\right| < 1, \tag{B.2}$$

which is equivalent to

$$|q| \cdot \lim_{n\to\infty} \left|\frac{M_{n+1}}{M_n}\right| < 1. \tag{B.3}$$

If $\lim|\frac{M_{n+1}}{M_n}| < 1$ then we must have $|q| \leq 1$ so that the inequality (B.3) is satisifed.

The dipole moment function as an infinite power series in $u = r - r_e$ can be written as

$$M(u) = m_0 + \sum_{n=1}^{\infty} m_n u^n = m_0 + \sum_{n=1}^{\infty} m_n r_e^n \left(\frac{r - r_e}{r_e}\right)^n.$$

Assuming that $\lim_{n\to\infty}|\frac{m_{n+1}}{m_n} r_e| < 1$, then from Eq. (B.3) this series will converge if $|\frac{r-r_e}{r_e}| \leq 1$, or $|r - r_e| \leq r_e$, or

$$0 \leq r \leq 2r_e. \tag{B.4}$$

For HF,

$$0 \leq r \leq 1.8336 \text{ Å}. \tag{B.5}$$

For the power series in the variable $y = 1 - e^{-a(r-r_e)}$,

$$M(y) = M_0 + \sum_{n=1}^{\infty} M_n y^n,$$

if $\lim|\frac{M_{n+1}}{M_n}| < 1$, then from Eq. (B.3) the condition for its convergence is [38]

$$|y| \leq 1 \quad \text{or} \quad -1 \leq y < 1.$$

This imposes a condition on r:

$$r_e - \frac{1}{a}\ln 2 \leq r \leq \infty. \tag{B.6}$$

In particular, for HF the convergence range is

$$0.6346 \text{ Å} \leq r \leq \infty. \tag{B.7}$$

Similarly, the convergence of the infinite power series in $z = e^{a(r-r_e)} - 1$,

$$M(z) = T_0 + \sum_{n=1}^{\infty} T_n z^n,$$

requires that

$$|z| \leq 1 \quad \text{or} \quad -1 \leq z \leq 1,$$

or

$$-\infty < r < r_e + \frac{1}{a}\ln 2. \tag{B.8}$$

Applying this relation to HF, we obtain

$$-\infty \leq r \leq 1.1990 \tag{B.9}$$

APPENDIX C

EVALUATING DIFFERENT POWER SERIES

The following infinite power series can be represented by simple analytical functions [38,39]:

$$\sum_{n=1}^{\infty} x^n = x(1+x+x^2+\cdots) = \frac{x}{1-x}; \tag{C.1}$$

$$\begin{aligned}\sum_{n=1}^{\infty} nx^n &= x\sum_{n=1}^{\infty} nx^{n-1} = x\frac{d}{dx}(\sum_{n=1}^{\infty} x^n), \\ &= x\frac{d}{dx}(\frac{x}{1-x}) = \frac{x}{(1-x)^2};\end{aligned} \tag{C.2}$$

$$\begin{aligned}\sum_{n=1}^{\infty} \frac{x^n}{n} &= -(-x-\frac{x^2}{2}-\frac{x^3}{3}\cdots-\frac{x^n}{n}), \\ &= -\ln(1-x);\end{aligned} \tag{C.3}$$

$$\begin{aligned}\sum_{n=1}^{\infty} \frac{x^n}{n(n+1)} &= \sum_{n=1}^{\infty}(\frac{x^n}{n}-\frac{x^n}{n+1}) = \sum_{n=1}^{\infty}\frac{x^n}{n}-\frac{1}{2}\sum_{n=1}^{\infty}\frac{x^{n+1}}{n+1}, \\ &= -\ln(1-x)-\frac{1}{x}(-x+\sum_{n=1}^{\infty}\frac{x^n}{n}), \\ &= -\ln(1-x)-\frac{1}{x}(-x-\ln(1-x)), \\ &= 1+(\frac{1-x}{x}\ln(1-x);\end{aligned} \tag{C.4}$$

$$\begin{aligned}
\sum_{n=2}^{\infty} \frac{x^n}{n(n-1)} &= \sum_{n=2}^{\infty} \left(-\frac{x^n}{n} + \frac{x^n}{n-1}\right), \\
&= -\sum_{n=2}^{\infty} \frac{x^n}{n} + x \sum_{n=2}^{\infty} \frac{x^{n-1}}{n-1}, \\
&= x - \sum_{n=1}^{\infty} \frac{x^n}{n} + x \sum_{n=1}^{\infty} \frac{x^n}{n}, \\
&= x + \ln(1-x) - x \ln(1-x), \\
&= x + (1-x) \ln(1-x). \qquad (C.5)
\end{aligned}$$

APPENDIX D

NUMEROV METHOD

The Numerov method is usually used for solving a linear, second order, and self adjoint differential equation of the form [35]

$$y'' = F(x,y).$$

We proceed by the method of undetermined coefficients:

$$y_{k+1} = Ay_k + By_{k-1} + h^2(CF_{k+1} + DF_k + EF_{k-1}) + R. \quad (D.1)$$

We start from the Taylor series expansions of y_{k+1}, y_{k-1}, F_{k+1}, and F_{k-1}, around point x:

$$\begin{aligned} y_{k+1} &= y_k + hy_k^{(1)} + \frac{1}{2}h^2 y_k^{(2)} + \frac{1}{3!}h^3 y_k^{(3)} \\ &\quad + \frac{1}{4!}h^4 y_k^{(4)} + \frac{1}{5!}h^5 y_k^{(5)} + \frac{1}{6!}h^6 y^{(6)}, \qquad (D.2a) \\ y_{k-1} &= y_k - hy_k^{(1)} + \frac{1}{2!}h^2 y_k^{(2)} - \frac{1}{3!}h^3 y_k^{(3)} \\ &\quad + \frac{1}{4!}h^4 y_k^{(4)} - \frac{1}{5!}h^5 y_k^{(5)} + \frac{1}{6!}h^6 y^{(6)}, \qquad (D.2b) \\ h^2 F_{k+1} &= h^2 y_k^{(2)} + h^3 y_k^{(3)} + \frac{1}{2!}h^4 y_k^{(4)} + \frac{1}{3!}h^5 y_k^{(5)} \\ &\quad + \frac{1}{4!}h^6 y^{(6)}, \qquad (D.2c) \\ h^2 F_{k-1} &= h^2 y_k^{(2)} - h^3 y_k^{(3)} + \frac{1}{2!}h^4 y_k^{(4)} - \frac{1}{3!}h^5 y_k^{(5)} + \frac{1}{4!}h^6 y^{(6)}. \qquad (D.2d) \end{aligned}$$

Substituing y_{k+1}, y_{k-1} h^2F_{k+1}, and h^2F_{k-1} from Eq. (D.2) into Eq. (D.1) and matching the coefficients of different powers of h (up to h^4) on both sides of Eq. (D.1) we get

$$A = 1,\ B = -1,\ C = \frac{1}{12},\ D = \frac{5}{6},\ E = \frac{1}{12},\ \text{and}\ R = -\frac{h^6 y^{(6)}}{6!}.$$

Thus, we obtain

$$y_{k+1} = 2y_k - y_{k-1} + \frac{1}{12}h^2(F_{k+1} + 10F_k + F_{k-1}) + R, \qquad (D.3)$$

which is the basic formula of the Numerov method. The radial Schrödinger equation can be written in a unitless form as

$$\frac{d^2\psi_i}{dr^2} = [V_i - E]\psi_i. \qquad (D.4)$$

Using Eq. (D.3) we can find the numerical solution to Eq. (D.4) as [35]

$$\psi_{i+1} = 2\psi_i - \psi_{i-1} + \frac{1}{12}h^2[\psi_{i+1}(V_{i+1} - E) + 10\psi_i(V_i - E) + \psi_{i-1}(V_{i-1} - E)],$$

which is equivalent to the pair of equations

$$Y_{i+1} + Y_{i-1} - 2Y_i = h^2(V_i - E)\psi_i$$

$$Y_i = [1 - (h^2/12)(V_i - E)],$$

where h is the separation between adjacent r values and E is a trial eigenvalue.

APPENDIX E

1. Relationship Between m_n and M_n

In Chapter IV we introduced three infinite power series [Eq. (4.1)], [38],

$$M(u) = m_0 + \sum_{n=1}^{\infty} m_n u^n, \qquad (E.1)$$

$$M(y) = M_0 + \sum_{n=1}^{\infty} M_n y^n, \qquad (E.2)$$

$$\text{and} \quad M(z) = T_0 + \sum_{n=1}^{\infty} T_n z^n, \qquad (E.3)$$

where $m_0 = M_0 = T_0$. If the coefficients of one series are known, then corresponding coefficients of the other two series can be evaluated as shown in the following. Using $y = 1 - \exp(-au)$ and the binomial theorem, we can write

$$\begin{aligned} y^n &= (1 - e^{-au})^n = \sum_{k=0}^{n} (-1)^k \binom{n}{k} e^{-auk}, \\ &= \sum_{k=0}^{n} \sum_{m=0}^{\infty} (-1)^{k+m} \binom{n}{k} \frac{k^m a^m u^m}{m!}, \qquad (E.4a) \\ &= \sum_{k=0}^{n} (-1)^k \binom{n}{k} + \sum_{m=1}^{\infty} \sum_{k=1}^{n} (-1)^{k+m} \binom{n}{k} \frac{k^m (au)^m}{m!}. \qquad (E.4b) \end{aligned}$$

The summation $\sum_{k=0}^{m}(-1)^k\binom{n}{k}$ can be shown to be zero (replace e^{-au} by

1 in both sides of the Eq. (E.4a)). The Eq. (E.4b) can now be written as

$$y^n = \sum_{m=n}^{\infty} A_m^n (au)^m, \qquad (E.5)$$

where $A_m^n = \sum_{k=1}^{n} (-1)^{m+k} \binom{n}{k} \frac{k^m}{m!}$, $A_n^n = 1$, and $\binom{n}{k} = \frac{n!}{k!(n-k)!}$. Putting Eq. (E.5) into Eq. (E.2) and changing the order of summations, then comparing to Eq. (E.1), we finally get

$$\overline{m}_m = \frac{m_m}{a^m} = \sum_{n=1}^{m} A_m^n M_n, \qquad (E.6)$$

where A_m^n satisfy the following recurrence relation [38]

$$A_m^n = \frac{1}{m-n} \sum_{k=n}^{m-1} (-1)^{m-k+1} \left[\frac{n(m-k+1)-k}{(m-k+1)!} \right] A_k^n. \qquad (E.7)$$

2. Relationship Between m_n and T_n

Using $z = e^{au}$ and the binomial theorem, we write

$$\begin{aligned} z^n &= (e^{au}-1)^n = (-1)^n \sum_{k=0}^{n} (-1)^k \binom{n}{k} e^{auk} \\ &= (-1)^n \sum_{k=0}^{n} \sum_{m=0}^{\infty} (-1)^k \binom{n}{k} \frac{k^m}{m!} (au)^m, \qquad (E.8a) \\ &= (-1)^n \sum_{m=1}^{n-1} \sum_{k=1}^{n} [(-1)^k \binom{n}{k} \frac{k^m}{m!}] (au)^m, \\ &+ (-1)^n \sum_{m=n}^{\infty} \sum_{k=1}^{\infty} [(-1)^k \binom{n}{k} \frac{k^m}{m!}] (au)^m. \qquad (E.8b) \end{aligned}$$

The summation $(-1)^n \sum_{m=1}^{n-1} \sum_{k=1}^{n} [(-1)^k \binom{n}{k} \frac{k^m}{m!}]$ turns out to be zero in Eq. (E.8b), which hence reduces to

$$z^n = \sum_{m=n}^{\infty} C_m^n (au)^m, \tag{E.9}$$

where C_m^n is given by

$$C_m^n = \sum_{k=1}^{n} (-1)^{n+k} \binom{n}{k} \frac{k^m}{m!}. \tag{E.10}$$

Substituting Eq. (E.9) into Eq (E.3) and comparing with Eq. (E.1) we find

$$\overline{m}_m = \frac{m_m}{a^m} = \sum_{n=1}^{m} C_m^n T_n. \tag{E.11}$$

T_n can also be evaluated in terms of $\overline{m}_n$ by matrix inversion [38]:

$$T_n = \sum_{m=1}^{n} D_n^m \overline{m}_m,$$

where

$$D_n^m = \frac{1}{n-m} \sum_{k=m}^{n-1} (-1)^{n-k} \left[\frac{n(n-k+1)-k}{n-k+1} \right] D_k^m. \tag{E.12}$$

3. Relationship Between M_n and T_n

Using $y = z(1+z)^{-1}$ and the binomial theorem, we can write

$$y^n = \sum_{k=0}^{\infty} (-1)^k \binom{n+k-1}{k} z^{n+k}, \tag{E.13a}$$

$$= \sum_{m=n}^{\infty} (-1)^{m-n} \binom{m-1}{m-n} z^m, \tag{E.13b}$$

where $m = n + k$. Substituting Eq. (E.13b) into Eq. (E.2) and comparing with Eq. (E.3) we get [38]

$$T_m = \sum_{n=0}^{m} G_m^n M_n, \tag{E.14}$$

where

$$\begin{aligned} C_m^n &= (-1)^{m-n}\binom{m-1}{m-n} = (-1)^{m-n}\frac{(m-1)!}{(n-1)!(m-n)!}, \\ &= [\frac{m-1-n}{n-1}]G_m^{n-1} \qquad ,(E.15) \\ G_m^m &= 1. \end{aligned}$$

To obtain M_n in terms of T_m, we substitute $z = y(1-y)^{-1}$ into Eq. (E.3); and comparing to Eq. (E.2), we find [38]

$$M_n = \sum_{m=0}^{n} H_n^m T_m,$$

where

$$\begin{aligned} H_n^m &= \binom{n-1}{n-m} = [\frac{n-m+1}{m-1}]H_n^{m-1}, \qquad (E.16) \\ H_n^n &= 1. \end{aligned}$$

REFERENCES

1. A.B.F. Duncan, *J. Am. Chem. Soc.* 77, 2107 (1955).
2. D. Kastler, *J. Chem. Phys.* 50, 556 (1953).
3. A.C. Hurley, *Proc. Roy. Soc. (London)* A248, 119 (1958).
4. R.A. Ballinger, *Mol. Phys.* 2, 139 (1959).
5. G. Herzberg, Spectra of Diatomic Molecules, (Van Nostrand, New York, 1950), 2nd ed.
6. J.I. Steinfeld, Molecules and Radiation (The MIT Press, Massachusetts, 1981).
7. A.C. Hurley, Introduction to the Electron Theory of Small Molecules, (Academic Press, New York, 1976).
8. M.B. Born and R. Oppenheimer, *Ann. Physik* 84, 457 (1927).
9. J.L. Dunham, *Phys. Rev.* 41, 721 (1932).
10. J.N. Huffaker, *J. Chem. Phys.* 64, 4564 (1976).
11. J.N. Huffaker, *J. Chem. Phys.* 70, 2720 (1979).
12. J.L. Dunham, *Phys. Rev.* 41, 15 (1932).
13. P.M. Morse, *Phys. Rev.* 34, 57 (1929).
14. J.N. Huffaker, *J. Chem. Phys.* 64, 3175 (1976).
15. G. Simons, R.G. Parr, and J.M. Finlan, *J. Chem. Phys.* 59, 3229 (1973).

16. R. Rydberg, *Z. Phys.* 73, 376 (1931); O. Klien, *Z. Phys.* 76, 226 (1932); J.T. Vanderslice *et al.*, *J. Mol. Spect.* 3, 17 (1959).

17. J.N. Huffaker, *J. Mol. Spect.* 65, 1 (1977).

18. E.W. Kaiser, *J. Chem. Phys.* 53, 1686 (1970).

19. J.N. Huffaker and P.H. Dwivedi, *J. Math. Phys.* 16, 862 (1975).

20. J.N. Huffaker, *J. Mol. Spect.* 71, 160 (1978).

21. J.N. Huffaker, *J. Chem. Phys.* 72, 2601 (1980).

22. P.R. Bunker and R.E. Moss, *Mol. Phys.* 33, 417 (1977).

23. P.R. Bunker, *J. Mol. Spect.* 5, 478 (1972).

24. G. Arfken, Mathematical Methods for Physicists (Academic Press, New York, 1970), 2nd ed.

25. Brice Carnahan, HA. Luther, James O. Walker, Applied Numerical Methods (John Wiley & Sons, Inc., New York).

26. R.N. Sileo and T.A. Cool, *J. Chem. Phys.* 65, 117 (1976).

27. G.C. Lie, *J. Chem. Phys.* 60, 2991 (1973).

28. W. Mayer and P. Rosmus, *J. Chem. Phys.* 63, 2356 (1975).

29. R.L. Spellicy, R.E. Meredith, and F.G. Smith, *J. Chem. Phys.* 57, 5119 (1972).

30. J.K. Cashion, *J. Chem. Phys.* 48, 94 (1968).

31. J.K. Cashion, *J. Chem. Phys.* 39, 1872 (1963).

32. G.D. Lanadro and A.E. Douglas, *Can. J. Phys.* 51, 434, (1973).

33. K. Cashion, *J. Mol. Spect.* 10, 182 (1963).

34. R.S. Mulliken, *J. Chem. Phys.* 2, 400 (1934).

REFERENCES

1. M. Chester and L.C. Yang, *Phys. Rev. Lett.* **31**, 1377 (1973)

2. J.M. Kosterlitz and D.J. Thouless, **Progress in Low Temperature Physics**, Vol. VIIB (edited by D.F. Brewer), North-Holland, New York (1978), chapter 5, p. 371

3. T. Ando, A.B. Fowler, and F. Stern, *Rev. Mod. Phys.* **54**, 437 (1982)

4. For a review of two-dimensional physics, see reference 2

5. S.C. Yang, *Phys. Rev. B* **3**, 4160 (1971)

6. D.C. Licciaredello and D.J. Thouless, *Phys. Rev. Lett.* **35**, 1475 (1975)

7. J.F. Janak, *Phys. Rev.* **178**, 1416 (1969)

8. E. Arnold, *Surface Science* **58**, 60 (1976)

9. C.C. Grimes and G. Adams, *Phys. Rev. Lett.* **42**, 795 (1979)

10. R. Dingle, H.L. Störmer, A.C. Gossard, and W. Wiegmann, *Appl. Phys. Lett.* **33**, 665 (1978)

11. G.H. Döhler, *Phys. Stat. Sol. B* **52**, 79 (1972)

12. K. von Klitzing, G. Dorda, and M. Pepper, *Phys. Rev. Lett.* **45**, 484 (1980)

13. D.C. Tsui, H.L. Störmer, and A.C. Gossard, *Phys. Rev. Lett.* **48**, 1559 (1982)

14. H.L. Störmer, A. Chang, D.C. Tsui, J.C.M. Hwang, A.C. Gossard, and W. Wiegmann, *Phys. Rev. Lett.* **50**, 1953 (1983)

15. R.B. Laughlin, *Phys. Rev. Lett.* **50**, 1395 (1983)

16. For a comprehensive review of device physics, see S.M. Sze, **Physics**

of Semiconductor Devices, Second edition, Wiley and Sons, New York (1981)

17. F. Stern, *Phys. Rev. B* 5 (1972)

18. H.H. Wieder, *Appl. Phys. Lett.* **25**, 206 (1974)

19. J.R. Sites and H.H. Wieder, *CRC Crit. Rev. Solid State Sci.* **5**, 385 (1975)

20. H.A. Washburn, *Thin Solid Films* **45**, 135 (1977)

21. See S.M. Sze, reference 16, chapter 7, p. 362

22. See, for example, N.W. Ashcroft and N.D. Mermin, **Solid State Physics**, Holt, Rinehart and Winston, New York (1976), chapter 2, p. 30

23. G.A. Antcliffe, R.T. Bate, and R.A. Reynolds, **Proceedings of the Conference on the Physics of Semimetals and Narrow-Gap Semiconductors**, 1970, (edited by D.L. Carter and R.T. Bate), Pergamon, New York (1971), p. 499

24. H. Reisinger, H. Schaber, and R.E. Doezema, *Phys. Rev. B* **24**, 5960 (1981)

25. F.J. Ohkawa and Y. Uemura, *J. Phys. Soc. Japan* **37**, 1325 (1974)

26. H.A. Washburn, J.R. Sties, and H.H. Wieder, *J. Appl. Phys.* **50**, 4872 (1979)

27. F. Stern, *Phys. Rev. B* **5**, 4881 (1972)

28. F.F. Fang and W.E. Howard, *Phys. Rev. Lett.* **16**, 797 (1966)

29. J.C. Maan, Ch. Uihlein, L.L. Chang, and L. Esaki, *Solid State Comm.* **44**, 653 (1982)

30. F. Stern, *Phys. Rev. Lett.* **33**, 960 (1974)

31. T. Ando, *J. Phys. Soc. Japan* **39**, 411 (1975)

32. See, for example, W.A. Harrison, **Solid State Theory**, Dover, New York (1979) p. 73

33. See, for example, P. Lorrain and D.R. Corson, **Electromagnetic Fields and Waves**, Second Edition, Freeman and Company, San Francisco

(1970) p. 153

34. F. Stern, *J. Computational Physics* **6**, 56 (1970)
35. See, for example, L.D. Landau and E.M. Lifshitz, Quantum Mechanics (Nonrelativistic Theory), Third Edition Pergamon Press, Oxford (1977), chapter 7, p. 164
36. F. Stern and W.E. Howard, *Phys. Rev.* **163**, 816 (1967)
37. T. Ando and Y. Uemura, *J. Phys. Soc. Japan* **36**, 959 (1974)
38. T. Ando, Y. Matsumoto, and Y. Uemura, *J. Phys. Soc. Japan* **39**, 279 (1975)
39. R.B. Laughlin, *Phys. Rev. B* **23**, 5632 (1981)
40. M. Wanner, R.E. Doezema, and U. Strom, *Phys. Rev. B* **12**, 2883 (1975)
41. O. Madelung, **Physics of III-V Compounds**, Wiley and Sons, New York (1964)
42. Von G. Gieseche and G.H. Pister, *Acta. Crystl.* **11**, 369 (1958)
43. F. Matossi and F. Stern, *Phys. Rev.* **111**, 472 (1958)
44. D. Long, *J. Appl. Phys.* **33**, 1682 (1962)
45. S. Zwerdling, B. Lax, and L.M. Roth, *Phys. Rev.* **108**, 1402 (1957)
46. J.R. Dixon and J.M. Ellis, *Phys. Rev.* **123**, 1560 (1961)
47. T.C. Harman, H.L. Goering, and A.C. Beer, *Phys. Rev.* **104**, 1562 (1956)
48. E.D. Palik and R.F. Wallis, *Phys. Rev.* **123**, 131 (1961)
49. E.O. Kane, **Semiconductors and Semimetals, Vol. 1, Physics of III-V Compounds** (edited by R.K. Willardson and A.C. Beer), Academic Press, New York (1966), chapter 3, p. 75
50. A.B. Fowler, F.F. Fang, W.E. Howard, and P.J. Stiles, *Proceedings of the International Conference on the Physics of Semiconductors*, Kyoto, 1966, *J. Phys. Soc. Japan* **21**, Supplement p. 331

51. F.F. Fang and P.J. Stiles, *Phys. Rev.* **174**, 823 (1968)

52. T. Ando and Y. Uemura, *J. Phys. Soc. Japan* **37**, 1044 (1974)

53. C.R. Pidgeon, D.L. Mitchell, and R.N. Brown, *Phys. Rev.* **154**, 737 (1967)

54. H. Reisinger, Diplom Thesis, Technische Universität München (1978), unpublished

55. R.J. Wagner, T.A. Kennedy, and H.H. Wieder, *Proceedings of the Third International Conference on the Physics of Small Gap Semiconductors*, Warsaw, 1977 p. 427

56. For sample 31-A2(10^{15}) see references 55, 26, 62, and see also 18-20. For sample IAS/34(10^{17}) see references 24 and 54.

57. O.G. Lorimor and W.G. Spitzer, *J. Appl. Phys.* **36**, 1841 (1965)

58. B.O. Seraphin and H.E. Bennett, **Semiconductors and Semimetals, Vol. 3, Optical Properties of III-V Compounds** (edited by R.K. Willardson and A.C. Beer), Academic Press, New York (1967) p. 499

59. D.C. Tsui, *Phys. Rev. B* **4**, 4438 (1971); see also reference 68 and references therein

60. J.A. Appelbaum and G.A. Barraff, *Phys. Rev. B* **4**, 1235 (1971); see also G.A. Barraff and J.A. Appelbaum, *Phys. Rev. B* **5**, 475 (1972) and references therein

61. D.C. Tsui, *Solid State Comm.* **9**, 1789 (1971)

62. H.A. Washburn and J.R. Sites, *Surface Science* **73**, 537 (1978)

63. H. Reisinger and F. Koch, *Solid State Comm.* **37**, 429 (1980)

64. L.L. Chang, E.E. Mendez, N.J. Kawai, and L. Esaki, *Surface Science* **113**, 306 (1982)

65. J.R. Clement and E.H. Quinnel, *Rev. Sci. Inst.* **23**, 213 (1962)

66. G.K. White, **Experimental Techniques in Low Temperatures Physics**, Second Edition, Clarendon Press, Oxford (1968), appendix table A, p. 307

67. R.J. Donnelly, **Experimental Superfluidity**, University of Chicago Press,

Chicago (1967), Appendix C, Table 1, p. 214

68. D.C. Tsui, *Phys. Rev. B* **8**, 2657 (1978)

69. H.L. Störmer, A.C. Gossard, and W. Wiegmann, *Solid State Comm.* **41**, 707 (1982)

70. Y. Uemura, Proceedings of the Twelfth International Conference on the Physics of Semiconductors, Stuttgart, 1974, (edited by M.H. Pilkuha), B.G. Teubner, Stuttgart (1974) p. 665

71. W. Beinvogl, A. Kamgar, and J.F. Koch, *Phys. Rev. B* **14**, 4274 (1976)

72. Th. Englert, J.C. Maan, D.C. Tsui, and A.C. Gossard, *Solid State Comm.* **45**, 989 (1983)

73. R.E. Doezema, M. Nealon, and S. Whitmore, *Phys. Rev. Lett.* **45**, 1593 (1980)

74. J.C. Portal, R.J. Nicholas, M.A. Brummell, A.Y. Cho, K.Y. Cheng, and T.P. Pearsall, *Solid State Comm.* **43**, 907 (1982)

75. J.C. Maan, Th. Englert, Ch. Uihlein, H. Künzel, A. Fischer, and K. Ploog, *Solid State Comm.* **47**, 383 (1983)

76. E.D. Palik and J.R. Stevenson, *Phys. Rev.* **130**, 1344 (1963)

77. T. Ando, *J. Phys. Soc. Japan* **37**, 1233 (1974)

78. E.N. Adams and T.D. Holstein, *J. Phys. Chem. Solids* **10**, 254 (1959)

79. K. Seeger, **Semiconductor Physics**, Second Edition, Springer-Verlag, New York (1982) p. 279

80. R.B. Dingle and D. Shoenberg, *Nature* (London) **166**, 652 (1950); see also R.B. Dingle, *Proc. Royal Soc. London* **A211**, 517 (1952)

81. G. Bauer and H. Kahlert, *Phys. Rev. B* **5**, 566 (1972)

82. W. Beinvogl and J.F. Koch, *Phys. Rev. Lett.* **40**, 1736 (1978)

83. S.K. Bhattacharya, *Phys. Rev. B* **25**, 3756 (1982)

84. M. Nealon, S. Whitmore, R.R. Bourassa, and R.E. Doezema, *Surface Science* **113**, 282 (1982)

85. S. Tansal, A.B. Fowler, and R.F. Cotellessa, *Phys. Rev.* **178**, 1326, (1969)

86. N. Kotera, Y. Katayama, and K.F. Komatsubara, *Phys. Rev.* B5, 3065 (1972)

87. Th. Englert, J.C. Maan, D.C. Tsui, and A.C. Gossard, *Solid State Comm.* **45**, 989 (1983)

88. F. Koch, **Physics in High Magnetic Fields** (edited by S. Chikazumi and N. Miura), Springer-Verlag, Berlin (1981) p. 262

89. F. Koch, private communication

90. H. Schaber and R.E. Doezema, *Phys. Rev. B* **20**, 5257, (1979)

91. J.H. Crasemann and U. Merkt, *Solid State Comm.* **47**, 917 (1983)

92. J.H. Crasemann, U. Merkt and J.P. Kotthaus, *Phys. Rev. B* **28**, 2271 (1983)

93. A Därr, J.P. Kotthaus, and J.F. Koch, *Solid State Comm.* **17**, 455 (1975)

94. L.L. Chang, N.J. Kawai, E.E. Mendez, C.-A. Chang, and L. Esaki, *Appl. Phys. Lett.* **38**, 30 (1981)

95. M. Nealon and R.E. Doezema, *Solid State Comm.* **50**, 661 (1984)

96. A.B. Fowler and A.M. Hartstein, *Surface Science* **98**, 169 (1980)

97. A.M. Voshchenkov and J.N. Zemel, *Phys. Rev. B* **9**, 4410 (1974)

98. Reference 3, p.442

99. A. Hartstein and A.B. Fowler, *Phys. Rev. Lett.* **34**, 1435 (1975)

100. A.B. Fowler and A. Hartstein, *Philosophical Mag. B* **42**, 949 (1980)

101. Y. Yafet, R.W. Keyes, and E.N. Adams, *J. Phys. Chem. Solids* **1**, 137 (1956)

102. E.H. Putley, **Semiconductors and Semimetals**, Vol. 1, Physics of III-V Compounds (edited by R.W. Willardson and A.C. Bear), Academic Press, New York (1966), Chapter 9, p. 289

103. Reference 79, p. 282

104. R.W. Keyes and R.J. Sladek, *J. Phys. Chem. Solids* **1**, 143 (1956)

105. M. von Ortenberg, *J. Phys. Chem. Solids* **34**, 397 (1973)

106. A. Hartstein and A.B. Fowler, *Physica* **117B & 118B**, 655 (1983)

107. H. Reisinger, A.B. Fowler and A. Hartstein, Proceedings of the Fifth International Conference on Electronic Properties of Two-Dimensional Systems, Oxford, 1984. To be published in *Surface Science*

108. J. Yoshino, H. Sakaki, and T. Hotta, *ibid.*

109. D.C. Tsui, *Phys. Rev. Lett.* **24**, 303 (1970).